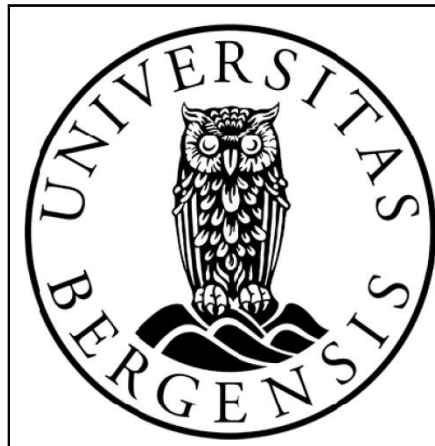


**Low Salinity Waterflood in Combination with
Surfactant/Polymer;
Effect of Surfactant Slug Size**

Adnan Ibrahim Al-Ajmi

Master Thesis
Petroleum Technology – Reservoir Physics



Department of Physics and Technology
Centre for Integrated Petroleum Research (Uni CIPR)
University of Bergen
June 2014

Acknowledgement:

I would like to express my sincere gratitude to my advisor Professor Arne Skauge for his guidance, scientific advice and assistance in my thesis work. It was a great experience to study and work under his supervision.

I would like to thank my co-supervisors Edin Alagic and Behruz Shaker for their assistance and guidance during the experimental work. I am also grateful to all the CIPR staff for their help and contribution during the laboratory experience.

I want to acknowledge Inger Thosen and Kristin Høge for their keen interest, affection and help shown towards me during my study period. Also my thank goes to Terje Finnekas for all his help as a student counselor.

I am always grateful to Hamed Al-Hadhrami for giving me the opportunity to study the master degree at CIPR, University of Bergen.

A special thank to my parents, brothers, sisters and the rest of my family for their support, encouragement and motivation during whole my study.

Last but not least, I thank all my friends for their help and for all great time we spent together.

Adnan Ibrahim Al-Ajmi

Bergen, May 2014

Abstract:

In last years, there has been a growing interest in the effect of reducing salinity of injected water in oil recovery. Many studies have showed that low salinity waterflooding is a promising method that can lead to a significant reduction in residual oil saturation compared to traditional waterflooding. The mechanisms behind improved oil recovery by low salinity waterflooding are not fully understood, but many researchers have claimed wettability alteration.

In this study, the effect of low salinity waterflooding on improving oil recovery is investigated in six Berea sandstone cores. In addition a combined low salinity and surfactant-polymer slugs injection were carried out in tertiary mode to determine and optimize its effectiveness in increasing oil production.

The results of this study indicated that the performance of low salinity waterflooding was affected by wettability of the cores. Thus, investigating the potential of increasing oil recovery by low salinity waterflooding requires establishing initial reservoir wettability state (non-waterwet).

The tertiary low salinity surfactant-polymer slugs injection showed an increased in oil recovery with increasing size of surfactant slug injected at constant surfactant concentration. The wettability of the cores had impact on the efficiency of the slugs injected on oil recovery.

A low salinity polymer slug injected at the end with higher concentration resulted in producing additional oil from the cores. However the performance of this injection varied due to different residual oil saturation obtained after tertiary low salinity surfactant and polymer slugs injection.

Table of contents:

| | |
|--|------|
| Acknowledgement | i |
| Abstract | ii |
| Table of contents | iii |
| List of Figures | vi |
| Nomenclature | viii |
| | |
| 1. Introduction | 1 |
| | |
| 2. Fundamental Concepts and Definitions | 2 |
| 2.1. Basic Core Properties | 2 |
| 2.1.1 Porosity | 2 |
| 2.1.2 Absolute Permeability | 3 |
| 2.1.3 Fluid Saturation..... | 4 |
| 2.2 Special Core Analysis..... | 5 |
| 2.2.1 Effective and Relative Permeability..... | 5 |
| 2.2.2 Capillary Pressure..... | 6 |
| 2.2.3 Wettability..... | 10 |
| 2.3 Liquid Properties..... | 13 |
| 2.3.1 Viscosity..... | 13 |
| 2.3.2 Interfacial/Surface Tension..... | 15 |
| | |
| 3. Low Salinity Waterflooding | 16 |
| 3.1 Introduction..... | 16 |
| 3.2 Summary of Previous Studies in Low Salinity Waterflooding..... | 16 |
| 3.3 Suggested Mechanisms of Low Salinity Waterflooding..... | 19 |
| 3.3.1 Fine Migration..... | 19 |
| 3.3.2 pH Variation..... | 20 |
| 3.3.3 Multicomponent Ionic Exchange (MIE) | 21 |
| 3.3.4 Wettability Alteration and Double Layer Expansion..... | 23 |
| | |
| 4. Enhanced Oil Recovery (EOR) | 25 |
| 4.1 Mobility Ratio, M..... | 25 |
| 4.2 Capillary Number and Capillary Distribution Curve..... | 26 |
| | |
| 5. Surfactant | 29 |
| 5.1 Surfactant Properties..... | 29 |
| 5.2 Types of Surfactants..... | 29 |
| 5.3 Phase Behavior..... | 31 |
| 5.4 Surfactant Retention..... | 35 |
| 5.5 Surfactant Flooding..... | 36 |
| | |
| 6. Polymer | 37 |
| 6.1 Types of Polymer..... | 37 |
| 6.2 Rheology..... | 38 |
| 6.3 Effect of Polymer Concentration..... | 40 |
| 6.4 Apparent Viscosity..... | 40 |
| 6.5 Polymer Flooding..... | 40 |

| | |
|---|----|
| 7. Experimental Apparatus and Procedures | 42 |
| 7.1 Experimental Apparatus..... | 42 |
| 7.1.1 Densitometer..... | 42 |
| 7.1.2 Rheometer..... | 44 |
| 7.1.3 Spinning Drop Tensiometer..... | 45 |
| 7.1.4 Core Holder..... | 46 |
| 7.1.5 Fraction Collector..... | 47 |
| 7.1.6 Pumps, Cylinders and Pressure Transducer..... | 48 |
| 7.1.7 Core Material..... | 49 |
| 7.2 Experimental Procedure..... | 49 |
| 7.2.1 Core Preparation..... | 49 |
| 7.2.2 Pore Volume and Porosity Measurement..... | 49 |
| 7.2.3 Experimental Setup..... | 50 |
| 7.2.4 Permeability Measurements..... | 50 |
| 7.2.5 Drainage..... | 51 |
| 7.2.6 Aging..... | 51 |
| 7.2.7 Synthetic Sea Water and Low Salinity Waterflooding..... | 52 |
| 7.2.8 Low Salinity Surfactant and Polymer Slugs Injection..... | 52 |
| 7.2.9 Low Salinity Polymer Slug Injection..... | 53 |
| 8. Preparation of Samples | 54 |
| 8.1 Synthetic Sea Water (SSW)..... | 54 |
| 8.2 Low Salinity Water (LS)..... | 54 |
| 8.3 Oils..... | 55 |
| 8.4 Surfactants Solution..... | 55 |
| 8.5 Polymer Solution..... | 56 |
| 9. Results and Discussion | 58 |
| 9.1 Measurements of Liquids Properties..... | 59 |
| 9.1.1 Density..... | 59 |
| 9.1.2 Viscosity..... | 59 |
| 9.1.3 Interfacial Tension Measurements..... | 60 |
| 9.2 Basic Physical and Petrophysical Properties of the Rocks..... | 62 |
| 9.3 Synthetic Sea Water (SSW) and Low Salinity (LS) Waterflooding in Unaged Cores..... | 63 |
| 9.3.1 Production Profiles of Secondary Injection..... | 63 |
| 9.3.2 Comparison Between the Synthetic Sea Water (SSW) and Low Salinity (LS) Waterflooding as Secondary Mode..... | 64 |
| 9.3.3 Low Salinity Waterflooding as Tertiary Mode..... | 65 |
| 9.4 Low Salinity (LS) Waterflooding in Aged Cores..... | 66 |
| 9.4.1 Oil Recovery of Low Salinity Waterflooding..... | 66 |
| 9.4.2 Wettability..... | 68 |
| 9.4.3 Pressure Profiles..... | 70 |
| 9.5 Low Salinity Surfactant and Polymer Slugs Injection..... | 73 |
| 9.5.1 Oil Recovery in Aged Cores (LS-S-P)..... | 73 |
| 9.5.2 Pressure Profiles..... | 76 |
| 9.5.3 Comparison of Tertiary Low Salinity Surfactant and Polymer Slugs Injection in Aged and Unaged Cores..... | 79 |
| 9.6 Low Salinity Polymer Slug Injection..... | 80 |

| | |
|---|------------|
| 9.6.1 Oil Recovery..... | 81 |
| 9.6.2 Pressure Profiles..... | 82 |
| 9.7 Capillary Number, N_c | 85 |
| 9.8 Summary and Discussion..... | 86 |
| 10. Conclusions..... | 89 |
| 11. Further Work..... | 91 |
| 12. References..... | 92 |
| Appendix A – Drainage Data | 98 |
| Appendix B – Density Measurements..... | 100 |
| Appendix C – Viscosity Measurements..... | 101 |
| Appendix D – Interfacial Tension Measurements..... | 107 |
| Appendix E – Measurements of the cores size..... | 108 |

List of Figures:

| | |
|---|----|
| Fig.2.1 : Illustration of porosity of porous medium with (1) matrix, (2) interconnected pores, (3) disconnected pores..... | 2 |
| Fig.2.2 : Illustration of measuring permeability of core plug in laboratory [5]..... | 3 |
| Fig.2.3 : Typical water/oil relative permeability of (a) strongly water-wet system and (b) strongly oil-wet system [13]..... | 6 |
| Fig.2.4 : Pressure relation in capillary tubes for air-water (left) and oil-water (right) systems [53]..... | 8 |
| Fig.2.5 : Capillary pressure curve of oil/water system measured for water-wet Berea sandstone [14]..... | 9 |
| Fig.2.6 : Illustration of contact angle, fluid-fluid, and solid-fluid interactions in oil-water-solid system [65]..... | 10 |
| Fig.2.7 : Illustration of intermediate wettability states [26]..... | 11 |
| Fig.2.8 : Variation in waterflood remaining oil saturation over 350 core floods from 30 different oil reservoirs [20]..... | 12 |
| Fig.2.9 : Illustration of parallel plate model..... | 13 |
| Fig.2.10 : Flow curves illustrating Newtonian and non-Newtonian fluid behavior [12]..... | 14 |
| Fig.3.1 : Illustration of bonding between clay surfaces and oil in highly saline and low saline brine environment [44]..... | 24 |
| Fig.4.1 : Typical capillary distribution (CDC) curve [56]..... | 27 |
| Fig.4.2 : Effect of the pore size distribution on the CDC curve [56]..... | 28 |
| Fig.5.1 : Illustration of a surfactant molecule by " tadpole" symbol, where the polar head group is the hydrophilic component and the non-polar tail is the lipophilic component..... | 29 |
| Fig.5.2 : Classification of surfactant..... | 30 |
| Fig.5.3 : Critical micelles concentration (CMC) [56]..... | 31 |
| Fig.5.4 : Schematic representation of surfactant type II(-) system..... | 32 |
| Fig.5.5 : Schematic representation of surfactant type II(+) system..... | 33 |
| Fig.5.6 : Schematic representation of surfactant type III system..... | 34 |
| Fig.5.7 : Interfacial tension versus brine salinity [58]..... | 35 |
| Fig.6.1 : Molecular structure of partially hydrolyzed polyacrylamide (HPAM)..... | 37 |
| Fig.6.2 : Molecular structure of Xanthan..... | 38 |
| Fig.6.3 : Illustration of Carreau model for viscosity of polymer..... | 39 |
| Fig.7.1 : An Anton Paar K.G. DMA 60 density meter and a Heto Birkerød temperature controller..... | 42 |
| Fig.7.2 : Kinexus rheometer form Malvern Instruments Ltd..... | 44 |
| Fig.7.3 : SITE 100 spinning drop tensiometer..... | 45 |
| Fig.7.4 : Hassler-type core holder..... | 46 |
| Fig.7.5 : Foxy Jr. fraction collector..... | 47 |
| Fig.7.6 : Pharmacia LKB P-500 pump..... | 48 |
| Fig.7.7 : Left picture: Piston cylinder. Middle picture: Fuji electric FCX-FKC differential pressure transducer. Right picture: Back pressure regulator.... | 48 |
| Fig.7.8 : Experimental set-up..... | 50 |
| Fig.9.1 : IFT measurements of equilibrated XOF 25s surfactant solution with diluted crude oil..... | 60 |

| | |
|---|-----|
| Fig. 9.2 : IFT measurements of equilibrated XOF 26s surfactant solution with diluted crude oil..... | 61 |
| Fig.9.3 : Production profile of SSW and DSSW in unaged cores A1 and A2..... | 63 |
| Fig.9.4 : Production profile of core A1..... | 65 |
| Fig.9.5 : Production profiles of low salinity waterflooding in aged cores..... | 67 |
| Fig.9.6 : Recovery profiles of secondary waterflooding for all six cores..... | 68 |
| Fig.9.7 : Production and Pressure profiles of LS waterflooding in core A3..... | 71 |
| Fig.9.8 : Production and pressure profiles of LS waterflooding in core A4..... | 71 |
| Fig.9.9 : Production and pressure profiles of LS waterflooding in core A5..... | 72 |
| Fig.9.10 : Production and pressure profiles of LS waterflooding in core A6..... | 72 |
| Fig.9.11 : Oil recovery of tertiary low salinity surfactant and polymer slugs injection done in the aged cores..... | 74 |
| Fig.9.12 : Oil recovery of tertiary low salinity surfactant and polymer slugs injection based on the residual oil after secondary low salinity waterflooding..... | 75 |
| Fig.9.13 : Relation between oil recovery and surfactant slug size injected at constant surfactant concentration..... | 76 |
| Fig.9.14 : Pressure and production profile of LS-S-P flooding in core A3..... | 77 |
| Fig.9.15 : Pressure and production profile of LS-S-P flooding in core A4..... | 77 |
| Fig.9.16 : Pressure and production profile of LS-S-P flooding in core A5..... | 78 |
| Fig.9.17 : Pressure and production profile of LS-S-P flooding in core A6..... | 78 |
| Fig.9.18 : Recovery profiles of cores A1(unaged), A2 (unaged), and A5 (aged)..... | 80 |
| Fig.9.19 : Oil recovery of low salinity polymer slug injection..... | 81 |
| Fig.9.20 : Pressure and production profiles of LS-P flooding in core A1..... | 82 |
| Fig.9.21 : Pressure and production profiles of LS-P flooding in core A2..... | 83 |
| Fig.9.22 : Pressure and production profiles of LS-P flooding in core A3..... | 83 |
| Fig.9.23 : Pressure and production profiles of LS-P flooding in core A4..... | 84 |
| Fig.9.24 : Pressure and production profiles of LS-P flooding in core A5..... | 84 |
| Fig.9.25 : Pressure and production profiles of LS-P flooding in core A6..... | 85 |
| Fig.9.26 : Capillary distribution curve of Berea sandstone [72]..... | 88 |
| | |
| Fig.C.1 : Viscosity of Marcol 152 measured at different temperature..... | 101 |
| Fig.C.2 : Viscosity of North Sea crude oil measured at different temperature..... | 102 |
| Fig.C.3 : Viscosity of diluted crude oil measured at different temperature..... | 102 |
| Fig.C.4 : Viscosity synthetic sea water measured at different temperature..... | 103 |
| Fig.C.5 : Viscosity of 3000 ppm NaCl brine measured at different temperature.... | 103 |
| Fig.C.6 : Viscosity measurement of 100 ppm polymer solution..... | 104 |
| Fig.C.7 : Viscosity measurement of 300 ppm polymer solution..... | 104 |
| Fig.C.8 : Viscosity measurement of 600 ppm polymer solution..... | 105 |
| Fig.C.9 : Viscosity measurement of 1000 ppm polymer solution..... | 105 |
| Fig.C.10 : Viscosity measurement of stock polymer solution..... | 106 |
| Fig.D.1: IFT measurements of fresh sample of XOF 25s surfactant with diluted crude oil..... | 107 |
| Fig.D.2 : IFT measurements of fresh sample of XOF 25s surfactant with diluted crude oil..... | 107 |

Nomenclature:

| | |
|-----------|--|
| A | area |
| BP | British Petroleum |
| c | interface shape |
| cm | centimeter |
| cp | centipoises |
| CDC | capillary distribution curve |
| CMC | critical micelles concentration |
| COBR | crude oil/brine/rock |
| C_p | polymer concentration |
| Ca | calcium |
| $CaCl_2$ | calcium chloride |
| C° | degree Celsius |
| DLVO | Deryaguin-Landau-Verwey-Overbeek |
| DSSW | diluted synthetic sea water |
| EOR | enhanced oil recovery |
| E_D | microscopic displacement efficiency |
| E_r | recovery factor |
| E_{vol} | volumetric displacement efficiency |
| F | force |
| FW | fractional-wet |
| g | gram |
| g | gravity acceleration |
| G | Gibbs free energy |
| h | height |
| HPAM | hydrolyzed polyacrylamide |
| IFT | interfacial tension |
| J | joule [unit] |
| K | permeability |
| K_{abs} | absolute permeability |
| K_{eff} | effective permeability |
| k_{rel} | relative permeability |
| k_{rw} | end-point relative permeability of water |
| k_{ro} | end-point relative permeability of oil |
| kg | kilogram |
| L | length |

| | |
|----------------|-------------------------------------|
| LS | low salinity |
| LS-S-P | low salinity surfactant and polymer |
| <i>m</i> | consistency parameter |
| M | mobility ratio |
| mbar | millibar |
| mD | millidarcy |
| Mg | magnesium |
| min | minute |
| MIE | multicomponent ionic exchange |
| ml | milliliter |
| mN | millinewton [unit] |
| mPa | millipascal [unit] |
| MWL | mixed-wet large |
| MWS | mixed-wet small |
| m | meter |
| m ² | square meter |
| m ³ | cubic meter |
| N | Newton [unit] |
| NA | not aged |
| NaCl | sodium chloride |
| N | oil originally in place |
| N _p | oil produced |
| N _c | capillary number |
| OIIP | oil initially in place |
| PAM | synthetic polymer polyacrylamide |
| Pa | Pascal [unit] |
| pH | -log[H ⁺] |
| ppm | part per million |
| PV | pore volume |
| PF | polymer flooding |
| P _c | capillary pressure |
| P _o | oil pressure |
| P _w | water pressure |
| <i>Q</i> | flow rate |
| <i>r</i> | radius |
| <i>R</i> | radius |
| RF | recovery factor |
| s | second |
| SI | international system of units |
| SOB | surfactant – oil – brine |
| SSW | synthetic sea water |

| | |
|-----------------------------|---|
| S_g | gas saturation |
| S_o | oil saturation |
| S_w | water saturation |
| S_{wi} | initial water saturation |
| S_{or} | residual oil saturation |
| S_{oi} | initial oil saturation |
| $S_{or,LS}$ | residual oil saturation after low salinity |
| $S_{or @ LS-S-P}$ | residual oil saturation after low salinity surfactant and polymer slugs injection |
| $S_{or \text{ after LS-P}}$ | residual oil saturation after low salinity polymer slug injection |

TDS total dissolved solid

| | |
|-------|--------------|
| V_b | bulk volume |
| V_g | gas volume |
| V_o | oil volume |
| V_p | pore volume |
| V_w | water volume |

WBT water break-through

Symbols

| | |
|---------------------------|--|
| \emptyset | porosity |
| Δp | differential pressure |
| μ | viscosity |
| μ_o | oil viscosity |
| μ_w | water viscosity |
| μ_{∞} | infinite shear rate viscosity |
| μ_{sol} | solution viscosity |
| μ_{slov} | solvent viscosity |
| σ | interfacial tension |
| θ | contact angle |
| ρ_w | water density |
| ρ_o | oil density |
| ρ | density |
| σ_{ow} | oil-water interfacial tension |
| σ_{so} | solid-oil interfacial tension |
| σ_{sw} | solid-water interfacial tension |
| τ | shear stress |
| $\dot{\gamma}$ | shear rate |
| $\partial v / \partial y$ | velocity gradients |
| Π | disjoining pressure |
| λ | mobility |
| λ_w | water mobility |
| λ_o | oil mobility |
| u | Darcy's velocity |
| α | constant related to the pore geometry and type of porous media |

1. Introduction:

Water-flooding is the most used method among fluid injection methods to improve recovery from oil reservoir. The purpose of waterflooding is to maintain the reservoir pressure and sweep the mobilized oil toward the producing wells. The residual oil trapped in the reservoir after waterflooding can be mobilized by using enhanced oil recovery (EOR) techniques. The EOR is defined as oil recovery by injection of materials that are not normally present in the reservoir such as surfactants and polymers [1]. The main objectives of the EOR methods are to increase the volumetric displacement efficiency and/or to remobilize oil that is capillary trapped in the water flooded zones therefore reducing the residual oil saturation.

In the last decade, a consideration has been given to study the effect of water chemistry in the performance of oil recovery. Reducing salinity of the injected water has been shown experimentally to increase oil recovery compared to the high salinity waterflooding in both secondary and tertiary mode [29,31,34].

In this thesis, an experimental investigation has been carried out to study the effect of reducing salinity of the injected water and to determine and optimize the effectiveness of a combined process of low salinity surfactant and polymer slugs injection as tertiary mode.

The investigation of fluid flow in a porous medium requires understanding of the fundamental concepts and properties of rock and fluids. These fundamentals will be described in chapter 2.

Chapter 3 of this thesis, includes a review of previous studies performed on low salinity waterflooding and the proposed mechanisms behind increased oil recovery.

In chapter 4, the principles of enhanced oil recovery techniques are described and the fundamental concepts about surfactant and polymer are listed in chapter 5 and 6 respectively.

The experimental apparatus and procedures used during the study are explained in chapter 7. Chapter 8 includes the chemical composition and the preparation procedures of the fluids samples used either for displacement experiments or for other measurements.

The main results of the measurements and experiments conducted are presented and discussed in chapter 9 followed by conclusion of the study in chapter 10.

2. Fundamental Concepts and Definitions:

The fundamental concepts and properties of a porous medium should be understood in order to investigate and study the fluid flow in the rock. In this chapter, the basic and special rock properties and the liquid properties are defined and discussed.

2.1 Basic Core Properties:

2.1.1 Porosity:

porosity is a measure of the void space within a rock that is available for storage of fluids and it is expressed as a fraction of the bulk volume of the rock as shown by equation 2.1. It is one of the most important rock properties in describing porous medium and it is classified based on connectivity into total porosity and effective porosity as illustrated in figure 2.1 . Total porosity is defined as the ratio of total pore space - taking into account the interconnected and disconnected pores - to the bulk volume of the rock. While the effective porosity is defined as the ratio of the interconnected pore space to the bulk volume.

$$\phi = \frac{V_p}{V_b} \quad (2.1)$$

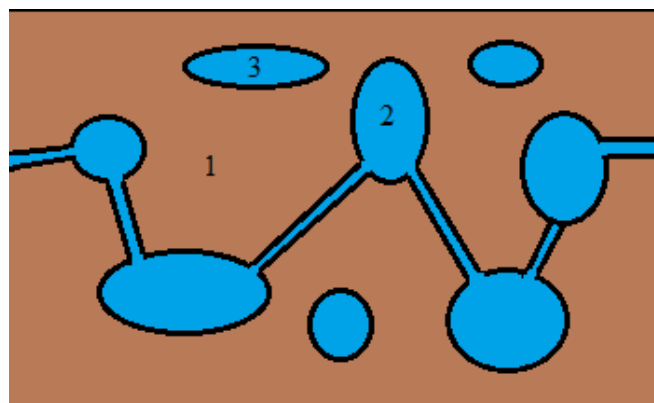


Fig. 2.1 : Illustration of porosity of porous medium with (1) matrix , (2) interconnected pores, (3) disconnected pores.

The fluids flow inside the rock through the connected pores, therefore it is the effective porosity which is of importance to reservoir engineering. In this experimental work the measured porosities are effective porosities.

Porosity is controlled by many factors such as, rock type, grain size and shape, grain sorting and packing, cementation, and compaction. The typical porosity of the two major rock types which are sandstone and carbonate are found to be in the region of 15% to 40% [1].

2.1.2 Absolute Permeability:

Another important parameter of a porous medium is permeability. In general, permeability is a measure of the ability of a porous material to allow fluids to pass through it. When the pore volume of the rock is fully saturated with single fluid, the permeability measured by definition is the absolute permeability of the rock.

Darcy's law is used to measure the absolute permeability of horizontal linear flow and it is given by equation 2.2 :

$$Q = \frac{-K \cdot A \cdot \Delta p}{\mu \cdot L} \quad (2.2)$$

where, Q is the flow rate, K is the absolute permeability of the rock, A is the cross sectional area of the rock, Δp is the pressure difference across the measuring points, μ is the viscosity of the flowing fluid and L is the length of the rock. The negative sign in the equation takes into account the pressure decline in the direction of flow. The unit of the permeability is called Darcy which is equivalent to m^2 in the SI unit's system.

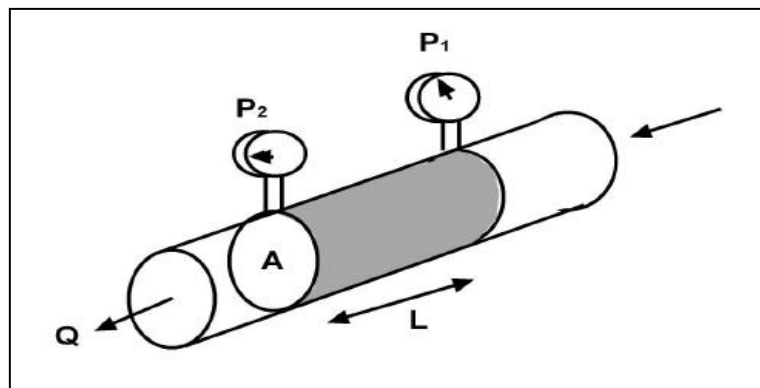


Fig.2.2 : Illustration of measuring permeability of core plug in laboratory [5].

The above equation is valid under the following conditions [50]:

- The core should be 100% saturated with only one fluid.
- Steady-state laminar viscous fluid flow within the core.
- No reactions between the fluid and core. Common reactions that must be avoided are water hydrating clays in the rock matrix, water dissolving minerals, such as salt, in the rock matrix and small rock particles (fines) moved within the rock matrix.

Permeability is an isotropic property where the vertical permeability is lower than horizontal permeability. During the depositional time, the presence of grain-scale or layer-scale heterogeneities which have a preferred orientation is thought to be the reason of the permeability anisotropy [51]. The burial diagenetic processes including compaction, dissolution, and cementation of grains may further modify the permeability anisotropy [4].

The grain structure and grain size of the rock influence both the porosity and permeability where clean, coarse grain sandstone and oolitic limestone have large pores and high permeability. While fine grain sandstone and intercrystalline limestone have small pores and low permeability [50].

2.1.3 Fluid Saturation:

Different type of fluids such as gas, oil and water, could present in the pore space of the rock and the volume of each fluid is determined by its saturation. Therefore, fluid saturation is the measure of the fluid volume present in the pore volume of the rock. It is referred as a fraction and defined as :

$$\text{water saturation: } S_w = V_w/V_p \quad (2.3)$$

$$\text{oil saturation: } S_o = V_o/V_p \quad (2.4)$$

$$\text{gas saturation: } S_g = V_g/V_p \quad (2.5)$$

The summation of the fluids saturation is equal to unity since the pore space is completely filled with fluids.

2.2 Special Core Analysis:

The special core analysis to measure rock properties which are affected by rock and fluids are defined in this section.

2.2.1 Effective and Relative Permeability:

In a petroleum reservoir, the rock is usually saturated with two or three fluids. The flow of each fluid will be affected by the presence of other fluids therefore, each fluid will have different permeability. This permeability referred as effective permeability which defined as the measure of the conductance of a porous medium for one fluid phase when the medium is saturated with more than one fluid.

Darcy's law is extended to describe multiphase flow and effective permeability under steady state conditions as given by equation 2.6:

$$K_{eff,i} = \frac{\mu_i \cdot L \cdot Q_i}{A \cdot \Delta p_i} \quad (2.6)$$

where, $K_{eff,i}$ is the effective permeability of phase i , μ_i is the viscosity of phase i , L is the length of the core, Q_i is the volumetric flow of the phase i , A is the cross-sectional area of the core, Δp_i is the pressure difference of the phase i .

Effective permeability ranges between 0 and absolute permeability, K , and the sum of the effective permeabilities is always less than the absolute permeability [3].

The ratio of effective permeability of a fluid at a given saturation to the absolute permeability is defined as relative permeability as shown by equation 2.7:

$$k_{rel,i} = \frac{K_{eff,i}}{K} \quad (2.7)$$

Relative permeability must be between zero and one and it is strongly affected by fluid saturation, geometry of the pore spaces, pore size distribution, wettability, and fluid saturation history. The curve of the relative permeability is normally plotted as a function of the water saturation. Figure 2.3 shows a typical curves of relative permeability of two phase system oil and water in strongly water-wet and strongly oil-wet conditions.

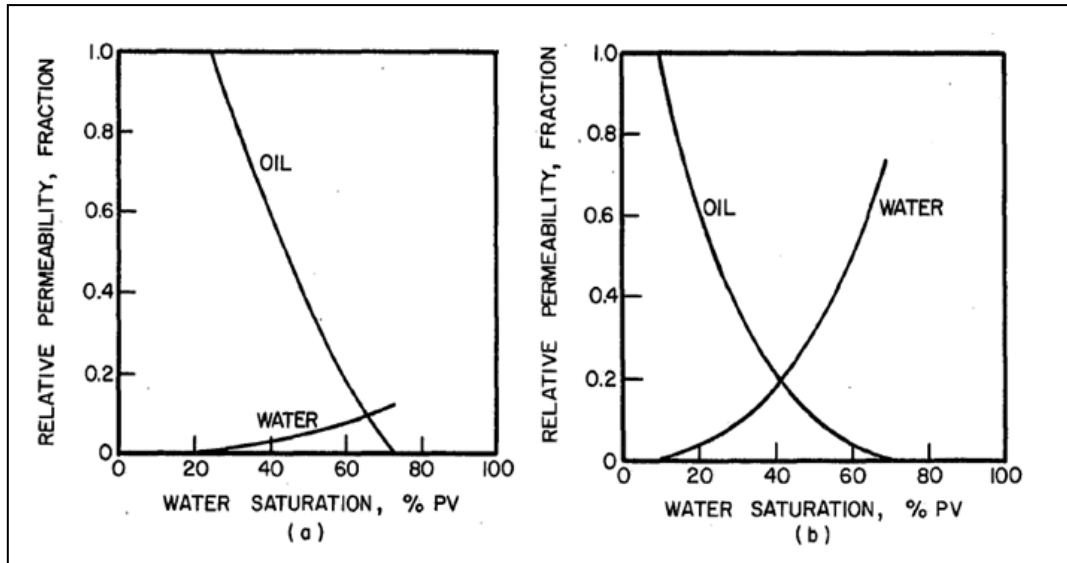


Fig. 2.3: Typical water/oil relative permeability of (a) strongly water-wet system and (b) strongly oil-wet system [13].

Some observations can be noted from figure 2.3 regarding the effect of wettability in the relative permeability curves:

- The connate water saturation, S_{wi} , is higher in strongly water-wet system compared to strongly oil-wet system.
- As the water saturation increases the water relative permeability increases and the oil relative permeability decreases. The increase in the water relative permeability is more pronounced in the strongly oil-wet system because of water flow through the large pores.
- The end-point relative permeability to water measured at maximum water saturation is generally less than 0.3 in strongly water-wet system while in strongly oil-wet system it is greater than 0.5.
- The relative permeability to water and to oil are equal at water saturation higher than 0.5 for strongly water-wet system and less than 0.5 for strongly oil-wet system.

2.2.2 Capillary Pressure:

In reservoir engineering capillary pressure is a major factor controlling the fluid distribution in reservoir rock. It is the most fundamental rock-fluid characteristic in multi-phase flow. The capillary pressure defined as the pressure difference existing across the interface separating two immiscible fluids [52]. This pressure difference is

caused by the interfacial tension effect that makes curved interface, therefore generally the capillary pressure, P_c , is defined as :

$$P_c = \sigma \cdot c \quad (2.8)$$

where σ is the interfacial tension between the fluids and c is the shape of the interface between the two fluids.

When oil and water present in the porous medium, one fluids (for example water) wets the surface of the formation rock in preference to the other fluid (for example oil). In this case, water is called the wetting phase and oil is called the non-wetting phase. The capillary pressure then defined by Laplace's equation [14]:

$$P_c = P_o - P_w = \sigma \left(\frac{1}{R_1} + \frac{1}{R_2} \right) \quad (2.9)$$

where P_o is the oil pressure, P_w is the water pressure, σ is the interfacial tension between oil and water and R_1 and R_2 are the radii of the interface curvatures.

When fluids other than oil and water are used, the capillary pressure is usually defined as :

$$P_c = P_{non-wetting} - P_{wetting} \quad (2.10)$$

However in most porous medium the capillary pressure is very difficult and complicated to be determined. The capillary tube experiment which consider the porous medium as a collection of capillary tubes is used to measure the capillary pressure as a function of geometry, wettability and interfacial tension. Figure 2.4 shows a capillary tube immersed in air-water and oil-water systems where the water which is the wetting phase in these systems rises in the tube due to capillarity.

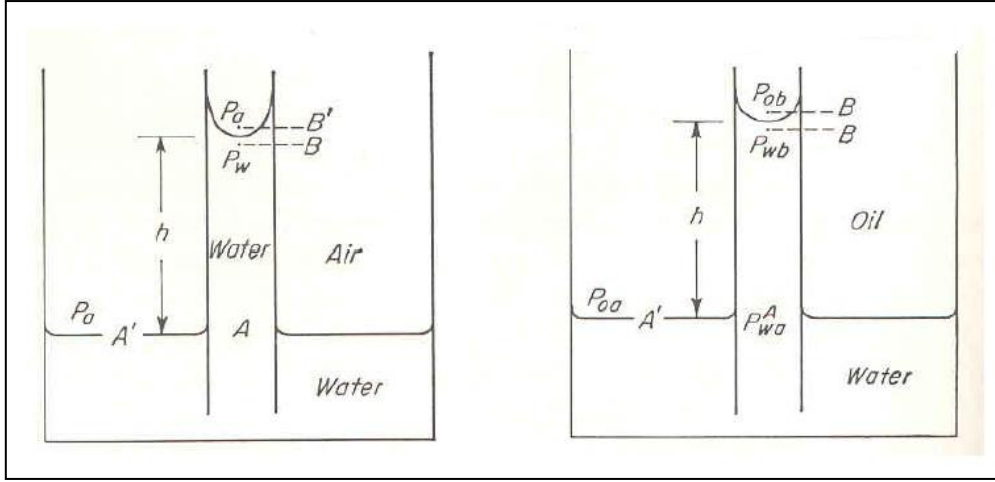


Fig. 2.4: Pressure relation in capillary tube for air-water (left) and oil-water (right) systems [53].

The capillary pressure is expressed in term of the tube radius and the interfacial tension as follows:

$$P_c = \frac{2 \sigma \cos\theta}{r} \quad (2.11)$$

where σ is the interfacial tension between the fluids, θ is the contact angle measured through the denser fluid, and r is the capillary tube radius. Also the capillary pressure in the above systems is related to the height at which the wetting phase rises inside the capillary tube. In case of oil-water system the relation is given by [53]:

$$P_c = P_o - P_w = (\rho_w - \rho_o)gh \quad (2.12)$$

where P_o and P_w are the oil and water pressure, ρ_w is the density of water, ρ_o is the density of oil, g is the acceleration due to gravity, and h is the height of the water column in the capillary tube with respect to reference point.

In laboratory, capillary pressure is measured as a function of the wetting fluid saturation. Therefore, capillary pressure curve can be plotted as shown in figure 2.5 which represents the oil/water capillary pressure curve of water-wet system. There are two types of fluids displacement process which are drainage and imbibition process. In the drainage process the non-wetting phase displaces the wetting phase in the porous medium which cause a decrease in the wetting phase saturation. While in the imbibition process the wetting phase displaces the non-wetting phase in the porous medium leads to an increase in the wetting phase saturation.

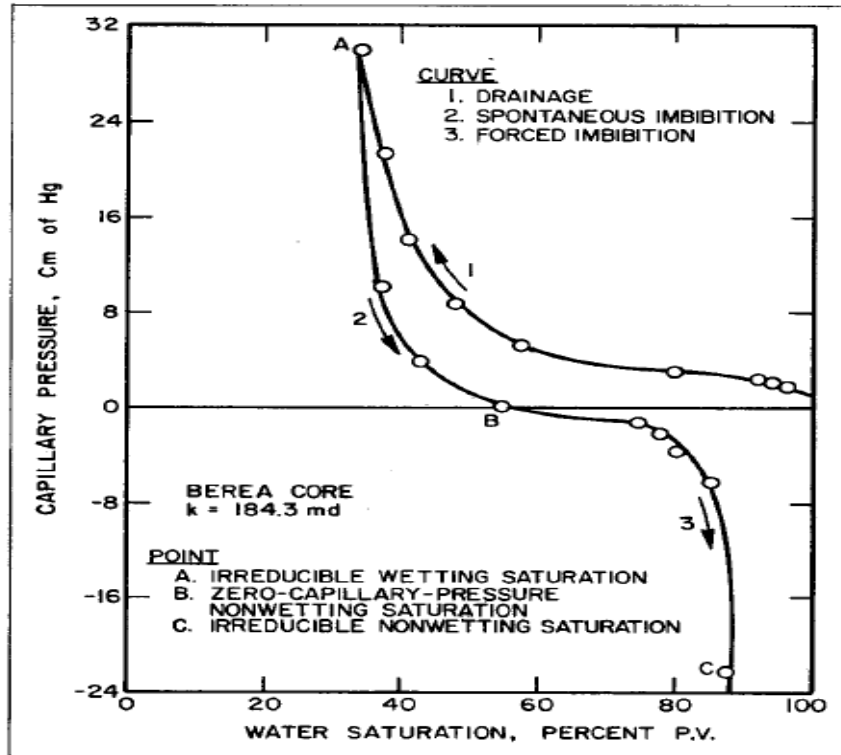


Fig. 2.5: Capillary pressure curve of oil/water system measured for water-wet Berea sandstone [14].

From the figure above the following observations are noted:

- In the drainage process the oil needs minimum pressure to start displacing water from the porous medium. This pressure is called the threshold pressure and it is the pressure needed to invade the largest pores of the porous medium.
- As the oil pressure increases the capillary pressure increases too and the oil displaces more water from the system. The water saturation decreases until no more water can be displaced and the capillary pressure increases to large values. The water saturation at this capillary pressure is called the irreducible water saturation, S_{wi} , as illustrated by point (A) in the figure 2.5.
- When the capillary pressure is reduced the water starts to imbibe into the system displacing the oil. The oil saturation decreases until there is no more oil can be displaced and the capillary pressure goes to large negative value. The oil saturation at this point – represented by point (C) in the figure 2.5 - is called the residual oil saturation, S_{or} .

2.2.3 Wettability:

Wettability of the reservoir is the most important factor that strongly controls the location, flow, and the distribution of fluids inside the reservoir. It also affects almost all types of core analysis including waterflood behavior, relative permeability, capillary pressure, irreducible water saturation, residual oil saturation, dispersion, simulated tertiary recovery, and electrical properties [12,50].

Wettability is defined as " the tendency of one fluid to spread on or adhere to a solid surface in the presence of other immiscible fluids" [12]. Therefore it is referred to the interactions between solid and fluid phases. In the reservoir the tendency of the rock to preferentially imbibe water, oil or both determines its wettability. When the rock has the tendency to imbibe water it is called water-wet rock and the water tends to occupy the small pores and contact the majority of the rock surface. While in oil-wet rock the oil occupies the small pores and contact the majority of the rock surface. However it is necessary to understand that wettability means the wetting preference and does not necessarily refer to the fluid in contact with the rock at any given time [12].

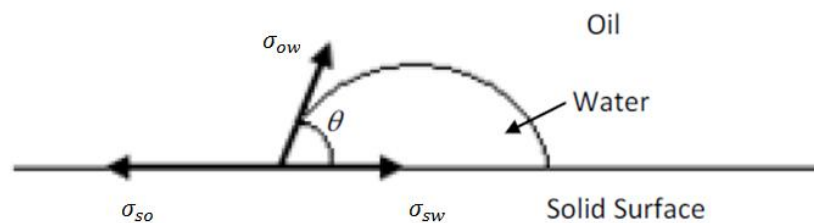


Fig. 2.6 : Illustration of contact angle, fluid-fluid, and solid-fluid interactions in oil-water-solid system [65].

When oil and water are in contact with solid surface, as shown in figure 2.6, there will be fluid-fluid and solid-fluid interactions which represented by Young's equation [1]:

$$\sigma_{ow} \cos \theta = \sigma_{so} - \sigma_{sw} \quad (2.13)$$

where σ_{ow} , σ_{so} , σ_{sw} , are the interfacial tension between oil-water, solid-oil, and solid-water respectively, and θ is the contact angle which measured through the denser phase. The wettability of the surface is determined by the direct measurement of contact angle where equation 2.13 can be rearranged into:

$$\cos\theta = \frac{\sigma_{os} - \sigma_{ws}}{\sigma_{ow}} \quad (2.14)$$

where contact angle, θ , of 0° indicates strongly water-wet surface while contact angle of 180° indicates strongly oil-wet surface. When the contact angle is less than 90° ($0^\circ < \theta < 90^\circ$) the system is known as weakly water-wet while the system with contact angle greater than 90° ($90^\circ < \theta < 180^\circ$) is known as weakly oil-wet. Contact angle of 90° indicates that the system is neutral which means the surface has same affinity toward water and oil.

A general classification of wettability based on contact angle is done by Anderson [12] where the rock is considered to be water-wet for contact angle between $0^\circ \sim 75^\circ$, intermediate-wet for contact angle between $75^\circ \sim 105^\circ$, and oil-wet for contact angle between $105^\circ \sim 180^\circ$. However the intermediate wettability is divided into three sub-classes which are fractional-wet (FW), mixed-wet large (MWL) and mixed-wet small (MWS) as shown in figure 2.7 [6, 20, 21].

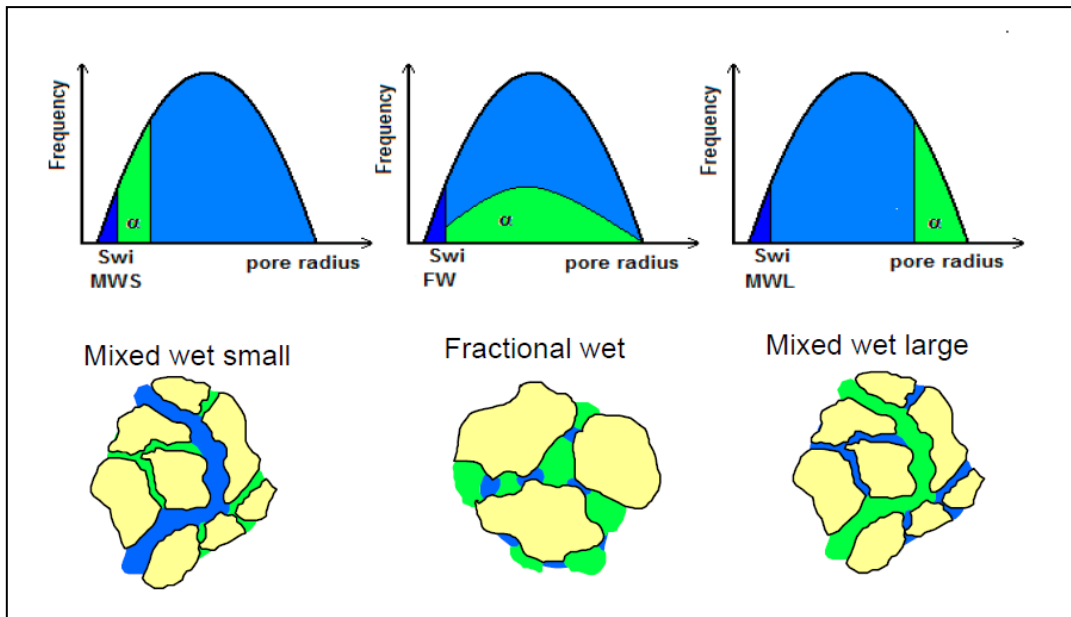


Fig. 2.7 : Illustration of intermediate wettability states [26].

In fractional wettability, the rock has local area that are strongly oil-wet, whereas most of the reservoir is strongly water-wet. This variation in local wettability is due to variable mineral compositions and surface chemistry of the rock. In mixed-wet large, the wetting phase is continuous where the largest pores are oil-wet while the small pores are water-wet. In mixed-wet small, the smallest pores are oil-wet while the

largest pores are water-wet. Mixed-wet small is regarded as a more unconventional mixed-wet state [21, 24].

Most common laboratory techniques that are used to measure wettability are the Amott method and USBM test which measure the average wettability of the core [13, 24]. Several studies showed that the wettability affects the residual oil saturation and oil recovery, see figure 2.8, where the minimum residual oil saturation and maximum oil recovery is obtained when the system is near neutral wettability or intermediate wettability [14, 20, 21].

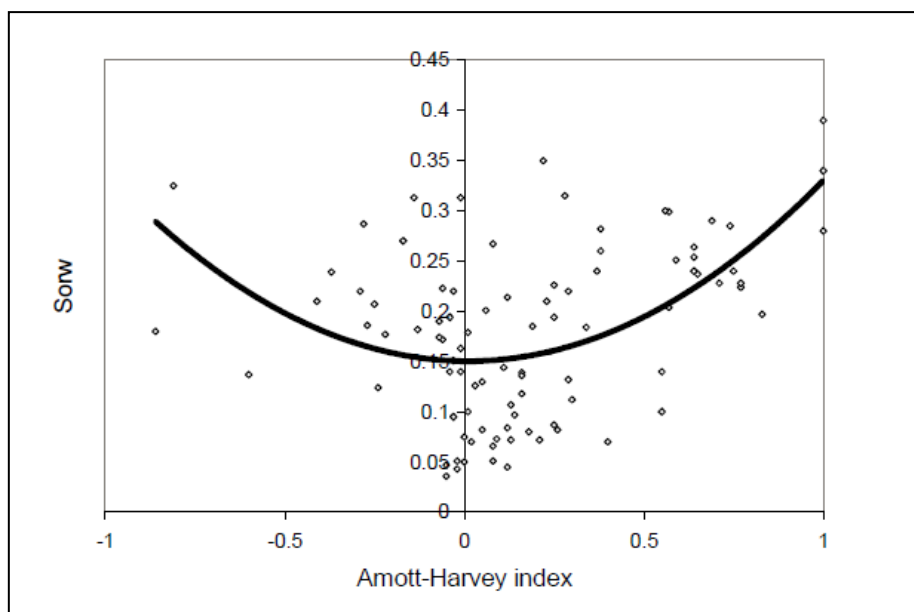


Fig. 2.8: Variation in waterflood remaining oil saturation over 350 core floods from 30 different oil reservoirs [20].

The wettability also affects the relative permeability curves of water and oil (see section 2.2.1 effective and relative permeability). The effect of wettability on the water/oil relative permeability curves is noted where the effective permeability of the wetting phase is lower than the effective permeability of the non-wetting phase. This is explained by the higher resistance of the wetting phase to flow while the non-wetting phase flows easily through the large pores.

2.3 Liquid Properties :

In the following section, the basic liquid properties which will be studied are described.

2.3.1 Viscosity:

The viscosity of fluid is an important property in analyzing fluid behavior and motion in porous medium and it is defined as a measure of a fluid's resistance to flow. Viscosity describes the internal friction of a fluid to deformation when a force is applied to move the fluid which can be illustrated by parallel plate model.

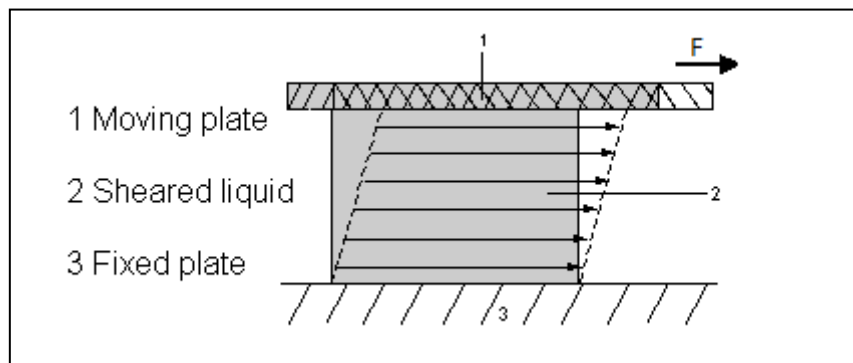


Fig. 2.9 : Illustration of parallel plate model.

Consider a fluid is trapped between two horizontal plates as shown in figure 2.9. When a force, F , is applied to the upper plate the adjacent layer of the fluid to that plate will move in the direction of the applied force. The adhesive force will cause movement transmission to the neighboring layers of fluid below but with diminishing magnitude. This causes a decrease in velocity of each fluid layer down to the bottom plate where velocity is at minimum ($v_x = 0$). In this system, the applied force is called a shear stress and the resulting deformation rate of the fluid is called shear rate [19]. Therefore, the viscosity of the fluid is described mathematically as follows:

$$\mu = \frac{\tau}{\dot{\gamma}} = \frac{(F/A)}{(\partial v / \partial y)} \quad (2.15)$$

where μ is the fluid viscosity, τ is the shear stress which is the force, F , per unit area, A , exerted by the fluid on the upper plate in the x -direction, $\dot{\gamma}$ is the shear rate which is defined as velocity gradients $\partial v/\partial y$.

The basic SI unit of viscosity is Pascal second [Pa · s] where $1 \text{ Pa} \cdot \text{s} = 1 \text{ N s m}^{-2}$. The most used unit of viscosity is centipoise [cp] where $1 \text{ cp} = 1000 \text{ Pa} \cdot \text{s}$.

The viscosity described by equation 2.15 is used only for laminar or streamline flow where it is referred to the molecular viscosity or intrinsic viscosity. While when the flow is turbulent the viscosity is comprised of contributions from the motion in addition to the intrinsic viscosity [19].

When the fluid viscosity is independent of shear rate, then the fluid is called a Newtonian fluid and a plot of the shear stress versus shear rate of the fluid results a straight line with a slope of viscosity, as shown in figure 2.10. While the fluid with a viscosity dependent on the shear rate is called non-Newtonian fluid such as polymer solutions.

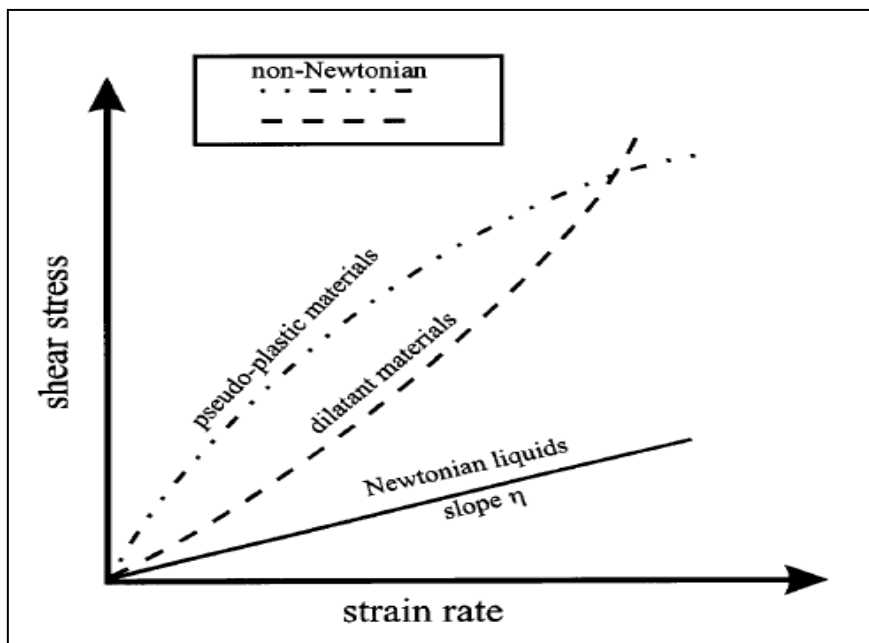


Fig 2.10 : Flow curves illustrating Newtonian and non-Newtonian fluid behavior [12].

The fluid viscosity largely depends on the temperature where the increase in temperature causes a reduction in the viscosity. Therefore, the temperature should be controlled during the measurement for accurate results. The pressure has a small effect in the viscosity of liquids and it requires a very high pressure to affect the viscosity.

2.3.2 Interfacial/Surface Tension:

When two immiscible phases are in contact with each other, the molecules at the interface experience different molecular interaction than the molecules in the bulk. This is caused by an imbalance of forces at the interface that lead to an excess free energy which defined as interfacial tension and thermodynamically expressed as [7,54]:

$$\sigma = \frac{\Delta G}{\Delta A} \quad (2.16)$$

where σ is the interfacial tension, ΔG is the free energy of the two phase system, and ΔA is the surface area of the fluids. From equation 2.16 the interfacial tension can be defined also as the energy required to increase the surface area of the interface by a unit amount. The SI unit of interfacial tension is J/m^2 , however the common used unit are dynes/cm or mN/m.

Generally when one of the two phases in contact is a gas, the excess energy exists at the interface is referred to as surface tension while when both of the phases are liquid it is referred to as interfacial tension. The interfacial tension is affected by temperature, pressure, and compositions of each phase.

3. Low Salinity Waterflooding:

3.1 Introduction:

Water-flooding is the most used method among fluid injection methods to improve recovery from oil reservoir. For over 100 years, the mechanisms of improving oil recovery by water-flooding have been thought of as physical mechanisms where water-flood maintains the reservoir pressure and sweeps the mobilized oil towards the producing wells.

In most of the oil reservoir, the sources used for water-flooding were mainly aquifer water and seawater which are high salinity water. In the last decade, a consideration has been given to the effect of water chemistry - the amount and composition of salt in the water used for flooding – in the oil recovery. Several studies were considered to investigate the effect of decreasing the salinity of the injected brine in improving the performance of waterflooding.

Low salinity waterflooding process involves injecting brine with a lower salt content or ionic strength. The ionic strength is typically in the range of 1000 – 5000 ppm which is much lower than the formation water or seawater. The low salinity waterflooding causes a shift in the thermodynamic equilibrium between crude oil, brine and rock system, that has been established during the geological time, which tends to favor improved oil recovery.

Several laboratory studies demonstrated the potential of low salinity water-flooding to improve oil recovery where the core flood experiments showed increase in oil recovery in both secondary and tertiary mode [29,31,34]. In addition, field trial of low salinity water-flooding has been carried out and showed significant success [33].

3.2 Summary of Previous Studies in Low Salinity Waterflooding :

Jadhunandan and Morrow [28] studied the variables that control the wettability of crude oil/brine/rock systems and investigated the relationship between wettability and oil recovery by waterflooding. Aged Berea sandstone cores with different aging temperature and period were used for more than 50 slow-rate laboratory waterfloods. Brines formulated from NaCl and CaCl₂ with varying concentrations were used to saturate the cores and also for displacement tests. The results of the study showed that aging temperature, initial water saturation, brine composition and crude oil are significant factors in determining the wettability of the crude oil/brine/rock system.

Wettability was measured after waterflooding and showed that for Moutary crude oil water wetness tends to decrease as calcium-ion content increases while for ST-86 crude oil the wettability was insensitive with changing in the brine composition at any level of wettability. Oil recovery by waterflooding for the crude oil/brine/rock systems studied increased with change in wettability from strongly water-wet to a maximum at close-to-neutral wettability.

Yalidiz and Morrow [27,34] extended the research of Jadhunandan and Morrow by studying the effect of brine composition in oil recovery by waterflooding. Berea sandstone cores aged for 10 days were tested using Moutary crude oil [27] and Prudhoe Bay crude oil [34]. Two brine compositions were used, sodium brine (4% NaCl + 0.5% CaCl₂) and calcium brine (2% CaCl₂) for displacement experiments. Different types of tests were conducted by varying the brine used to saturate the core or for displacement process. The tests in which the same brine was used for core saturation and displacements referred to as standard waterfloods. While tests in which the brine composition is changed one or more times during the test are referred to as mixed-brine tests. The study showed that in standard waterfloods when Moutary crude oil used, calcium brine gave higher oil recovery than sodium brine and the imbibition rate test indicated that calcium brine achieved less water wet conditions. In the other hand when Prudhoe Bay crude oil used, the standard waterfloods showed higher recovery for sodium brine than calcium brine.

In mixed-brine tests for Moutary crude oil, changes in brine composition found to be favorable to recovery as compared to standard waterfloods. The highest recovery was achieved when the core was initially saturated by calcium brine and subsequently flooded first with sodium brine until residual oil saturation thereafter flooding by calcium brine. However, mixed-brine tests for Prudhoe Bay crude oil gave oil recovery curves that fell between the standard waterfloods. Also, the breakthrough recoveries were intermediate to values for standard waterfloods. In these researches, the effects of brine composition found to be highly specific to the crude oil and aging conditions.

Sharma and Filoco [29,30] found that at a fixed connate water salinity of 3% NaCl, the oil recovery does not change by varying the salinity of the injected brine (0.3%, 3% and 20% NaCl) using Prudhoe Bay crude oil. However they observed that as the salinity of the connate water is decreased, the oil recovery increased. Therefore they suggested the connate water to be the primary factor controlling the oil recovery. They attributed this dependence on connate water salinity to the change in the wettability from water-wet conditions to mixed-wet conditions leading to lower residual oil saturation.

In 2006 **Zhang and Morrow** [31] conducted a series of core floods, both in secondary and tertiary mode. Four sets of Berea sandstone cores based on their permeability (60mD, 400mD, 500mD and 1100mD) were tested in the experiments. Three types of crude oil were used (CS crude, Minnelusa crude and a crude oil called

A) and the brines were prepared from distilled water and reagent grade chemicals corresponded to Minnelusa reservoir brine. In low salinity water flooding, the synthetic reservoir brine were diluted by a factor of 0.01. Based on the results and the observations of their experiments, sandstone properties are concluded to be the most significant factor in improved recovery by injection of low salinity brine. If injection of low salinity brine improves recovery, response is usually observed for both secondary and tertiary mode. The oil recovery of the outcrop sandstone were found to be depended on initial water saturation where higher initial water saturation gave a higher recovery for low salinity brine. Berea sandstone that has a permeability in the range of 60mD to 140mD does not usually responded to injection of low salinity brine. This lack of response was concluded to be related to the presence of relatively high amounts of chlorite in the cores.

Tang and Morrow [32] investigated the effect of temperature and composition of brine and oil on wettability and crude oil recovery by both spontaneous imbibition and waterflooding. Berea sandstone with three crude oils designated as Dagang, Prudhoe Bay and CS and three kinds of synthetic reservoir brines designated as Dagang (DG), Prudhoe Bay (PB) and CS were used in the displacement tests. The salinity of the brines was varied by diluting the original concentration of total dissolved solids in proportions. The study concluded that the salinity of the connate and invading brines can have a major influence on wettability and oil recovery at reservoir temperature. The water wetness and/or oil recovery by spontaneous imbibition and oil recovery by waterflooding increases with a decrease in salinity of both the connate and invading brine or decrease of either. In addition, they found the water wetness and oil recovery increased with increase in displacement temperature for all crude oils. Aging at high water saturation can increase water wetness.

In 2005, a hydraulic unit was converted to inject low salinity brine into an Alaskan reservoir by switching a single injection pad from high salinity produced water to low salinity water. An injector well and two close production wells were selected within a reasonably well constrained area. **Lager and Webb** [33] did a detailed analysis of the production, and the chemical composition of the produced water to show the effect of injection brine composition in improving recovery at reservoir scale. The salinity of the produced water used for injection was 16640 ppm of total dissolved solids, while the low salinity brine used has a salinity of 2600 ppm of total dissolved solids. The production data indicated that the process was successful where the oil production increased and the water cut dropped from 92% to 87%.

The produced water chemistry data showed that after 5 months of low salinity brine injection, the salinity in the well MPL-07 started to decline whilst the salinity from the well MPL-11 stayed above 12000 ppm TDS. This response from the well MPL-11 was attributed to the presence of sealing fault between the injector and the well and that was confirmed by seismic survey. The data also showed that the magnesium ion (Mg) concentration in produced water of well MPL-07 changed dramatically during the implementation of low salinity brine injection whereas the calcium ion (Ca)

concentration did not exhibit such changes. Additionally, the response of the reservoir to low salinity water injection was confirmed by single well chemical tracer test. The results showed there was no difference between high salinity water and the produced water. The non-optimized low salinity water decreased the S_{or} by 2 saturation units whilst the optimized brine lowered the S_{or} by 10 saturation units compared to the high salinity water.

3.3 Suggested Mechanisms of Low Salinity Waterflooding:

Many studies during the last years have shown the effect of low salinity waterflooding in improving the oil recovery over the high salinity waterflooding in sandstone. This effect has been investigated and observed in both secondary and tertiary mode. A number of mechanisms have been suggested in the literature to explain the increase in oil recovery due to low salinity waterflooding. Necessary conditions for observing the effect of low salinity were identified by systematic experimental work done by Tang and Morrow[32,62] and with some points taken from the work done by researchers at BP [33,63]. The listed conditions are [41,45,47]:

- Significant clay fraction must be present in the sandstone.
- Presence of initial formation water.
- Formation water must contain divalent cations that are, Ca^{2+} , Mg^{2+} .
- Crude oil must contain polar components where no effect of low salinity waterflooding have been observed using refined oil.
- The rock should be exposed to the crude oil to create mixed-wet conditions.

The crude oil/brine/rock interactions is highly affecting the performance of the low salinity waterflooding therefore it is more complicated to understand the recovery mechanisms under various circumstances. Probably the different mechanisms acting together during the low salinity waterflooding causing the increase in the oil recovery.

3.3.1 Fine Migration:

Tang and Morrow [62] studied the influence of the brine composition on crude oil/brine/rock interactions and oil recovery. They observed during their laboratory coreflood experiments on Berea sandstone an increase in the crude oil recovery with a decrease in the salinity of the brine injected. In addition they noticed during the low salinity waterflooding that fine particles, especially kaolinite, were eluted.

Furthermore Berea sandstone were fired and acidized in order to stabilize the clays and then tested for low salinity waterflooding. The crude oil recovery of fired and acidized cores was found to be independent in the salinity of injected brine. Therefore they proposed that the fine particles mobilization play a key role in the sensitivity of oil recovery to salinity.

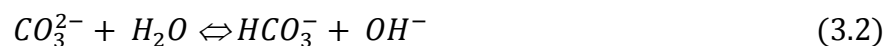
In order to explain the proposed mechanism, the DLVO (Deryaguin-Landau-Verwey-Overbeek) theory of colloidal was used. The balance between the mechanical and colloidal (DLVO) forces determine the stripping of mixed-wet fines from the pore walls. When the salinity of the injected brine is reduced, the electrical double layer between particles in the aqueous phase is expanded thus the tendency for stripping fines will increase causing an improve in oil recovery. [62]

The increase in the recovery caused by the fine migration could be explained by either wettability alteration or diversion of flow. The first mechanism requires an initial wettability state of weakly water-wet to mixed-wet state. In this wettability range, the mixed-wet particles are formed by adsorption of the polar components in the crude oil to the rock surface. Injecting low salinity brine will cause the mixed-wet particles to detached from the rock surface therefore increasing the wettability toward more water-wet.

The fine particles could accumulate at the pore throat resulting in blocking some of the flow channels. This will divert the flow into unswept area therefore causing an increase in oil recovery. This was observed by a reduction in the permeability when low salinity brine was injected. However core flood experiments done by BP have shown neither fines were produced in the effluent nor reduction in permeability [18].

3.3.2 pH Variation:

Some laboratory experiment studies have shown an increase in the effluent pH during the low salinity waterflooding [17,18]. This increase in the effluent pH is explained by two concomitant reactions occur inside the cores which are carbonate dissolution and cation exchange as follows:



The carbonate dissolution (i.e. calcite and/or dolomite) results in an excess of OH^- and cation exchange occurs between invading water and clay minerals. The

dissolution reactions are relatively slow and dependent on the amount of carbonate material present in the rock [18]. The clay minerals will change H^+ ions from the invading phase with cations previously adsorbed. Thus decreasing the concentration of H^+ ions in the liquid phase which will give a rise in the pH.

Based on the evidence of increasing pH during the low salinity waterflooding, McGuire et al [17] suggested that low salinity waterflooding behaves in fashion similar to alkaline flooding. Like alkaline flooding, low salinity waterflooding causes a reduction in the interfacial tension between reservoir oil and water. This is resulted from in-situ generation of surfactant occurs when the oil is contacted by the elevated-pH low salinity water. In addition, the elevated-pH water alters the wettability of the reservoir towards more water-wet therefore increasing the oil recovery.

However, contradictory evidence throws doubt on accepting this mechanism as cause of increasing oil recovery by low salinity waterflooding. The alkaline flooding requires high acid number to generate enough surfactant to induce wettability reversal and/or emulsion formation [64]. In contrast, low salinity waterflooding increased recovery even for crude oil with a very low acid number. No obvious correlation has been found between the increase in the oil recovery due to low salinity waterflooding and the acid number of the crude oil [18]. In addition, some core flood experiments observed a small change in the effluent pH of about 1 unit and it concluded that pH is not responsible for the increase in oil recovery due to the injection of low salinity water [48].

3.3.3 Multicomponent Ionic Exchange (MIE):

In 2006 Lager et al. [18] has proposed multicomponent ionic exchange as predominant mechanism that causes the increased oil recovery by low salinity waterflooding. The results of detailed analysis carried on the effluent of low salinity water injection done for North slope cores gave the evidence for multicomponent ionic exchange (MIE). The effluent analysis showed a sharp decrease in the concentration of Mg^{2+} and Ca^{2+} where their concentration dropped lower than the concentration in the injected low salinity brine. This indicates that the rock matrix has strongly retained Mg^{2+} and Ca^{2+} .

According to these results the multicomponent ionic exchange (MIE) was suggested to be responsible for improved oil recovery by low salinity waterflooding. The extended DLVO theory presents eight possible different mechanisms of organic matter adsorption onto clay mineral, see table 3.1. The dominant mechanism strongly depends on the condition of the clay surfaces and the organic functional group in the oil phase. Four of the eight mechanisms are strongly affected by cation exchange

occurring during low salinity waterflooding which are cation exchange, cation bridging, ligand bonding, and waterbridging.

Cation exchange occurs typically when molecules containing quaternized nitrogen or heterocyclic ring is replaced by metal cations initially bond to clay surfaces. The direct formation between a multivalent cation and a carboxylate group is referred as ligand bonding. Cation bridging is a weak adsorption mechanism between polar functional group and exchangeable cations on the clay surface. Water bridging occurs when the exchangeable cation is strongly solvated.

Table 3.1: Adsorption mechanisms of organic material onto mineral surface [65].

| Mechanism | Organic functional group(s) involved |
|----------------------------|--|
| Cation exchange | Amino, ring NH, heterocyclic N (aromatic ring) |
| Ligand exchange | Carboxylate |
| Cation bridging | Carboxylate, amines, carbonyl, alcoholic OH |
| Water bridging | Carboxylate, amino, carbonyl, alcoholic OH |
| Protonation | Amino, heterocyclic N, carbonyl, carboxylate |
| Anion exchange | Carboxylate |
| Hydrogen bonding | Amino, carbonyl, carboxyl, phenolic OH |
| Van der Waals interactions | Uncharged organic units |

The multivalent cations at the clay surface will tend to bond with polar compounds present in the oil phase thus forming organic-metallic complexes. These complexes have been shown to promote oil-wetness at the clay surfaces. Simultaneously, some of organic polar compounds will be adsorbed directly to the mineral surface causing an increase in the oil-wetness of the clay surface. By reducing the salinity of the injected brine, the multicomponent ionic exchange (MIE) mechanism will take place by replacing the organic polar compounds and organo-metallic complexes in the clay surface with uncomplexed cations. This desorption of polar compounds from the clay surfaces leads to a more water-wet state thus increasing oil recovery.

Lager et al. [18] performed an experiment on North Slope core in purpose to test the multicomponent ionic exchange (MIE) mechanism. In the experiment all the multivalent cations present on the mineral surface were replaced by Na^+ and two shut-ins were performed to make sure that no carbonate was left undissolved. The core was flooded first with high salinity NaCl brine, followed by injection of low salinity NaCl brine. Then a tertiary low salinity brine containing Ca^{2+} and Mg^{2+} was performed.

The first high salinity waterflooding (only containing NaCl) resulted a higher oil recovery due to the absence of oil adsorption by ligand formation and multivalent cation bridging and exchange. The injection of low salinity NaCl brine showed no additional oil recovery as all the mobile oil would have been mobilized already by the

primary high salinity waterflooding and no organo-metallic complexes are present to be adsorbed. The tertiary flooding by low salinity brine contains Ca^{2+} and Mg^{2+} also showed no additional oil produced because the mineral surface contains only the monovalent cations (i.e. Na^{2+}). These results indicated that waterflooding causes a higher recovery irrespective of salinity when the Ca^{2+} and Mg^{2+} removed from the rock surface. Therefore this experiment confirmed the importance of MIE in the low salinity waterflooding mechanism.

3.3.4 Wettability Alteration and Double Layer Expansion :

The most frequently suggested cause of improved oil recovery by low salinity waterflooding is the wettability alteration usually towards more water-wetness [45]. Tang and Morrow [32] concluded from their studies that the water wetness and/or oil recovery by spontaneous imbibition and oil recovery by waterflooding increase with a decrease in salinity. Also, other researchers have seen the increased recovery of low salinity combined with wettability alteration of the cores [44,66].

The initial wettability state of the cores can be altered during the wettability restoration where the crude oil would be adsorbed on the clay surfaces through specific interactions. This wettability alteration strongly depends on the stability of the water film exists between oil and mineral surface. The ability of oil to rupture the water film and therefore change the wettability of the clay surfaces explained by the concept of disjoining pressure, Π [2,26,67]. The disjoining pressure is an additional pressure within the water film and it represents the sum of the attractive and repulsive forces between the oil/water and clay/water surfaces. It depends on the water film thickness and increases positively as the interfaces approach each other until a critical disjoining pressure is reached at critical separation distance. Then further decrease in the water film will change the disjoining pressure from positive to negative leading to collapse the water film and thus altering wettability.

Ligthelm et al [44] explained the wettability alteration during the low salinity waterflooding as an effect of double layer expansion. In high salinity brine the presence of sufficient multivalent positive cations lead to lower the negative electrical potential at the slipping plane between the charged surfaces (oil and clay minerals) and the brine solution, see figure 3.1. Multivalent cations are believed to act as bridges between negatively charged oil and clay minerals and in high saline environment oil could react with clay surfaces resulting in forming organo-metallic complexes therefore change the local wettability. By lowering the brine salinity, the reduction in the multivalent cations will reduce the screening potential of cations. Therefore the electrical double layer will expand and the absolute level of zeta potential will increase. This in turn results in increasing the electrostatic repulsion between oil and clay particles. When the repulsive forces exceed the binding force via

multivalent cations bridges the oil might be desorbed from the clay surface. This would cause wettability alteration towards increasing water wetness.

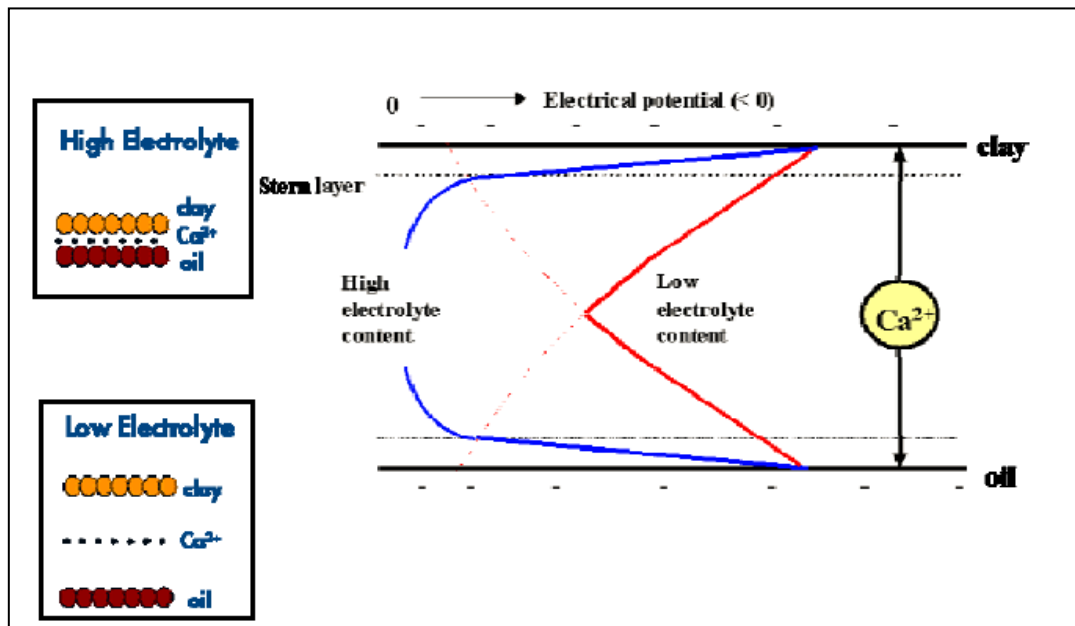


Fig.3.1 : Illustration of bonding between clay surfaces and oil in highly saline and low saline brine environment [44].

The experiments carried by Ligthelm et al [44] showed that low salinity waterflooding causes wettability modification towards increasing water wetness. They suggested that the mechanism of wettability alteration by low salinity injection relies primarily on expansion of electrical double layers and to lesser extent on cation exchange processes.

It seems from the suggested mechanisms in the literatures that probably different mechanisms acting together during the low salinity waterflooding causing the increase in the oil recovery. The multicomponent ionic exchange with double layer expansion could act together to alter the wettability toward more water-wet state therefore improve oil recovery. The release of fine particles and the increase in the pH could be attributed as effects of low salinity waterflooding rather than the mechanisms that cause the increase in oil recovery. However in many studies of low salinity waterflooding these effects have not been observed.

4. Enhanced Oil Recovery (EOR):

The recovery mechanisms of an oil reservoir are typically divided into three stages which are primary, secondary and tertiary recovery. In primary recovery stage, the drive mechanisms of recovery are natural water displacing oil toward wells, expansion of gas cap in the top of the reservoir, expansion of dissolved gas in the oil, and gravity drainage. These mechanisms are called natural drive mechanisms. During the primary mechanisms the reservoir pressure is depleted and at some point there will be insufficient reservoir pressure to produce oil therefore secondary recovery methods are implemented. These methods rely on supply an external energy into the reservoir by injecting fluids to increase reservoir pressure and to displace the oil toward the production wells. Water-flooding and gas injection are the most common secondary recovery mechanisms. The recovery factor after primary and secondary recovery stages is normally between 35 and 45% [71].

In order to increase the recovery, tertiary recovery mechanisms which known as enhanced oil recovery mechanisms were introduced. The EOR is defined as oil recovery by injection of materials not normally present in the reservoir such as surfactants and polymers [1]. The main objectives of the EOR methods are to increase the volumetric displacement efficiency and/or to remobilize oil that is capillary trapped in the water flooded zones therefore reducing the residual oil saturation.

The recovery factor, E_r is defined as :

$$E_r = N_p/N = E_D \cdot E_{vol} \quad (4.1)$$

where the ratio of the amount of oil produced, N_p , to the amount of oil originally in place, N , is equal to the product of the microscopic displacement efficiency, E_D , times the volumetric displacement efficiency, E_{vol} . According to the above equation the oil recovery could be increased by i) improving the volumetric sweep efficiency which can be done by getting a favorable mobility ratio, and/or by ii) increasing the microscopic displacement efficiency by lowering the interfacial tension between the fluids.

4.1 Mobility Ratio, M:

The mobility, λ , of a single fluid in a porous medium is defined as the ratio of the effective permeability of the fluid to the viscosity of that fluid :

$$\lambda_i = \frac{k_{ri} \cdot K}{\mu_i} \quad (4.2)$$

where λ_i is the mobility of the fluid, k_{ri} is the relative permeability of the fluid, K is the absolute permeability of a given medium and μ_i is the viscosity of the fluid.

The mobility ratio, M , is defined as the mobility of the displacing phase (for example water) divided by the mobility of the displaced phase (for example oil) as represented by equation 4.3 :

$$M = \frac{\lambda_w}{\lambda_o} = \frac{k_{rw} \cdot \mu_o}{k_{ro} \cdot \mu_w} \quad (4.3)$$

The mobility ratio is often given in the term of the end point mobility ratio :

$$M^\circ = \frac{k_{rw}^\circ \cdot \mu_o}{k_{ro}^\circ \cdot \mu_w} \quad (4.4)$$

where k_{rw}° is the end-point relative permeability of water at residual oil saturation and k_{ro}° is the end-point relative permeability of oil at initial water saturation.

The mobility ratio has a significant impact on the stability of displacement process. The favorable displacement process is attained when the mobility ratio is low ($M \leq 1$). At this condition the displacement will be in form of a piston like displacement when the porous medium is considered to be homogenous. Therefore this will give a late water break-through and smaller tail production. While a mobility ratio of greater than one ($M > 1$) gives unfavorable displacement process which will cause an early water break-through and long tail production of oil [1].

However the mobility ratio can be modified to be favorable by: i) Increasing the viscosity of the displacing phase (e.g. adding polymer to the injected water). ii) lowering the viscosity of the displaced phase (e.g. thermal injection such as steam injection) or iii) decreasing the end-point relative permeability of displacing phase (e.g. adding polymer to the injected water).

4.2 Capillary Number and Capillary Distribution Curve:

During the immiscible displacement, the capillary force is responsible for trapping oil in the porous medium. A dimensionless ratio called the capillary number, N_c , is introduced which is the ratio of viscous force to capillary force and it is described by the use of Darcy's law as follow:

$$N_c = \frac{\text{Viscous force}}{\text{Capillary force}} = \frac{u \cdot \mu}{\sigma} \quad (4.5)$$

where u is the Darcy's velocity of the displacing fluid, μ is the viscosity of the displacing fluid, and σ is the interfacial tension between the displacing fluid and displaced fluid. Many studies have shown that the residual oil saturation is related to the capillary number and the relationship is described graphically by a capillary distribution curve (CDC) [22,23,56].

A typical plot of capillary distribution curve is shown in figure 4.1 where at low capillary number, N_c , the residual oil saturation, S_{or} , is constant and this is called plateau region. At a critical capillary number a knee occurs in the curve and the residual saturation starts to decrease. Most of the water floods are well onto the plateau region of the capillary distribution curve [1].

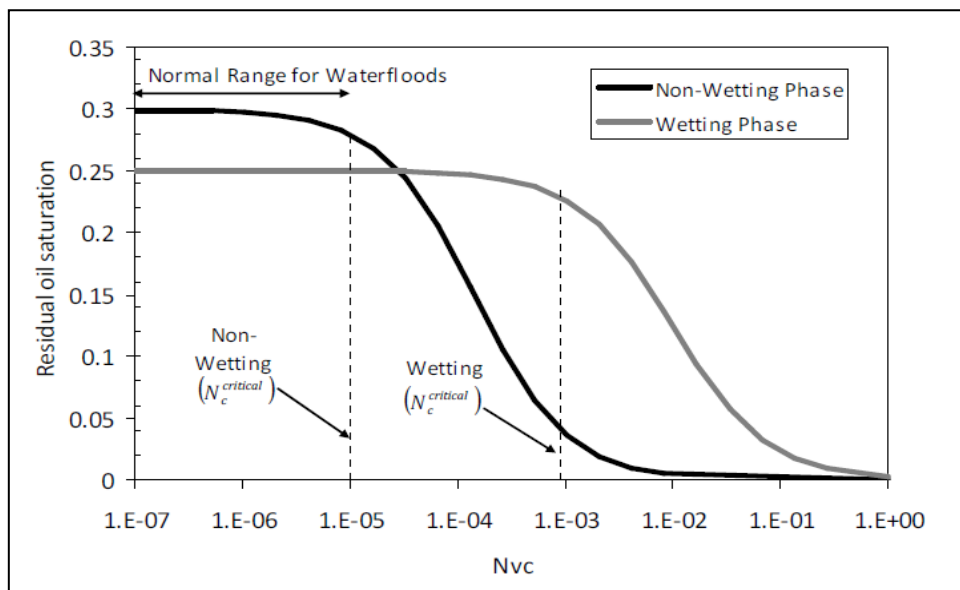


Fig. 4.1: Typical capillary distribution curve (CDC) [56].

The capillary distribution curve is affected by the pore size distribution and wettability of the porous medium. Figure 4.2 shows the effect of the pore size distribution on the curve where as the pore size distribution gets wider, the knee in the capillary distribution curve will be less pronounced.

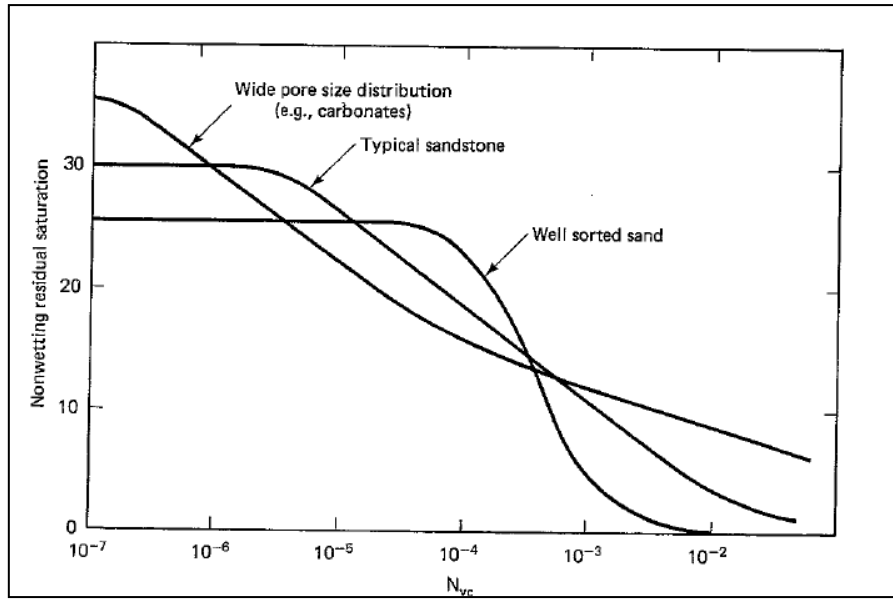


Fig. 4.2 : Effect of the pore size distribution on the CDC curve [56].

A high capillary number, N_c , is required in order to achieve low, S_{or} after water flood. Therefore, to increase the capillary number, one of the following should be done:

- Increase the velocity of the injected fluid. However a large increase in the velocity could cause a formation damage.
- Increase the viscosity of the injected fluid which can be done by adding polymer to the injected fluid.
- Reduce the interfacial tension between the displacing fluid and displaced fluid and this can be done by adding surfactant to the injected fluid.

5. Surfactant:

5.1 Surfactant Properties:

surfactant or surface-active agent is a substance which tends to reduce the surface tensions and interfaces between any two immiscible phases of liquid, allowing for easier spreading. A surfactant molecule is amphiphilic, that has a polar water-soluble portion, or moiety (hydrophilic component) attached to a non-polar insoluble hydrocarbon chain (lipophilic component) as shown in figure 5.1. This dual nature of the surfactant makes it reside at the interface between aqueous and organic phases thereby lowering the interfacial tension.

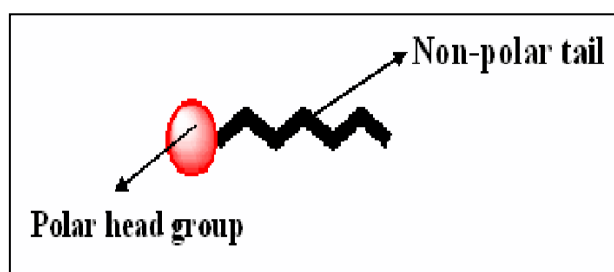


Fig. 5.1 : Illustration of a surfactant molecule by "tadpole" symbol, where the polar head group is the hydrophilic component and the non-polar tail is the lipophilic component.

5.2 Types of Surfactants :

Surfactants are classified into four main groups according to their charge and nature of their polar moieties (i.e. hydrophilic head) as illustrated in figure 5.2 [1,55].

Anionic surfactant contains negatively charged polar head group (e.g. sulphates, sulfonates, phosphates and carboxylates). These surfactants are dissociated in water in an amphiphilic anion and a cation, which is in general an alkaline metal (Na^+ , K^+) or a quaternary ammonium. They are the most used surfactants in the oil recovery because they are soluble in the aqueous phase, efficiently reduce IFT, relatively resistant to retention, stable, and not expensive.

Cationic surfactant contains positively charged polar head group and it is dissociated in water into an amphiphilic cation and an anion, most often of the halogen type. A very large proportion of this class corresponds to nitrogen compounds such as fatty amine salts and quaternary ammoniums, with one or several long chain of the alkyl

type, often coming from natural fatty acids. This type of surfactants have little use due to the high adsorption by the anionic surfaces of interstitial clays.

Non-ionic surfactants are bearing no apparent ionic charge and they do not ionize in aqueous solution because their hydrophilic group is of a non-dissociable type, such as alcohol, phenol, ether, ester, or amide. A large proportion of these nonionic surfactants are made hydrophilic by the presence of a polyethylene glycol chain, obtained by the polycondensation of ethylene oxide. These surfactants are mainly used as co-surfactants.

Amphoteric surfactants also called **Zwitterionic surfactants** contain two charged head groups of different signs e.g. carboxylate as anionic and ammonium as cationic. Some amphoteric surfactants are insensitive to pH, whereas others are cationic at low pH and anionic at high pH, with an amphoteric behavior at intermediate pH. Amphoteric surfactants are generally quite expensive and have not been used in oil industry.





| | | | |
|---|---|--|---|
|  |  |  |  |
| Anionics Sulfonates, sulfates, carboxylates, phosphates, etc. | Cationics quart. Ammonium, pyridinium, imidazolinium, piperidinium, sulfonium, compounds, others | Amphoterics Aminocarboxylic acids, others | Nonionics Alkyl-, Alkyl- aryl-, acyl, acylamino-, acylamino-poly- glycol ethers, polyol ethers, alkanolamides, and others |

Fig. 5.2: Classification of surfactant.

When an anionic surfactant is dissolved in an aqueous phase, molecules of the surfactant start to dissociate into a cation (Na^+) and an anionic monomer. At low concentration the surfactants are in the monomer form and if the concentration is increased, the monomers start to aggregate themselves into more energetically favorable form called micelles with lipophilic parts oriented inward and hydrophilic parts outwards. Further increase in the surfactants concentration causes only increase in the micelles concentration and not in that of monomers as illustrated in figure 5.3.

The concentration at which micelles are formed is called critical micelles concentration (CMC) and it is a characteristic of a particular surfactant. The CMC is typically quit low therefore the surfactant is predominantly in micelle form at nearly all practical concentrations.

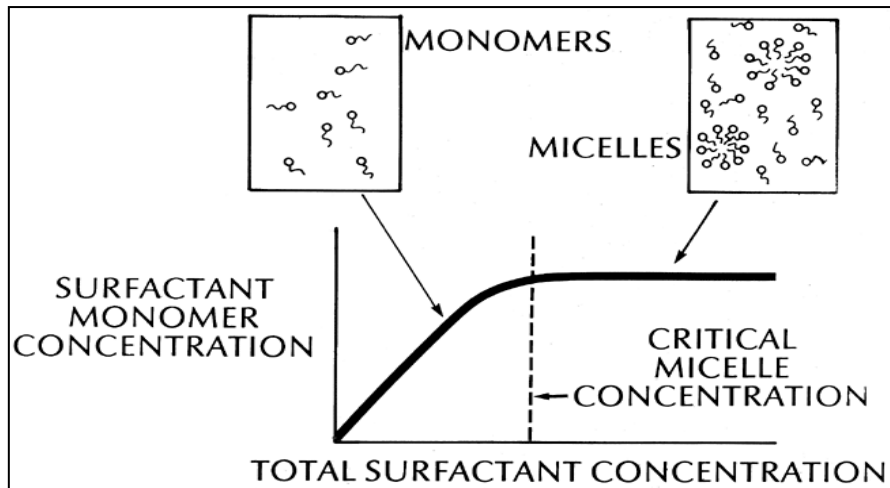


Fig. 5.3: Critical micelles concentration (CMC) [56].

When an aqueous phase with the dissolved surfactant contacts an oleic phase the surfactant, due to its dual nature tends to align at the interface so that the hydrophilic parts (heads) are in the water phase and lipophilic parts (tails) are in the oleic phase. As the concentration of the surfactant increases at the interfaces, the interfacial tension (IFT) between the two phases reduces dramatically. However, this process leads to the alteration of the solubility of the surfactant in the bulk oleic and aqueous phases which, in turn, might affect the interfacial tension. Thus, exploring the properties of surfactant – oil – brine behavior enables us to predict and to optimize the flood process.

5.3 Phase Behavior:

The surfactant – oil – brine (SOB) phase behavior is described by ternary diagrams introduced by Windsor 1954 [57]. In the ternary diagram the temperature and pressure are held constant and each corner of the diagram represents 100% of one of the three components of SOB system.

Salinity of brine has been reported to be the most important factor affecting the surfactant – oil – brine (SOB) behavior. Depending on the brine salinity three different types of phase systems can be formed.

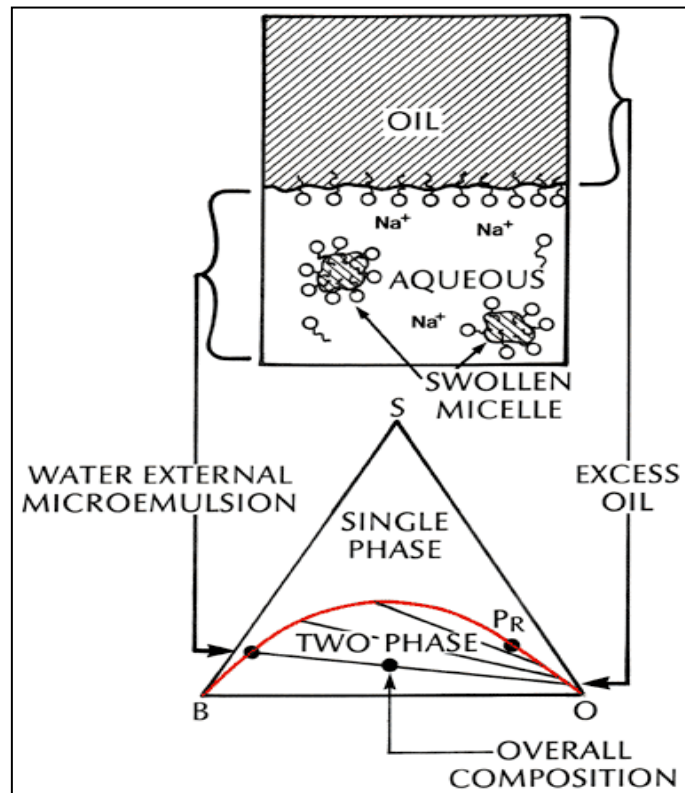


Fig. 5.4: Schematic representation of surfactant type II(-) system.

At low brine salinity, a typical surfactant will exhibit good aqueous phase solubility and poor oil phase solubility. Near the brine-oil boundary there will be an excess oil phase that is essentially pure oil and a water-external microemulsion phase that contains brine, surfactant and some solubilized oil in swollen micelles. This type of phase environment is called a type II(-) system which means that no more than two phases can be formed and the tie line within the two-phase region have a negative slope, see figure 5.4.

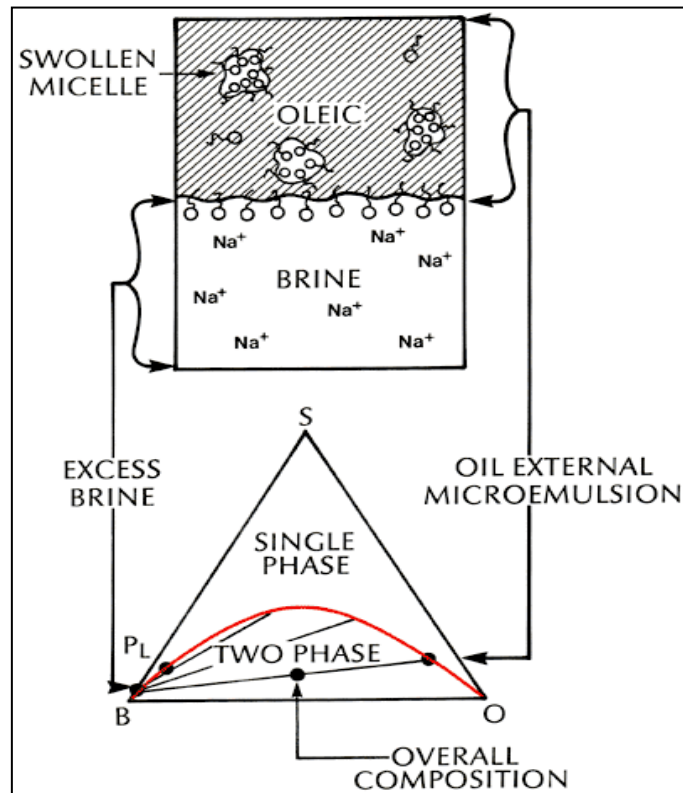


Fig. 5.5 : Schematic representation of surfactant type II(+) system.

At high brine salinity, shown in figure 5.5, the surfactant solubility in the aqueous phase will be drastically reduced due to electrostatic forces. The overall composition within the two phase region will split into an excess brine phase and an oil-external microemulsion phase that contains most of the surfactant and some solubilized brine in inverted swollen micelles. This type of phase environment is called type II(+) system which means no more than two phases can be formed and the tie line within the two phase region have a positive slope.

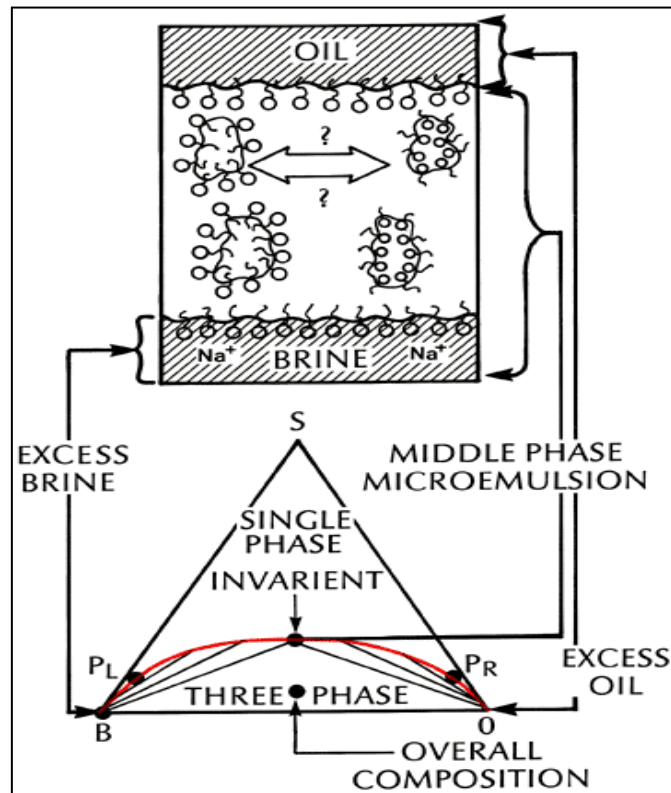


Fig. 5.6: Schematic representation of surfactant type III system.

At a salinities between the two extremes presented so far, there must be a continuous change between type II(-) and II(+) systems. There is no salinity where the solubility of the surfactant in the brine- and oil-rich phases are exactly the same, but there is a range of salinities where a third surfactant rich phase is formed. The mixture splits into excess oil and brine phases and into a microemulsion phase. This environment is called a type III system and it has two IFT's: between oil and microemulsion and between microemulsion and brine, see figure 5.6.

It has been observed in the experiments that type III system gives the lowest interfacial tension which makes this phase environment attractive for oil recovery by surfactant flooding as shown in figure 5.7 [1,8,9,10]. However the surfactant formulation should also consider retention and solubility of surfactant in addition to low interfacial tension. The optimum surfactant system is the system that gives low interfacial tension, low retention in the reservoir rock, and good solubility in the injected brine [58].

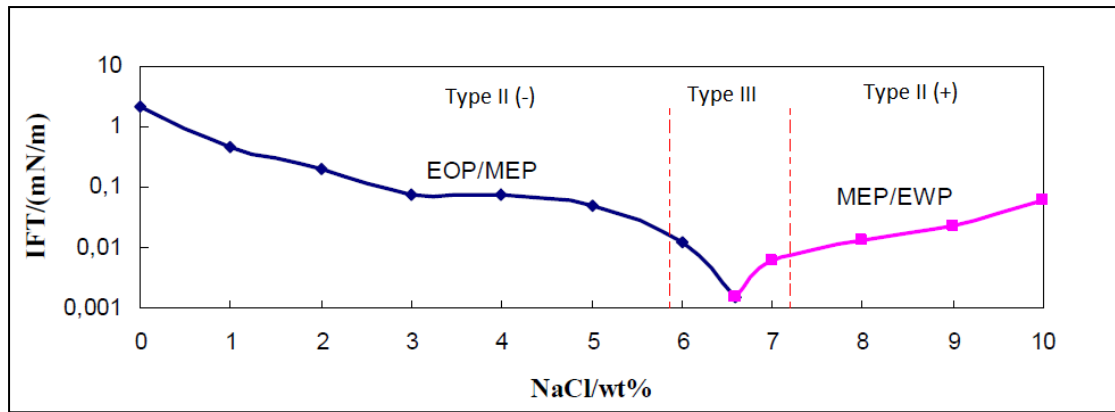


Fig. 5.7 : Interfacial tension versus brine salinity [58].

5.4 Surfactant Retention:

Surfactant retention is one of the most important factors that are affecting the economic feasibility of surfactant flooding. It is referred to the loss of surfactant concentration in the solution to the formation which will lead to less flooding efficiency. Therefore it is significantly important to determine the surfactant retention in order to design an efficient surfactant flooding. There are four mechanisms that cause the surfactant retention which are [1]:

Adsorption:

Surfactant monomers adsorbed through hydrogen bonding and ionically bond with cationic surface sites. At and above the critical micelle concentration, the supply of monomers becomes constant, as does the retention.

Precipitation:

In hard brines, the presence of divalent cations may cause formation of undesirable surfactant-divalent complexes that may precipitate. This will cause a decrease in the surfactant flooding performance.

Ion exchange:

When brine hardness is at level somewhat lower than those required for precipitation, ion exchange reactions between clay surface and the brine/surfactant system may occur which cause surfactant retention.

Phase trapping:

In phase environment of type II(+) and in the presence of oil, the surfactant will reside in the oil-external microemulsion phase. As interfacial tension of this phase

environment is relatively large because it lies above the optimal salinity region, the oil-external microemulsion and the dissolved surfactant can be trapped in the pores.

However, the dominant surfactant retention mechanism of the above mentioned mechanisms for a given application is not obvious. At high salinity and hardness, all mechanisms retain more surfactant. In low salinity brine, surfactant retention by precipitation and phase trapping could be eliminated.

5.5 Surfactant Flooding:

After waterflooding the residual oil trapped in the porous media is mainly due to the capillary force. Adding surfactant to the injected water will reduce the interfacial tension between oil and water resulting in higher capillary number and thus mobilizing the trapped residual oil. The interfacial tension should be lowered enough by surfactant in order to have a significant mobilization of residual oil.

In this study, the surfactant solution was prepared intentionally as type II(-) surfactant system by mixing 1 wt% of active surfactant with low salinity brine (i.e 3000 ppm NaCl brine). The phase behavior of the surfactant system is observed to be constant and gives low interfacial tension to mobilize trapped oil. The low salinity brine was used in preparing the surfactant solution in order to seek low retention of surfactant. low salinity surfactant slug will be injected into the cores as tertiary mode. The size of surfactant slug injected in each core is different and that is done for a purpose of optimizing the surfactant slug size needed to improve oil recovery.

6. Polymer:

Polymer is a substance contains large molecules that are composed of many repeated subunits known as monomers. It can be formed naturally or synthetically and the process of forming polymers is called polymerization. Depending on the structure of the polymer the physical properties of the polymer vary.

6.1 Types of Polymer:

There are two types of polymers that are used most frequently in polymer flooding and they are produced in synthetic or microbial process. These polymers are [1,59] :

- The synthetic polymer polyacrylamide, PAM, or hydrolyzed polyacrylamide, HPAM (with a typical degree of hydrolysis of 30 to 35%). This type of polymer is formed from acrylamide subunits which is combination of carbon, hydrogen, oxygen and nitrogen. The molecular structure is randomly coiled as shown in figure 6.1. The degree of hydrolysis is important with respect to water solubility, viscosity and retention. When degree of hydrolysis is too small that causes polymer to be not water soluble. While too large degree of hydrolysis makes the polymer properties too sensitive to salinity.
- The biopolymer Xanthan, which is produced by polymerization of saccharide molecules in fermentation process with micro-organism *Xanthomonas campestris*. The X-ray diffraction studies suggested that xanthan has a helical and rod-like structure. Figure 6.2 shows the primary chain structure of xanthan. This type of polymer is an efficient viscosifier of water.

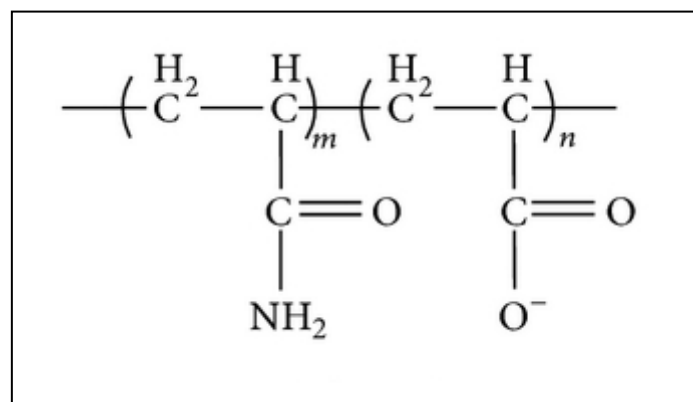


Fig. 6.1: Molecular structure of partially hydrolyzed polyacrylamide (HPAM).

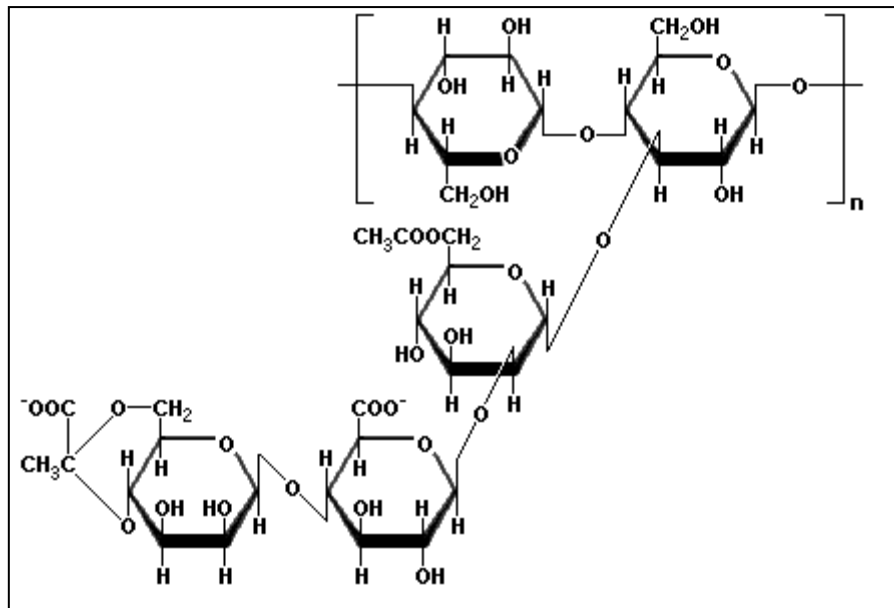


Fig. 6.2 : Molecular structure of Xanthan.

6.2 Rheology:

In polymer flooding, the viscosity of polymer solution is an important property that should be considered. The polymer is added to the injection brine in order to increase brine viscosity, which in turn improve oil-water mobility ratio and leads to increase sweep efficiency. However the polymer solutions, unlike water and oil, have shear-dependent viscosity flow behavior and this type of fluids called non-Newtonian fluid.

The most common model that relates the shear stress and shear rate is the power law model which is given by the expression [1,59]:

$$\mu = m \cdot \dot{\gamma}^{n-1} \quad (6.1)$$

where μ is the viscosity of solution, m is the consistency parameter, $\dot{\gamma}$ is the shear rate, and n is the flow index.

For a Newtonian fluid $n = 1$ and m is simply the constant viscosity, μ . When n is less than one, the viscosity will decrease with increasing shear rate. When n is greater than one, the viscosity increases with increasing shear rate. However many non-Newtonian fluids, like polymer solutions, have Newtonian regime for low shear rates

and very high shear rates, and a pseudoplastic regime in between where the power law is valid. A more satisfactory model that describes the shear regimes of the polymer solution is the Carreau model [1,59]:

$$\frac{\mu - \mu_{\infty}}{\mu_0 - \mu_{\infty}} = [1 + (\lambda \cdot \dot{\gamma})^2]^{(n-1)/2} \quad (6.2)$$

where ;

- μ : viscosity
- μ_0 : zero shear rate viscosity
- μ_{∞} : infinite shear rate viscosity
- λ : relaxation constant
- $\dot{\gamma}$: shear rate
- n : power law exponent ($n < 1$)

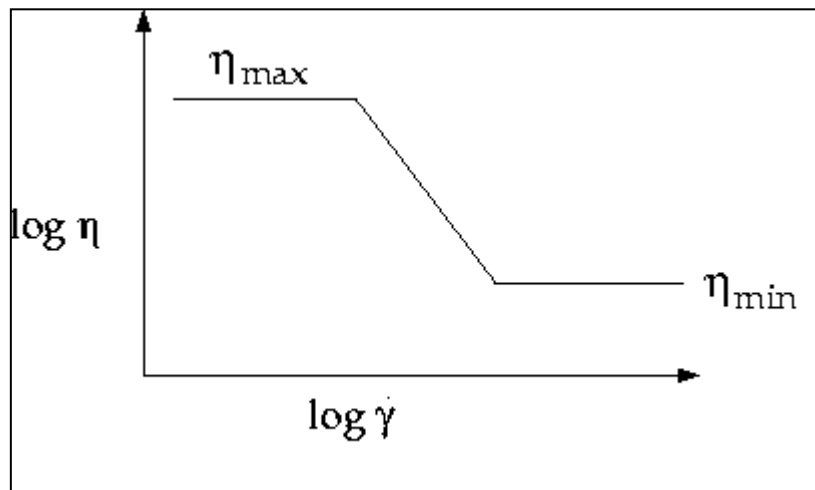


Fig. 6.3 : Illustration of Carreau model for viscosity of polymer.

The polymer solution behavior is explained by Carreau model as follows:

- At low shear rates macromolecules rotate at a constant angular velocity without significant conformation change. Therefore, the viscosity remains constant and the flow regime is Newtonian.
- As shear rate increases, the macromolecules start to deform (PAM / HPAM) and/or orient themselves in the direction of flow (Xanthan) which causes a viscosity reduction.
- At very high shear rates all the macromolecules are oriented in the flow direction and do not affect the viscosity of polymer solution.

6.3 Effect of Polymer Concentration :

Flory-Huggins equation is used to model the relation between the concentration of polymer solution and viscosity as follows [1].

$$\mu_{sol} = \mu_{slov} [1 + a \cdot C_p + b \cdot C_p^2 + \dots \dots \dots] \quad (6.3)$$

where, μ_{sol} is the solution viscosity, μ_{slov} is the brine (solvent) viscosity, C_p is the polymer concentration in the aqueous phase, and a, b etc. are constants. The linear term in the equation accounts for the dilute range where the polymer molecules act independently. The unit used for polymer concentration is g/m^3 of solution and it is approximately same as ppm. Generally the viscosity of polymer solution increases as the concentration increases.

6.4 Apparent Viscosity:

The shear rate in a porous medium is a strong function of rock properties (porosity and permeability) and fluid velocity. An averaged value of the polymer solution viscosity called apparent viscosity should be used in order to predict the performance of polymer flooding. The effective shear rate can be determined based on a simple capillary bundle model using the following equation:

$$\dot{\gamma} = \alpha [4 \cdot u / (8 \cdot \phi \cdot k)^{\frac{1}{2}}] \quad (6.4)$$

where $\dot{\gamma}$ is the effective shear rate, α is a constant related to the pore geometry and type of porous medium.

6.5 Polymer Flooding:

In polymer flooding, polymer is mixed with the injected water in order to increase the viscosity of the water therefore making the mobility ratio between oil and water more favorable. In consequence this will improve the macroscopic sweep efficiency. In principle, as the viscosity of the injected water, μ_w , increases, the capillary number, N_c , increases too and therefore gives lower oil residual, S_{or} as described by equation 4.5. However, the reduction is small since it takes a major change of N_c (order of magnitudes) in order to affect the S_{or} significantly [1].

Polymer flooding usually used for high viscous oil reservoirs to improve the mobility ratio, or for heterogeneous reservoirs to decrease the permeability of high permeable zones and divert flooding into low permeable zones. In addition, polymers may be used for near-well treatment in order to gain more favorable water-cut development.

In this thesis, the partially hydrolysed polyacrylamide (HPAM) polymer has been used for polymer slug injection. The concentration of the injected polymer solution was chosen based on the viscosity measurements. In the tertiary mode a polymer slug was injected into the core directly after surfactant slug in order to have a more stable displacement behind surfactant and then followed by low salinity water flood. At the end of the tertiary low salinity slugs injection when the oil production is ceased, a polymer slug of higher concentration was injected then followed by low salinity water flood.

7. Experimental Apparatus and Procedures:

The experimental equipments used in this study were to analyze fluids properties and to perform the displacement experiments. The experimental apparatus and displacement procedures done on the Berea sandstone cores are described in this section.

7.1 Experimental Apparatus:

7.1.1 Densitometer:

An Anton Paar K.G. DMA 60 density meter and a DMA 602 density-measuring cell were used to measure density of the fluids used in the experiments. The measure cell was connected to a water bath thermo stated by a Heto Birkerød temperature controller and the temperature in this bath was checked with a Fluke 2180A digital thermometer.

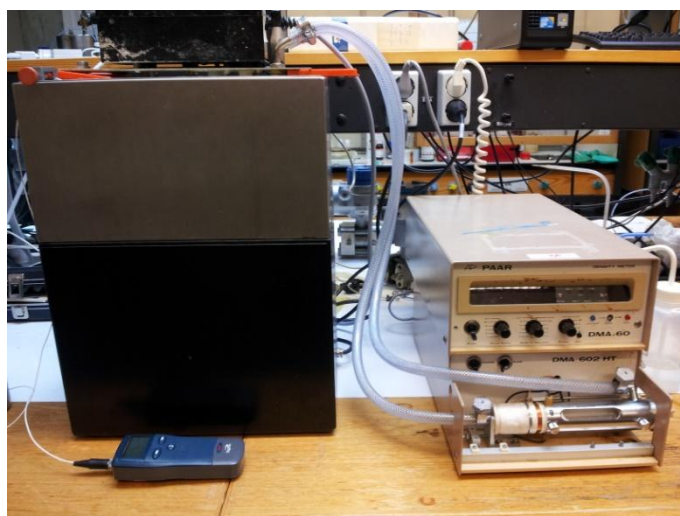


Fig. 7.1: An Anton Paar K.G. DMA 60 density meter and a Heto Birkerød temperature controller.

The density meter consists of a hollow U-formed glass tube (measuring cell), where fluids can be injected and an electromagnet which forces harmonic waves (oscillations) to occur within the tube. The frequency of the measuring cell is a function of the density of the fluid inside it. The density meter measures the time for pre-set number of cycles. When the density of the solvent is known the density of the solution is given by:

$$\rho - \rho^* = \frac{1}{A}(T^2 - T^{*2}) \quad (7.1)$$

Where;

- T : the time period of solution (s)
T* : the time period of pure solvent (s)
A : apparatus constant (g/cm³)
ρ : density of solution (g/cm³)
ρ* : density of the pure solvent (g/cm³)

The apparatus constant, A, can be found by measuring T for two fluids with known density. Distilled water and air were used in this experiments to measure the apparatus constant. The density of air as function of temperature, pressure and relative air humidity is given by following equation:

$$\rho_{air} = 0.46464 * \frac{B - 0.08987 * F}{T} . 10^{-3} \quad (7.2)$$

where;

- ρ_{air} : density of air (g/cm³),
T : working temperature (K),
B : atmospheric air pressure (mmHg),
F : relative humidity of air (%).

The density of water at a given temperature at atmospheric pressure were taken from the work of Kell [60]. The apparatus constant depends on room temperature and therefore it should be measured for each temperature used.

The density of solution was measured by carefully injecting the solution into the hollow U-tube with a sterile syringe. The tube holds approximately 1 ml and around 3 ml was injected into the tube so that the tube was flushed with solution. The syringe was held in position and the other end of the tube was gently closed with a rubber plug. After approximately 5 minutes and when the temperature was constant, the time period was recorded. Once the measurements of one fluid is done the tube was cleaned and dried with pressurized air to conduct a good measurement for another sample. The uncertainty of the measurements was estimated to be ± 10⁻⁴ g/ml with variation in the thermostatic water bath temperature of ± 0.2 C°.

7.1.2 Rheometer:

Viscosity measurements for all fluids used in the experiments were performed using Kinexus rheometer from Malvern Instruments Ltd. The Kinexus rheometer is an advanced rotational platform which coupled with a software system called rSpace based on one flexible interface that can be configured for the user's rheological requirements. At the heart of rSpace is the rFinder search engine which allows the user to locate information and appropriate tests relevant to a particular application[61].



Fig. 7.2: Kinexus rheometer form Malvern Instruments Ltd.

The rheometer is equipped with different types of cartridge and geometry. In this study, the double gap geometry was used to measure viscosity of brines, oils and surfactant solution and the measurements were conducted at single shear rate of 100 s^{-1} . The cone and plate geometry was used for polymer solutions viscosity measurements and the measurements were conducted at different shear rates from 0 to 1000 s^{-1} . The temperature during the measurements is controlled by heat exchangers connected to the rheometer.

The uncertainty of the measurements was estimated to be approximately 5% of the absolute value obtained. The fluid samples used for measurements were checked visibly to be free from foam and air bubbles.

7.1.3 Spinning Drop Tensiometer:

The interfacial tension of the surfactant system used in the experiments were measured using A SITE 100 spinning drop tensiometer from Krüss Company. The spinning drop method is one of the methods used to measure IFT and it is founded based on the principles of balancing the centrifugal forces against interfacial attractive forces. This method is preferred for accurate measurements of IFT below 10^{-2} mN/m.



Fig.7.3 : SITE 100 spinning drop tensiometer.

The measurements are carried out in a rotating horizontal tube filled with a denser fluid. A drop of less dense liquid is placed inside the tube and a centrifugal force is created by rotating the horizontal tube. This force will push the densest fluid toward the wall of the tube while the drop of the less dense liquid will start to deform into an elongated shape. The elongation stops when the centrifugal force and the interfacial tension between the fluids are balanced.

The applied rotational speed should be high enough so that the length of the droplet will be at least 3 times greater than its radius therefore its shape can be approximated as a straight cylindrical shape. Under this condition the following expression can be used to measure the IFT:

$$\sigma = \frac{\Delta\rho \omega^2 R^3}{4} \quad (7.3)$$

where; σ is the IFT between the fluids, $\Delta\rho$ is the density difference between the used fluids, ω is the rotational speed and R is the droplet radius.

The SITE 100 spinning drop tensiometer measures the interfacial tension down to 10^{-6} mN/m and it uses DSA-2 software that is connected to a camera to analyze the drop diameter.

In this study, the interfacial tension of two types of surfactants were measured. The surfactant with lower interfacial tension was selected to prepare the surfactant solution used for the core flooding experiments. All the interfacial tension measurements were conducted at temperature of 23 C° and a water bath was used to control the temperature during the experiments. The tube was filled with the surfactant solution and a needle with a diameter of 0.8 mm was used to calibrate the DSA-2 software. After calibration, the tube was rotated to get rid of the gas bubbles that could be trapped at the ends of the tube and more surfactant solution was added. Then, a drop of the oil was injected to the tube using a micro-syringe and a rotational speed of 2400-4000 rpm was set for the tube.

A continuous measuring of the IFT with different spinning rate was recorded and the measurement of each sample was repeated to double check the obtained values. The uncertainty of the measurements is estimated to be 20 % of the obtained value. However in some samples it was difficult to get rid of gas phase or a clear water phase from the oil drop and in some cases the software could not find the oil drop for measurements.

7.1.4 Core Holder:

Hassler-type core holder was used to mount the cores and conduct the experiments. This type of core holder is routinely used for gas and liquid permeability and other core flooding experiments. Figure 7.4 illustrates the components of the Hassler-type core holder.

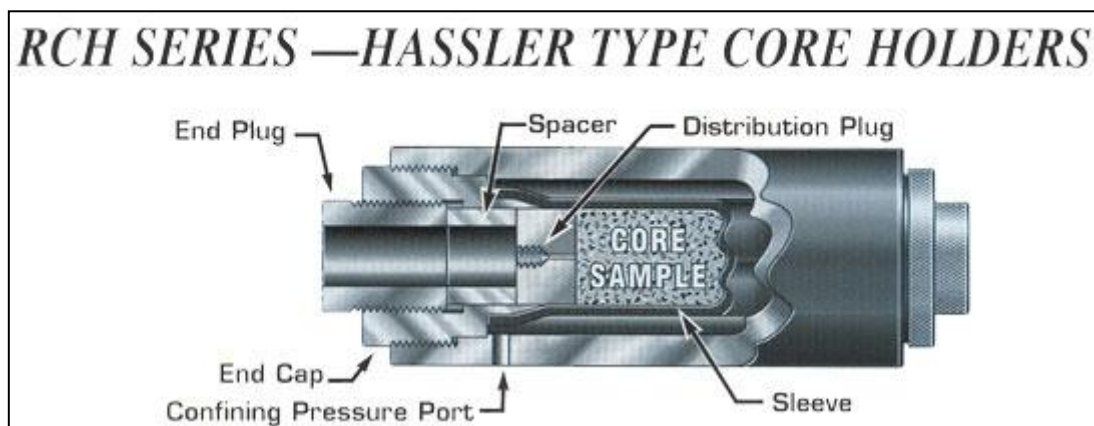


Fig.7.4: Hassler-type core holder.

The core first placed in a proper rubber sleeve and two dead ends were added and tightened to the rubber sleeve by metal wire. Then the core mounted into the core holder and the end plug with end cap and spacer was sealed properly. A confining pressure was applied by filling the space between the sleeve and the core holder with a liquid injected through the confining pressure port. The confining pressure is required to prevent fluids from bypassing core during running experiments. In this study, a confining pressure of 25 bar was applied to all cores used in the experiments.

7.1.5 Fraction Collector :

A Foxy Jr. fraction collector was used to collect effluent fluid samples. It can operate at different collection programs depending on the user requirements. In this experiments the faction collector was set to operate by time so, that for each set of time the fraction collector will change the tube that receives fluid to new tube. Test tubes that can hold up to 14 ml were used and the time for fraction collector was set so that approximately 3 , 5 or 8 ml were collected in each test tube depending on the injection rate. A back-pressure regulator was used in this study to prevent air bubbles in the system , however it could cause variation in the fluid volume of the tubes. Therefore, each tube had to be measured separately to find the exact volume.



Fig.7.5: Foxy Jr. fraction collector.

7.1.6 Pumps, Cylinders and Pressure Transducer:

Edwards RV3 vacuum pump was used to evacuate the cores before saturation with brine and measuring porosity. The pump has capacity to eject air from the core down to 750 mTorr. A Quizix computer-aided pump was used to measure the porosity by saturating the cores with synthetic sea water brine. In the displacement experiments Pharmacia LKB P-500 pump was used to inject fluids and a piston cylinder was placed between the pump and the core to distribute the fluids during the experiments.

A Fuji electric FCX-FKC differential pressure transducer was used to measure the pressure drop across the core. In order to prevent the development of air bubbles in the system, a back pressure regulator was used.



Fig.7.6: Pharmacia LKB P-500 pump.



Fig.7.7: Left picture: Piston cylinder. Middle picture: Fuji electric FCX-FKC differential pressure transducer. Right picture: Back pressure regulator.

7.1.7 Core Material:

The cores used in this study were Berea sandstone cores. Over than 40 years Berea sandstone cores have been widely used in petroleum industry as a model rock to investigate and understand the fluid flow and oil recovery mechanisms. The Berea sandstone is a sedimentary rock and it is composed mainly of quartz with other types of minerals in different content percent such as chlorite, kaolinite, illite, and smectite. The use of Berea sandstone rather than reservoir material in the core flooding experiments is attractive because it is inexpensive, relatively homogeneous, and commercially available [39,40].

7.2 Experimental Procedure:

In this section, the procedures of the experiments performed are described. The experimental setup and the different types of the flooding process carried on the cores used are explained.

7.2.1 Core Preparation:

Berea sandstone block was used to cut the six cores used in this study to desire length and diameter. The cores were put in the oven at temperature of 90 C° for couple of days to dry them properly and then the length and diameter of the cores were measured. The dead ends volumes were measured before mounting the core into the core holder to make correction for later calculations. Then a confining pressure of about 27 bar was applied to the core and the core holder was checked to make sure there is no leakage.

7.2.2 Pore Volume and Porosity Measurement :

The core holder was connected to a vacuum pump from one end and a vacuum pressure gage from the other end. The vacuum pump was turned on and the core was evacuated until the core pressure dropped below 1 mbar, then the pump was switched off and the pressure reading was checked for stabilization around half an hour to make sure there is no leakage in the core holder. After that the core was connected to a Quizix computer-aided pump through a piston cylinder filled with synthetic sea water. Before starting saturating the core, the pump was set to hold a pressure of 5 bars which will be the pressure in the cylinder and lines as well. After the pressure was stabilized in the system, the inlet valve of the core-holder was opened and the brine was sucked into the core. The pump has to deliver more synthetic sea water to fill the

pore volume of the core and to maintain the pressure of 5 bar. This was maintained until there was almost no change in the cumulative volume of added brine which represents the pore volume (V_p), of the core used. The bulk volume (V_b) of the core calculated based on the geometrical measurements done during the core preparation. The porosity of the core then measured using equation 2.1.

The core was put aside for one week after saturation to allow synthetic sea water to reach the ionic equilibrium with the core.

7.2.3 Experimental Setup :

The fundamental experimental setup for the displacement experiments in this study is shown in figure 7.8 below.

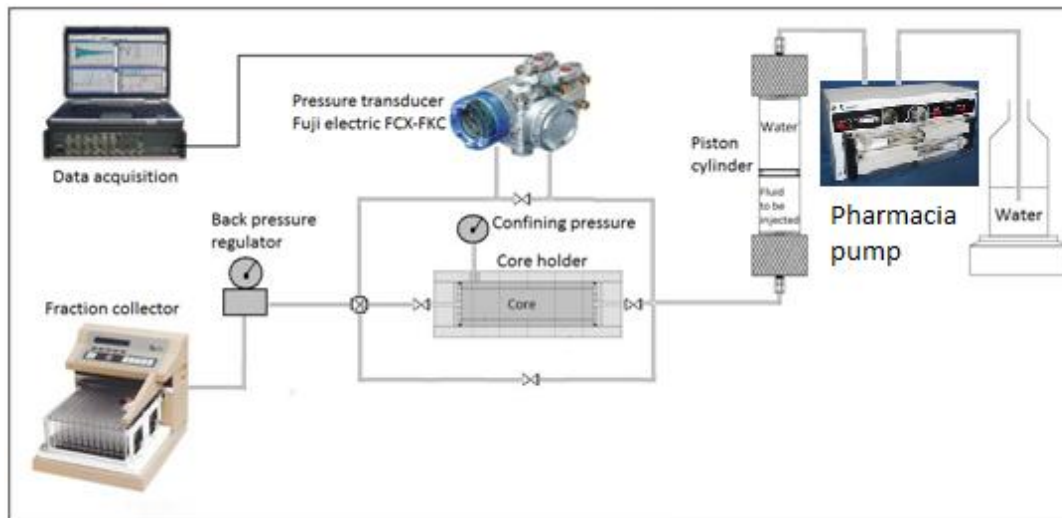


Fig.7.8: Experimental set-up.

7.2.4 Permeability Measurements :

The permeability is measured using the Darcy law equation and the experimental set-up for measurements is as shown in figure 7.8 except the fraction collector was replaced by glass beaker. For the absolute permeability, the core was first flushed with 2 PV of synthetic sea water before conducting the permeability measurements. After that the differential pressure across the core was recorded for five different flow rates applied for injection. The permeability is calculated by finding the slope of the relationship of the flow rate versus the differential pressure and by knowing the viscosity of the injected brine and the sizes of the core.

The effective and relative permeability were measured in this study using the same procedure and the measurements were conducted before aging, after aging, after low salinity flooding and after the surfactant and polymer flooding.

7.2.5 Drainage:

Primary drainage process for the cores was established by using Marcol 152 which is a high viscous oil. The process was done with the core oriented vertically to make use of the gravitational force. The injection started with slow flow rate of 0.1 ml/min and the drained sea water was collected in graduated flask to measure the water saturation. The injection rate was increased stepwise when water production was ceased and the direction of the flow was reversed to reduce the end-effect. The results of the drainage process are summarized in Appendix A.

After the initial water saturation was achieved, the end-point effective permeability of Marcol 152 was conducted. Then 3 PV of filtered North Sea crude oil or diluted crude oil was used to displace Marcol 152 in the core and the displacement process started with slow rate which was increased stepwise and the direction of the injection was reversed. Also the end-point effective permeability was measured afterward.

7.2.6 Aging:

After the primary drainage process the cores were aged in a heating cabinet for about 4 weeks at a temperature of $110 \pm 1 \text{ C}^\circ$ to alter the wettability of the cores. During the aging time, a fresh crude oil was injected to the cores to replace the old crude oil and the displacement was done either by continuous injection of crude oil at a very slow flow rate or by injecting 1 PV of crude oil after each week. Back pressure regulator of 5 bars was used to control the expansion and evaporation of light components of the crude oil due to the high temperature used.

Cores A3, A4, A5, and A6 were aged for 4 weeks while cores A1 and A2 were not aged to observe the effect of aging in the performance of displacement experiments.

After aging, 3 PV of diluted North Sea crude oil which contains 40% of octane was used to flush the cores and displace the crude oil. The diluted crude oil was used in order to have a better mobility ratio since it has a viscosity of about 3 cp. The effective permeability measurements of the cores after flushing with diluted crude oil was conducted and compared with the measurements before aging to observe the wettability alteration.

7.2.7 Synthetic Sea Water and Low Salinity Waterflooding:

The effect of reducing salinity of the injected brine was investigated in the unaged cores in both secondary and tertiary mode. The synthetic sea water was injected first in core A1 as secondary mode then followed by 22 times diluted sea water as tertiary mode. Core A2 was flooded directly from the beginning by 22 times diluted sea water. The aged cores A3, A4, A5, and A6 was flooded by 3000 ppm NaCl brine (low salinity brine) as secondary injection. During the flooding experiments all the cores were subjected to a confining pressure of 25 bar and the experimental set-up for flooding process is as shown in figure 7.8. Before starting the flooding in each core the system was pressurized to 8 bars by using the back pressure regulator to prevent the development of air bubbles.

The flooding process started with slow flow rate of 0.1 ml/min in order to avoid the fingering displacement that causes the early water break-through. When the oil production was stopped, the injection was continued at same rate for 2 more pore volume. After that the flow rate was increased in order to observe the effect of increasing the viscous force in the oil recovery. Also the injection continued for almost 2 pore volume after the oil production was ceased. The flow rates used in the experiments were 0.1, 0.5, and 1 ml/min.

During the flooding, samples of production were collected using the fraction collector. The volume of oil and water produced in each tube was measured volumetrically and the calculations of the production profiles and saturations were carried out. The pressure profile during the displacement was continuously monitored.

After flooding the unaged cores A1 and A2 with synthetic sea water and 22 times diluted synthetic sea water. The cores were flooded by 3000 ppm NaCl brine (low salinity brine) to replace the previous brine. This was done to use the unaged cores for low salinity surfactant and polymer slugs injection and compare their recoveries with the aged cores.

7.2.8 Low Salinity Surfactant and Polymer Slugs Injection:

The tertiary low salinity surfactant and polymer slugs injection was performed in all six cores used in this study. However the size of the slugs injected was varied. In the aged cores the different size of surfactant slug injected was in order to determine the optimum slug size that gives high oil recovery. The unaged cores were flooded with same surfactant slug size and compared with the aged core to determine the effect of wettability. The polymer slug was injected directly after the surfactant slug in order to maintain a stable displacement behind the surfactant. Table 7.1 shows the slug size injected in each core. The surfactant solution used was made of 1 wt% of active

surfactant mixed with low salinity brine (i.e 3000 ppm NaCl brine). The type of polymer used was partially hydrolysed polyacrylamide (HPAM) with concentration of 300 ppm.

Table 7.1: The sizes of the surfactant and polymer slugs injected in each core.

| Core ID | Surfactant slug size [PV] | Polymer slug size [PV] |
|---------|---------------------------|------------------------|
| A1* | 1 | 1 |
| A2* | 1 | 1 |
| A3 | 0.3 | 0.5 |
| A4 | 0.5 | 1 |
| A5 | 1 | 1 |
| A6 | 2 | 1 |

* unaged cores 1

After the injection of the slugs, the cores were flooded with continuous low salinity brine until the oil production was ceased. The variation in the slug size injected in the aged cores was in order to investigate the optimum slug size injection. The unaged cores A1 and A2 was flooded with same slug size as the aged core A5 in order to investigate the effect of wettability in the performance of oil recovery.

The flow rate during the flooding processes was set to 0.1 ml/min and production samples were collected by fraction collector. The experimental setup is as shown in figure 7.8. The production profiles and saturation were calculated and the pressure drop was continuously monitored during the flooding processes.

7.2.9 Low Salinity Polymer Slug Injection:

After low salinity surfactant and polymer slug injection, all the six cores were flooded by a slug of polymer with higher concentration. This was in order to observe if additional oil recovery can be obtained from the cores. The slug size in all the core was 1 pore volume and the concentration of the HPAM polymer injected was 600 ppm. A continuous injection of low salinity brine (3000 ppm NaCl) was preformed after the polymer slug until the oil production was ceased. The flow rate was set to 0.1 ml/min during the flooding process and production samples were collected to calculate the production profile and saturations. The pressure drop was continuously monitored during the flooding processes.

8. Preparation of Samples:

The fluid samples used in this study are described and presented in this section. In addition the chemical composition and the preparation procedures are explained for each fluid. These fluids were either used for displacement experiments or for other measurement during the study.

8.1 Synthetic Sea Water (SSW):

All the cores were initially saturated with synthetic sea water. The chemical composition of the synthetic sea water is listed in table 8.1. The brine was prepared by mixing distilled water and the salts. The brine was put on a magnetic stirrer to dissolve the salts properly and then filtrated using 0.45 μm vacuum filter.

Table 8.1 : Chemical composition of synthetic sea water

| Salt | [g/kg solution] | Producer |
|---------------------------------------|-----------------|-----------------|
| NaCl | 24.886 | Sigma - Aldrich |
| CaCl ₂ · 2H ₂ O | 1.722 | Riedel-de Haen |
| MgCl ₂ · 6H ₂ O | 11.118 | Sigma - Aldrich |
| NaHCO ₃ | 0.192 | Fluka |
| Na ₂ SO ₄ | 4.054 | Riedel-de Haen |
| KCl | 0.672 | Fluka |

TDS: 42,656 ppm

The synthetic sea water was diluted 22 times to make low salinity brine used for injection in the unaged cores. The diluted synthetic sea water has TDS = 1939 ppm.

8.2 Low Salinity Water (LS):

The low salinity water used for secondary waterflooding in the aged cores was made by mixing distilled water and sodium chloride (NaCl). The brine contains 0.30 wt% of NaCl and the composition is listed in table 8.2:

Table 8.2: Chemical composition of low salinity water

| Salt | [g/kg solution] | Producer |
|------|-----------------|-----------------|
| NaCl | 3.000 | Sigma – Aldrich |

The brine made was put on a magnetic stirrer to dissolve the salts properly and then filtrated using 0.45 μm vacuum filter.

8.3 Oils:

Three types of the oils were used in this study either for displacement process or for aging. These oils are viscous mineral oil called Marcol 152, North Sea crude oil, and diluted North Sea crude oil. The diluted North Sea crude oil made of 40 wt% of octane (produced by Sigma – Aldrich Co.) and 60 wt% of North Sea crude oil. The addition of octane to the North Sea crude oil was in order to reduce its viscosity for better mobility ratio during the core flooding experiments.

First Marcol 152 was used for drainage process to establish initial water saturation, S_{wi} , in the cores. Then it was miscible replaced by injecting North Sea crude oil into the cores. After that the cores were aged with North Sea crude oil in order to alter the wettability of the cores during the aging. After the aging, the North Sea crude oil was also miscible replaced by diluted crude oil to get lower oil viscosity inside the cores before starting the flooding experiments.

The North Sea crude oil was filtrated using 0.5 μm in-line filter before it was used for either injection or making the diluted North Sea crude oil. The filtration was done to remove any unwanted particles and/or wax contents.

8.4 Surfactants Solution:

Two types of surfactants were used in this study they are both of type sodium alkyl benzene sulphonate from Huntsman. They are named XOF 25s and XOF 26s and table 8.3. shows the weight percent of active matter in each of surfactant mixture.

Table 8.3: The anionic active matter in each of surfactant mixture

| Surfactant ID | XOF 25s | XOF 26s |
|---------------------------|---------|---------|
| Anionic active matter (%) | 25.6 % | 24.5 % |

The surfactants solution were made of 1 wt% of active surfactant mixed with low salinity brine (i.e 3000 ppm NaCl brine). The solutions were put on the magnetic stirrer for 2 hours to homogenously mix the surfactant before using them for samples preparation. Sample of each surfactant solution was equilibrated with diluted crude oil in 1:1 ratio before conducting the interfacial tension measurements.

Based on the interfacial tension measurements the surfactant that gave the lowest value was chosen for tertiary low salinity surfactant slug injection.

8.5 Polymer Solution:

The type of polymer used in this study is the partially hydrolysed polyacrylamide (HPAM). The preparation of polymer solution took 2 days to be completed where first the polymer stock solution was prepared then diluted polymer solutions to the desired concentrations were made from the stock solution.

The stock solution was prepared by the following steps:

- 540.00 g of pre-filtered 0.30 wt% NaCl brine was added to 800 ml beaker.
- The beaker was placed on a magnetic stirrer and the speed was set to create a vortex extends about 75 % towards the bottom.
- 3.000 g of HPAM polymer weighted in a tray was added to the brine by carefully sprinkling the polymer powder just below the vortex shoulder.
- The speed of the magnetic stirrer was reduced to the lowest speed where the polymer particles still float in the solution and the beaker was covered with perforated parafilm.
- The solution was left on the magnetic stirrer overnight and then transferred to Duran flask with a cork and sealed with parafilm.

The HPAM powder activity is approximately 90 % thus the final concentration in ppm is calculated using the following equation:

$$C_{polymer} = 10^6 \times W_{polymer} \times 0.90 / (W_{polymer} + W_{brine}) \quad (8.1)$$

The diluted polymer solutions were prepared using the following steps:

- A coated magnet was put in a Duran flask and then about half of the 0.30 wt% of NaCl brine was added.
- Polymer from the stock solution was added by weight to the Duran flask.
- The rest of the brine was added so that the concentration of the polymer matches the final concentration wanted.
- The solution was put on a magnetic stirrer at low speed (< 100 rpm) then sealed by cork and parafilm and left stand overnight.
- The solution then filtrated using 40 μ m filter and vacuum apparatus before using it for viscosity measurements and flooding process.

The most important aspects should be avoided for polymer solution are shear degradation, unnecessary exposition to air, iron contamination, sample homogeneity and creation of microgels. Table 8.4 shows the concentrations of the polymer stock solution and the diluted polymer solutions made in this study.

Table 8.4 : Concentration of polymer solutions

| Polymer solution | Concentration [ppm] |
|--------------------------|---------------------|
| Stock polymer solution | 5000 |
| Diluted polymer solution | 1000 |
| Diluted polymer solution | 600 |
| Diluted polymer solution | 300 |
| Diluted polymer solution | 100 |

The viscosity measurements were conducted in all the polymer solutions made and the solution that gives the desired viscosity for flooding was chosen for tertiary slug injection.

9. Results and Discussion:

In this chapter, the main results of the different measurements and displacement experiments done during this study are presented and discussed. First the measured properties of different liquids used or prepared are listed and analyzed and these measured properties are density, viscosity, and interfacial tension. The surfactant used for the tertiary injection was selected based on the interfacial tension measurements while the polymer concentration was chosen based on the viscosity measurements.

Then the basic physical and petrophysical properties of the six Berea sandstone cores used for displacements experiments are listed and discussed. These cores are designated as A1, A2, A3, A4, A5, and A6. The cores A1 and A2 have not been aged while the other four cores were aged for almost four weeks at 110 C°.

Core A1 was flooded first with synthetic sea water then followed by 22 times diluted synthetic sea water in order to observe the effect of the low salinity waterflooding as tertiary mode. While core A2 was flooded directly by the 22 times diluted synthetic sea water as secondary mode and compared with core A1.

The aged cores were flooded by low salinity brine which is 3000 ppm NaCl brine and the oil recovery and pressure profiles are shown. The recovery parameters and wettability state of the cores are discussed and compared with the unaged cores to determine the effect of aging and low salinity waterflooding.

A combined process of low salinity surfactant and polymer slugs injection was investigated in this study to determine its effectiveness as tertiary injection mode in all six cores. The procedure of tertiary injection was carried out by injecting a surfactant slug followed by a polymer slug and then a continuous injection of low salinity brine. The aged cores has been flooded with a different size of surfactant slug with constant concentration in order to determine the optimum slug size that gives high oil recovery. The polymer slug was injected directly after the surfactant slug in order to maintain a stable displacement behind the surfactant. The production profile and parameters of the cores are discussed and compared.

The cores were flooded at the end by 1 PV of low salinity polymer with higher concentration followed by continuous low salinity brine injection to observe any further production. The capillary number for each type of flood is calculated and listed for each core.

9.1 Measurements of Liquids Properties :

In this section, the measured properties of the fluids used in this study are presented and discussed. The fluids were used during the study either for displacement experiments or for analyzing purposes.

9.1.1 Density:

The density measurements of the fluids used in this study are listed in Appendix B. The measurements for brines and oils were conducted at three different temperatures while for the two surfactant solutions prepared it was carried out at a temperature of 23 C°. The results show that the density of brines and oils decreases with increase in the temperature.

9.1.2 Viscosity:

The viscosity measurements of brines and types of oil used in this study were conducted at four different temperature and the results are shown in Appendix C. The uncertainty of the measurements was estimated to be approximately 5% of the absolute value obtained.

The fluid viscosity largely depends on the temperature and the results show that the viscosity of brines and oils used decreased with increasing temperature. The displacement experiments in this study were conducted at room temperature and the measured temperatures during the experiments were between 22 and 24 C°. The plots of viscosity measured at different temperature are shown also in Appendix C.

The viscosity measurements of the surfactant and polymer solutions were conducted at temperature of 23 C° and they are shown in the following table. For polymer solutions the viscosity were measured at different shear rates from 0 to 1000 s⁻¹ and value of viscosity at 100 s⁻¹ was used. The plots of polymer solutions viscosity at different shear rates are shown in Appendix C.

Table 9.1: Viscosity of surfactant and polymer solutions at 23 C° and $\dot{\gamma} = 100\text{s}^{-1}$.

| Fluid | Viscosity [mPa.s] |
|-------------------------------|-------------------|
| Surfactant solution [XOF 26s] | 1.13 ± 0.06 |
| Polymer stock solution | 84.23 ± 4.21 |
| 1000 ppm polymer solution | 11.04 ± 0.55 |
| 600 ppm polymer solution | 6.72 ± 0.34 |
| 300 ppm polymer solution | 3.57 ± 0.18 |
| 100 ppm polymer solution | 1.77 ± 0.09 |

The concentration of the polymer solution used for polymer slug injection in the tertiary mode was chosen based on the viscosity measurements in table 9.1. In the tertiary low salinity surfactant and polymer slugs injection, the concentration chosen for polymer slug was 300 ppm because its viscosity is close to the viscosity of the diluted crude oil, therefore the viscosity ratio will be around 1.

In the low salinity polymer slug injection which is the last flooding process, the concentration chosen for polymer slug was 600 ppm and that was in order to observe any additional oil can be produced by further improving in the viscosity ratio between oil and polymer solution.

9.1.3 Interfacial Tension Measurements:

The interfacial tension measurements of the two surfactant solutions prepared in this study were carried out at temperature of 23 C°. Figure 9.1 and 9.2 show the measurements of equilibrated surfactant solutions with diluted crude oil for two weeks and the average values of the obtained interfacial tensions are listed in table 9.2. The uncertainty of the measurements is estimated to be 20 % of the obtained value.

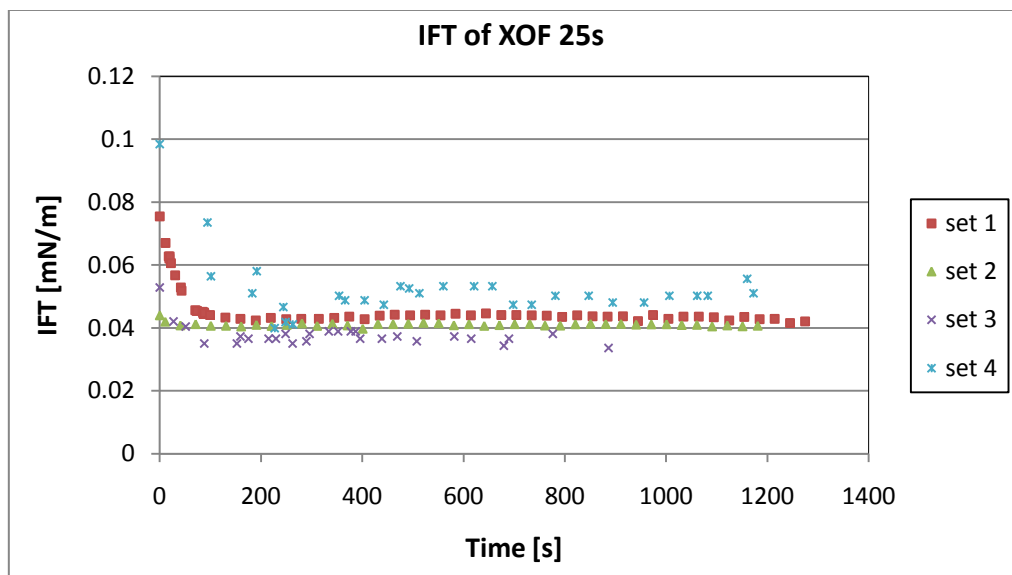


Fig. 9.1: IFT measurements of equilibrated XOF 25s surfactant solution with diluted crude oil.

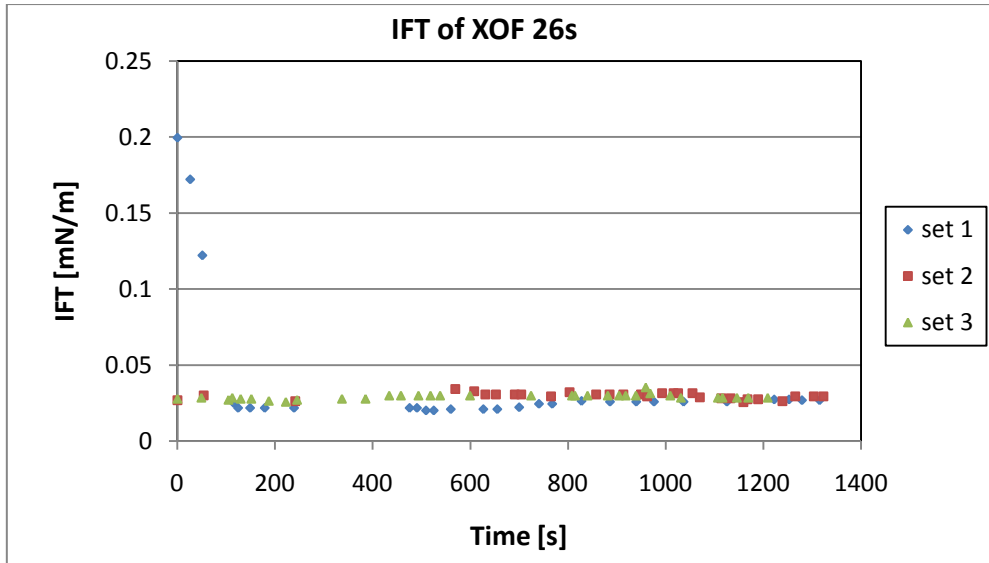


Fig. 9.2 : IFT measurements of equilibrated XOF 26s surfactant solution with diluted crude oil.

Table 9.2: Average value of IFT measurements for each surfactant solution.

| Surfactant | XOF 25s | XOF 26s |
|-----------------------------------|-------------------|-------------------|
| IFT of Equilibrated sample [mN/m] | 0.045 ± 0.009 | 0.028 ± 0.006 |

The IFT measurements of the equilibrated surfactant solutions started to stabilize after almost 2 minutes as shown in the above figures. As it is clear from table 9.2 that both surfactant solutions reduced the interfacial tension to the order of 10^{-2} , however surfactant XOF 26s has a lower interfacial tension value therefore it was chosen for the surfactant slug injection in the tertiary mode.

The interfacial tension measurements of a fresh sample of each surfactant solution with diluted crude oil were conducted as well and the results are shown in Appendix D. However the measurements could not be carried out for long time because a gas phase or a clear water phase got in contact with the oil drop and affected the readings.

9.2 Basic Physical and Petrophysical Properties of the Rocks:

The six Berea sandstone cores used in this study were designated as A1, A2, A3, A4, A5, and A6. The table below shows the basic properties of these cores.

Table 9.3: Physical properties of Berea sandstone cores sample.

| Core ID | Length (cm) | Diameter (cm) | Bulk volume (ml) | Pore volume (ml) | Porosity (%) | Abs.K _w (mD) |
|---------|-------------|---------------|------------------|------------------|--------------|-------------------------|
| | ± 0.01 | ± 0.01 | ± 0.1 | ± 0.01 | ± 0.1 | ± 5 |
| A1 | 6.29 | 3.79 | 71.1 | 15.64 | 22.0 | 356 |
| A2 | 6.48 | 3.80 | 73.3 | 16.16 | 22.0 | 332 |
| A3 | 6.40 | 3.81 | 73.0 | 16.60 | 22.7 | 371 |
| A4 | 6.30 | 3.82 | 72.2 | 16.38 | 22.7 | 390 |
| A5 | 6.33 | 3.81 | 72.2 | 16.28 | 22.6 | 346 |
| A6 | 6.34 | 3.81 | 72.2 | 17.39 | 22.7 | 377 |

Table 9.3 shows that the Berea sandstone cores have almost same porosities ranging from 22.0 – 22.7 % while the absolute permeabilities varies between 332 and 390 mD. The variation in the absolute permeabilities of the cores could be caused by the interactions between the SSW used for measurement and the rock minerals during saturation. In addition the differences in the pore structure of the cores could contribute to the permeabilities variation.

Table 9.4 shows initial parameters of the cores after the drainage process and also the permeability measurements conducted before and after the aging period.

Table 9.4: The initial parameters of the cores before flooding process

| Core ID | A1 | A2 | A3 | A4 | A5 | A6 |
|------------------------------------|---------|---------|---------|---------|---------|---------|
| S _{wi} [% PV] | 19.5 | 18.9 | 22.9 | 22.1 | 21.4 | 22.2 |
| S _{oi} [%PV] | 80.5 | 80.8 | 77.1 | 77.9 | 78.6 | 77.8 |
| K _{eff} [mD] before aging | 413 ± 5 | 447 ± 5 | 483 ± 5 | 496 ± 5 | 488 ± 5 | 423 ± 5 |
| K _{eff} [mD] after aging | NA* | NA* | 387 ± 5 | 394 ± 5 | 413 ± 5 | 394 ± 5 |

NA* means not aged

The cores A1 and A2 have not been aged and its initial water and oil saturations are almost same as shown in the table 9.4. The other four cores that were aged for almost four weeks at 110 C° showed a reduction in the effective permeability which indicates that the wettability of the cores has been altered during aging period. However the

reduction in permeability is more pronounced in the cores A3, A4, and A5 while core A6 showed about 7% reduction in permeability.

9.3 Synthetic Sea Water (SSW) and Low Salinity (LS) Waterflooding in Unaged Cores:

In this study, first the effect of decreasing the salinity of injected brine in the oil recovery of two unaged cores was tested. The brines used were synthetic sea water and 22 times diluted synthetic sea water and the experiments were carried out in secondary and tertiary mode. Core A1 was flooded first with synthetic sea water then followed by 22 times diluted synthetic sea water in order to observe the effect of the low salinity waterflooding as tertiary mode. While core A2 was flooded directly by the 22 times diluted synthetic sea water as secondary mode and compared with core A1. The results of flooding process are presented and discussed in this section.

9.3.1 Production Profiles of Secondary Injection:

The production profiles of secondary waterflooding of the unaged cores A1 and A2 are shown in figure 9.3. Core A1 was flooded with synthetic sea water while core A2 was flooded by the 22 times diluted synthetic sea water.

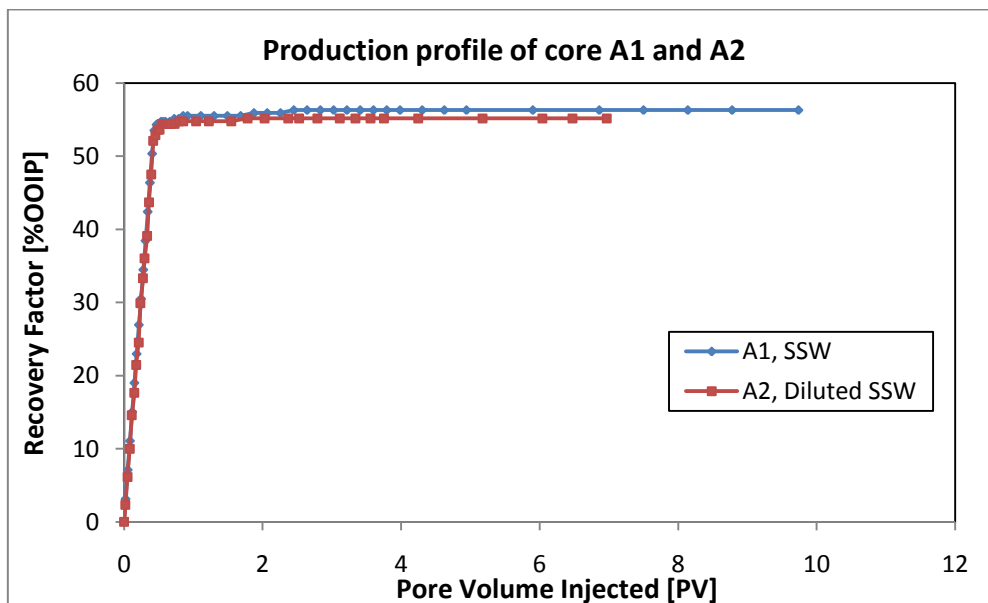


Fig. 9.3: Production profile of SSW and DSSW in unaged cores A1 and A2.

9.3.2 Comparison Between the Synthetic Sea Water (SSW) and Low Salinity (LS) Waterflooding as Secondary Mode:

Table 9.5 lists the production recovery parameters of synthetic sea water and low salinity waterflooding as both done as secondary mode waterflooding in unaged cores. The flooding procedures in both cores were same and the flow rate was increased when the oil production was ceased in order to observe the effect of increasing the viscous force. As it is clear from the table that both flooding types have almost same oil recovery where synthetic sea water gave 56.3% of oil recovery factor and the 22 time diluted synthetic sea water gave 55.2% of oil recovery factor.

Table 9.5: Production recovery parameters of SSW and LS waterflooding as secondary mode.

| Core | A1 [Secondary SSW] | A2 [Secondary LS] |
|--------------------------------------|---------------------|--------------------|
| PV Injected | 9.7 | 7.0 |
| RF [% of OIIP] | 56.3 | 55.2 |
| WBT [PV] | 0.50 | 0.42 |
| S _{or} [%PV] | 35.2 | 36.2 |
| K _{effe} at S _{or} | 35.5 | 37.9 |

In both experiments, it was observed that the oil production was stopped or continued at a high water/oil ratio once the water break-through was occurred. This type of production gives an indication that both cores have a strongly water-wet conditions [28]. In addition the high residual oil left after the flooding process which are 35.2 and 36.2 %PV for core A1 and A2 respectively reflects that the cores are at strongly water-wet.

Many studies showed that the reduction in the salinity of the injected brine gives higher oil recovery compared to high salinity brine. However these studies were conducted in aged cores where the aging period affected the crude oil/Brine/Rock (COBR) interaction and altered the wettability of the core to reflect the reservoir state. This alteration of wettability influences the performance of the waterflooding using different brine salinity [29,32,42,49]. A stated necessary condition for observing the effect of low salinity waterflooding is establishing the mixed wettability by exposure of the rock to crude oil [45].

9.3.3 Low Salinity Waterflooding as Tertiary Mode:

A tertiary low salinity water flooding was done in core A1 after the residual oil saturation was obtained by synthetic sea water flooding. The production profile is shown in figure 9.4 and the recovery parameters are listed in table 9.6:

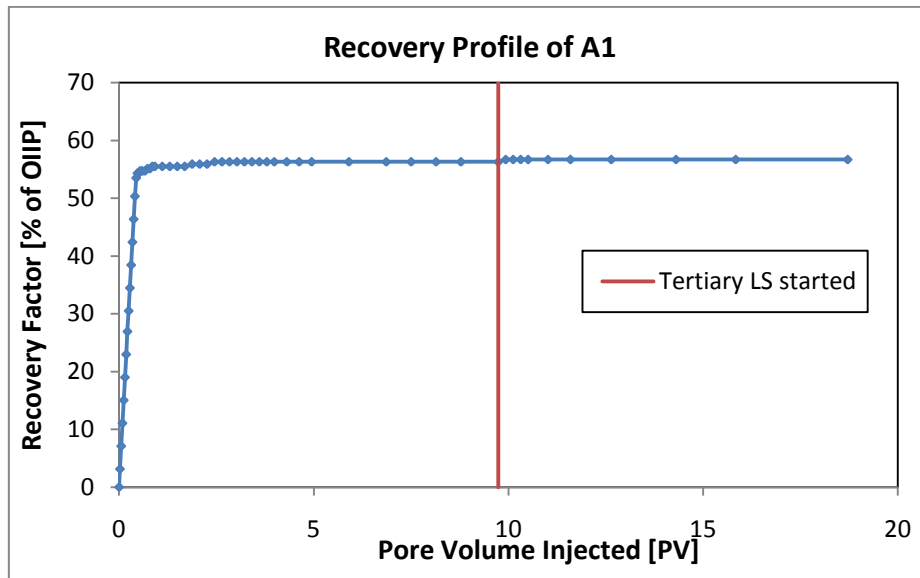


Fig. 9.4: Production profile of core A1.

Table 9.6: Parameters of secondary SSW and tertiary LS waterflooding in core A1.

| Parameters | Core A1 |
|---|---------|
| PV injected for secondary SSW flooding | 9.7 |
| RF [% of OIIP] after secondary SSW flooding | 56.3 |
| PV injected for tertiary LS flooding | 9.0 |
| RF [% of OIIP] after tertiary LS flooding | 56.7 |

From the table above and from figure 9.4, it appears that the tertiary low salinity waterflooding has no effect in the oil recovery of core A1 which is strongly water wet. The slight increase in the recovery factor could be related to the uncertainty in the reading measurements of the oil production which have been done volumetrically.

In strongly water wet cores, the water occupies the small pores and covers the surface of the large pores while oil occupies the large pores. After secondary waterflooding by synthetic sea water and establishing residual oil saturation, S_{or} , the trapped residual oil by capillary force in strongly water wet system would be in the largest pores. By using the low salinity waterflooding as tertiary mode to improve the oil recovery this would implies that low salinity brine should mobilize the trapped oil from the largest pores. Based on the pore scale theory, in order for the low salinity brine to increase

the recovery it should effectively reduce the interfacial tension or change the wettability of the system to become more water wet. However neither of these effects would occur because the interfacial tension between oil and water is not a very significant function of the brine salinity and for strongly water wet system, the rock surface has a little scope to become more water wet [48].

It seems from the flooding process in the unaged cores that the wettability state of the core has a great influence in the effect of low salinity water flooding. Therefore the other 4 cores were subjected to aging period before conducting the flooding experiments.

9.4 Low Salinity (LS) Waterflooding in Aged Cores:

In this section, the results of secondary low salinity waterflooding process done on the aged core (aged for 4 weeks at a temperature of 110 C°) are presented and discussed. The aged cores are A3, A4, A5, and A6 and the low salinity brine used for flooding is 3000 ppm NaCl brine. In the experiments the flow rate was increased when the oil production was ceased in order to observe the effect of increasing the viscous force. The effect of aging period in altering the wettability of the cores are discussed and the pressure profiles are presented.

9.4.1 Oil Recovery of Low Salinity Waterflooding:

Figure 9.5 shows the production profiles of the four aged core flooded with low salinity (3000 ppm NaCl brine) as secondary mode. The recovery parameters of the cores are shown in table 9.7 below.

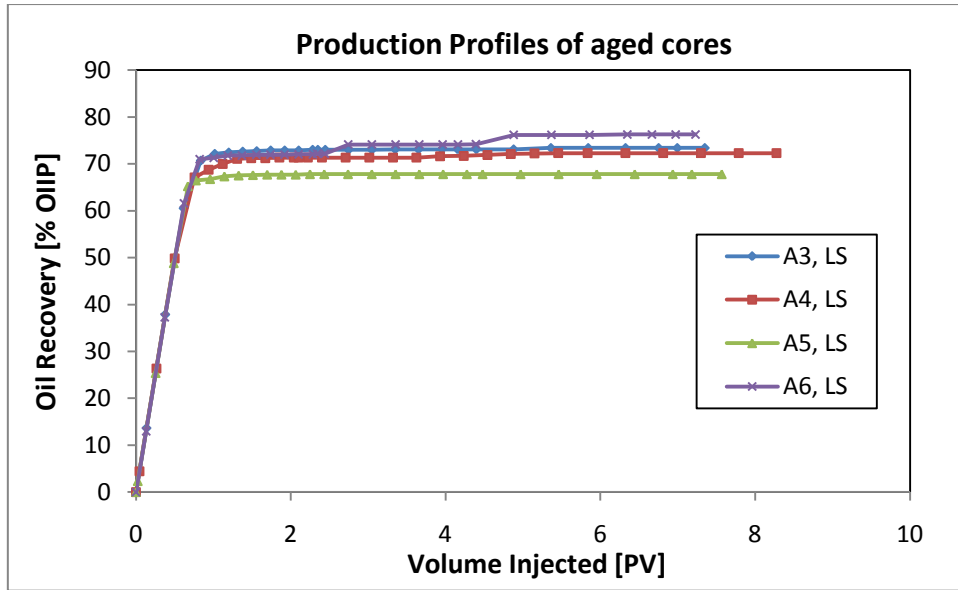


Fig. 9.5: Production profiles of low salinity waterflooding in aged cores.

Table 9.7: The recovery parameters of low salinity waterflooding the aged cores.

| Core ID | A3 | A4 | A5 | A6 |
|----------------------------|------|------|------|------|
| S_{wi} [%PV] | 22.9 | 22.1 | 21.4 | 22.2 |
| S_{oi} [%PV] | 77.1 | 77.9 | 78.6 | 77.8 |
| Pore volume injected [PV] | 7.4 | 8.3 | 7.6 | 7.2 |
| RF [%OIIP] | 73.4 | 72.3 | 67.8 | 76.3 |
| WBT [PV] | 0.54 | 0.56 | 0.58 | 0.53 |
| $S_{or,LS}$ [%PV] | 20.5 | 21.6 | 25.3 | 18.5 |
| K_{eff} at S_{or} [mD] | 65.5 | 89.1 | 65.0 | 72.2 |

The recovery factors, as it is shown in table 9.7, obtained for low salinity waterflooding in the four aged cores are ranging between 67.8 – 76.3 ± 2 % OIIP with highest recovery obtained from core A6. Although the four cores have almost same initial oil saturations, S_{oi} , in the range of 77.1 – 78.6 % PV, and the flooding procedures were identical, the recovery factors and residual oil varies among the cores. The wettability of the cores could be altered in the aging period at different degree which caused this variation in oil recovery. In a crude oil/brine/rock (COBR) system, the degree of interaction between surface-active constituents in the oil and the rock surface is influenced by many factors, such as rock mineral composition, brine composition, fluid content, oil composition, temperature, and pressure. This COBR interaction control wettability and the efficiency of oil recovery by a variety of possible mechanisms [12,28,32].

9.4.2 Wettability:

The wettability state of the COBR system has a great effect on the performance of waterflooding. A study of different COBR systems showed that the oil recovery by waterflooding increased with change in the wettability from strongly water-wet to a maximum at close to neutral wettability [28]. Figure 9.6 shows a comparison of the oil recovery obtained from all the six cores used in this study flooded in secondary stage.

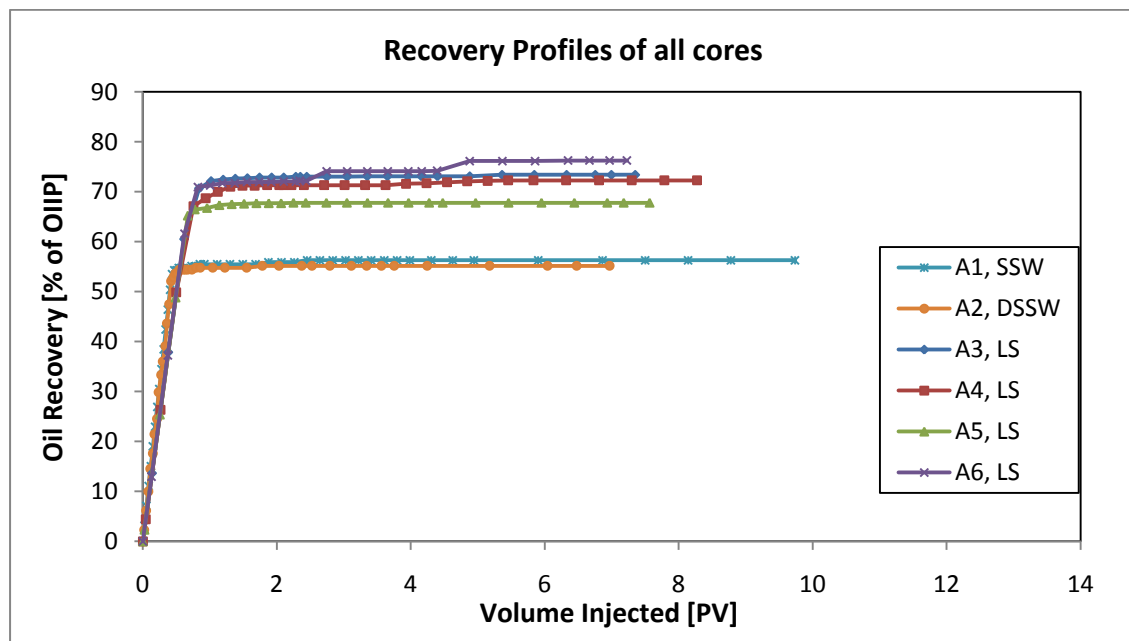


Fig. 9.6: Recovery profiles of secondary waterflooding for all six cores.

From figure 9.6, the results of secondary injection in both aged and unaged cores clearly indicate that the low salinity (3000 ppm NaCl brine) injection in aged cores gives higher recovery compared to injection of synthetic sea water and 22 times diluted sea water in the unaged cores. This results indicate that the aging period of the cores had a positive effect in changing the wettability of the cores toward less water wet conditions which is reflected in higher oil recovery. It has been reported in the literatures that both the aging time and aging temperature of cores influence the oil recovery where the oil recovery by waterflooding increases with increasing aging time and temperature [28,32].

The observed decrease in the oil permeability at initial water saturation before and after aging also could be a qualitative indication of changing in the wettability of the aged cores to less water wet state compared to the unaged (strongly water wet) cores. In strongly water wet cores the oil occupies the large pores and therefore will flow easily with minimal resistance having a high oil permeability. As the wettability

altered towards less water-wet conditions the flow resistance of oil will increase leading to reduce the oil permeability at initial water saturation. The cores A3, A4, and A5 showed 15 – 20 % reduction in the oil permeability after aging except core A6 that showed a reduction of 7% , see table 9.4.

It has been suggested in the literatures that during the low salinity waterflooding the wettability of the cores changes towards increasing water wetness and thus leading to increase recovery [45,68,69]. This mechanism has been discussed and explained physically using the pore scale network modeling and the percolation theory where the low salinity injection has been concluded to alter the wettability of the mixed wet cores towards more water wet conditions [48].

The relative permeability values to water, K_{rw} , can be obtained as a ratio of the endpoint permeability to water, K_{eff} , to the absolute permeability, K_{abs} , for the corresponding cores. The relative permeability values could serve as an indication of cores wettability after the low salinity waterflooding in the aged cores. These values are compared with the values of the unaged cores A1 and A2 (strongly water wet cores). Table 9.8 shows the residual saturation after secondary waterflooding and the relative permeability values of the six cores.

Table 9.8: Residual saturation and relative permeability values of all cores.

| Core | A1 | A2 | A3 | A4 | A5 | A6 |
|-------------------|------|------|------|------|------|------|
| S_{or} | 35.2 | 35.5 | 20.5 | 21.6 | 25.3 | 18.5 |
| K_{rw} after LS | 0.1 | 0.11 | 0.18 | 0.23 | 0.19 | 0.19 |

The unaged cores A1 and A2 which have shown a strongly water wet state have values of relative permeabilities of 0.1 and 0.11 respectively. However the typical values of the relative permeability for strongly water wet system is in the range of 0.05 to 0.1. The aged cores that flooded by low salinity brine show relative permeability values, as listed in table 9.8, between 0.18 – 0.23 which are in the range of the typical weakly water wet systems (the relative permeability of 0.1 – 0.3 is determined as weakly water wet). The intermediate water wet system has generally relative permeability of greater than 0.3.

The wettability of cores A3, A4, A5, and A6 has been altered toward less water wet during the aging which have been confirmed by the reduction in the oil permeability after the aging. During the low salinity flooding the wettability of the cores might be changed toward more water wet leading to release the oil from the rock surface and increase recovery.

9.4.3 Pressure Profiles:

The pressure profile combined with production profile of the low salinity waterflooding in the aged cores are shown in figures 9.7 - 9.10. As it can be seen from the figures that the pressure development of the cores have a quite similar trends. The pressure profile started increasing at the beginning of the low salinity injection until the peak value reached just before the water break-through then decreased and leveled off. The flooding started with injection rate of 0.1 ml/min to have a kind of stable displacement and avoid the fingering phenomena which causes early water break-through. The observed pressure peak at water break-through of the cores was in the range of 16 – 20 mbar and the oil volume produced at the breakthrough were 0.54, 0.56, 0.58, and 0.53 PV from A3, A4, A5, and A6 respectively. After the break-through the pressure leveled off with minor disturbance in the profile.

The increase in the differential pressure profile of the cores after almost 2.5 PV injection is a response of increasing the injection rate. The injection rate increased to 0.5 ml/min after the oil production ceased and then increased further to 1 ml/min as can be seen from the increase in the pressure profile. The production profiles of cores A3, A4, and A5 do not show any noticeable response of this increase in the injection rate, while core A6 produced more oil as the injection increased. The increase in recovery caused by rising flow rate is one of the indication that the wettability of the core is less water wet.

Most sandstone formations contain fine particles that could migrate in the porous medium and cause a reduction in the permeability of the formation by plugging the interconnecting pore throats [35,37]. At the same time, fine migration has been suggested to provide a mobility control to improve the performance of the waterflooding by diverting the flow from the water swept zones to un-swept zones. Salinity of the injected brine, flow rate, pH, and temperature have been found to be significant factors affecting the fine migration process [35,36,37].

In addition, fine migration has been observed and proposed in the literatures as one of the mechanisms that causes an increase in the oil recovery by low salinity waterflooding [31,32,38,62]. However core flood experiments done by BP have shown neither fines were produced in the effluent nor reduction in permeability [18].

In this study, fine particles have not been observed visually in the produced effluent during the coreflood experiments of secondary low salinity water flooding. The pressure profiles of the cores, presented in figures 9.7 - 9.10, seems to be stable during the low salinity injection and increased only as a response of rising the flow rate. Therefore this indicates that the swelling of clay in the Berea sandstone is not significant, otherwise it will be observed as a noticeable increase in the pressure profile.

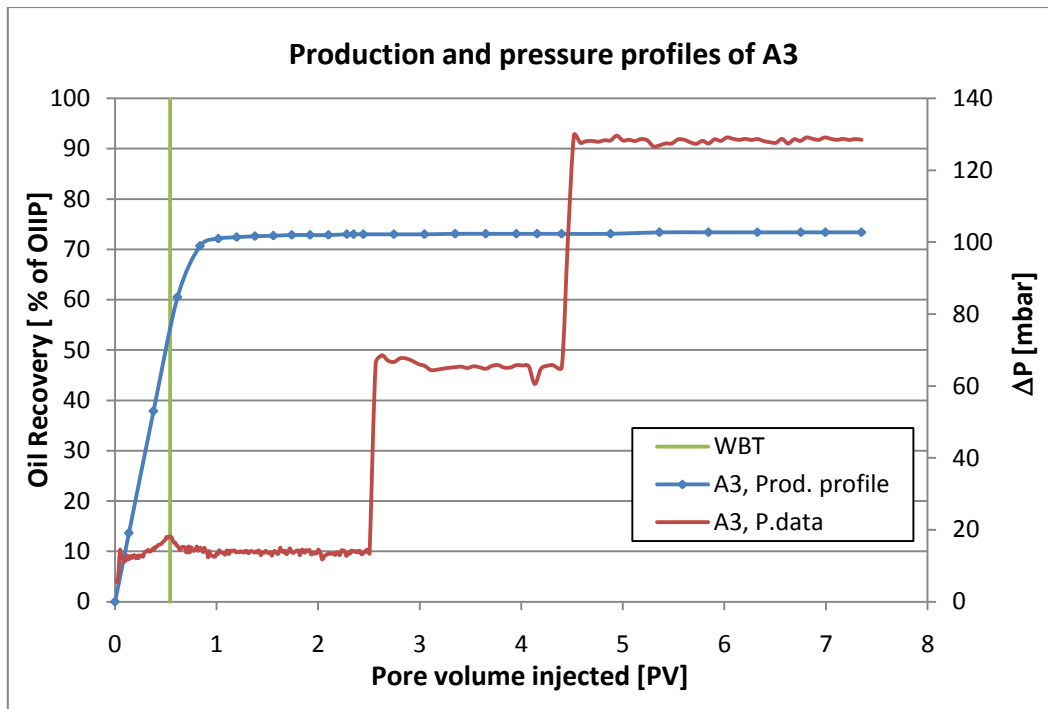


Fig. 9.7: Production and Pressure profiles of LS waterflooding in core A3.

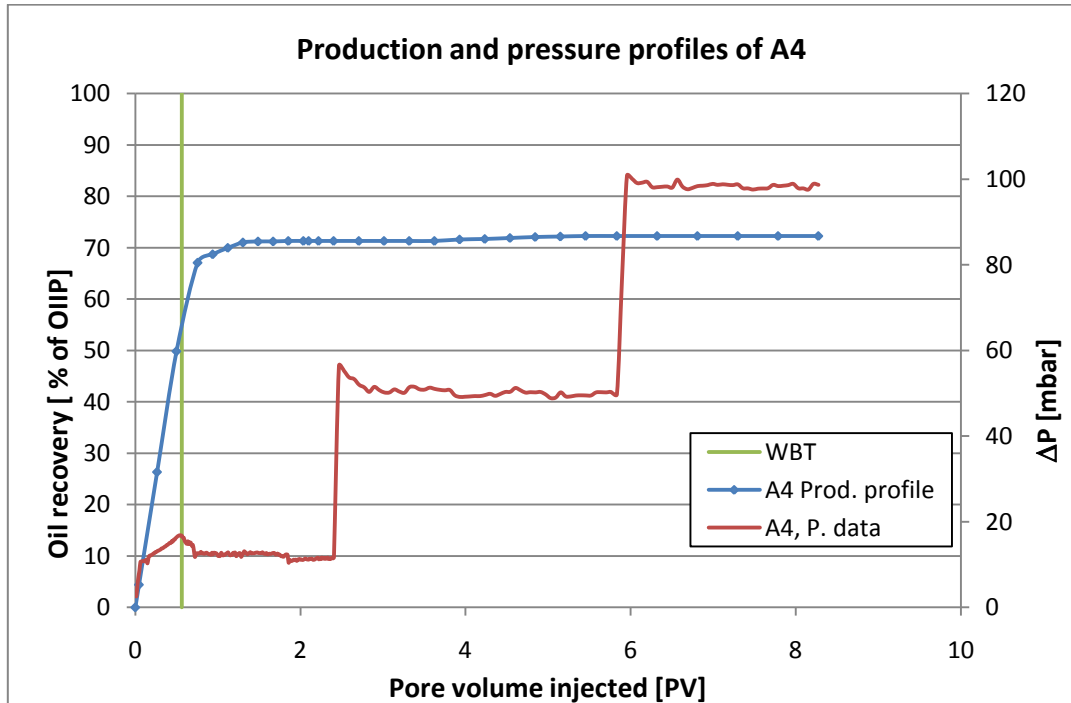


Fig. 9.8: Production and pressure profiles of LS waterflooding in core A4.

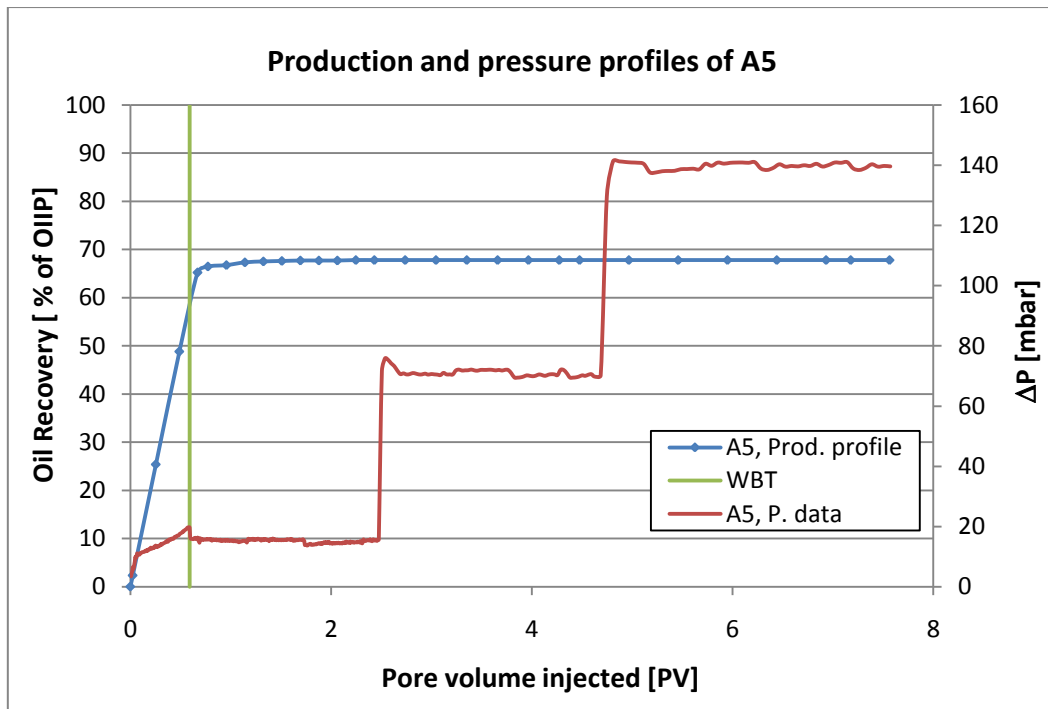


Fig. 9.9: Production and pressure profiles of LS waterflooding in core A5.

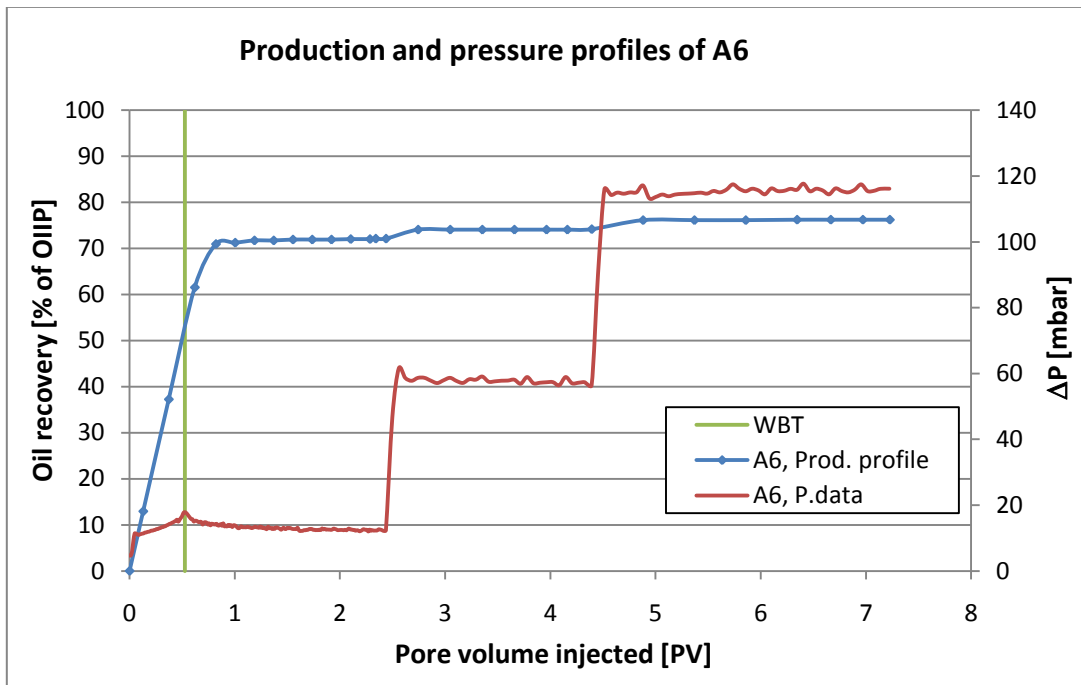


Fig. 9.10: Production and pressure profiles of LS waterflooding in core A6.

9.5 Low Salinity Surfactant and Polymer Slugs Injection:

The combined process of low salinity surfactant and polymer flooding was investigated in this study to determine its effectiveness as tertiary injection mode. The experiments were carried out by injecting a surfactant slug followed by a polymer slug and then a continuous injection of low salinity brine. Each of the aged cores has been flooded with a different size of surfactant slug at a constant concentration in order to determine the optimum slug size that gives high oil recovery. The polymer slug was injected directly after the surfactant slug in order to maintain a stable displacement behind the surfactant.

The surfactant used in this investigation was XOF 26s which was chosen based on interfacial tension measurements, see section 9.1.3. The surfactant system was prepared intentionally as type II(-) surfactant system, still giving a low interfacial tension, and the observations of surfactant behavior detected that the surfactant remained in the aqueous phase. The composition of the surfactant system was always kept at constant 1:1 surfactant to mixed-oil ratio.

The polymer solution used in this study was prepared using HPAM and the concentration was chosen based on the viscosity measurement, see table 9.1. The concentration of 300 ppm of HPAM was chosen since it gives a viscosity of 3 cp which is close to diluted oil viscosity, therefore the viscosity ratio is about 1.

A Summary of the experimental parameters of low salinity surfactant and polymer slugs injection are listed in table 9.9 and will be discussed in this section.

Table 9.9 : Experimental parameters of low salinity surfactant and polymer slugs injection.

| Core ID | A1* | A2* | A3 | A4 | A5 | A6 |
|-----------------------------|------|------|------|------|------|------|
| $S_{or@LS}$ [% PV] | 34.8 | 35.6 | 20.5 | 21.6 | 25.3 | 18.5 |
| PV inj. of Surfactant | 1 | 1 | 0.3 | 0.5 | 1 | 2 |
| PV inj. of Polymer | 1 | 1 | 0.5 | 1 | 1 | 1 |
| PV inj. of LS | 2.0 | 2.0 | 3.0 | 2.3 | 2.8 | 3.3 |
| RF [% of OIIP] | 6.4 | 3.8 | 1.6 | 7.0 | 16.9 | 15.4 |
| RF [% of S_{or} after LS] | 17.0 | 10.0 | 6.2 | 25.1 | 52.6 | 65.0 |
| $S_{or@LS-S-P}$ [% PV] | 29.6 | 32.5 | 19.3 | 16.2 | 12.0 | 6.5 |

* Unaged core

9.5.1 Oil Recovery in Aged Cores (LS-S-P):

The oil recovery of tertiary low salinity surfactant and polymer slugs injection done in the aged cores are presented in figure 9.11. As It is clear from the figure that the slugs injection have mobilized and produced oil from the cores as tertiary recovery after the

secondary low salinity flooding. The amount of produced oil varies in cores depending on the size of the surfactant slug injected.

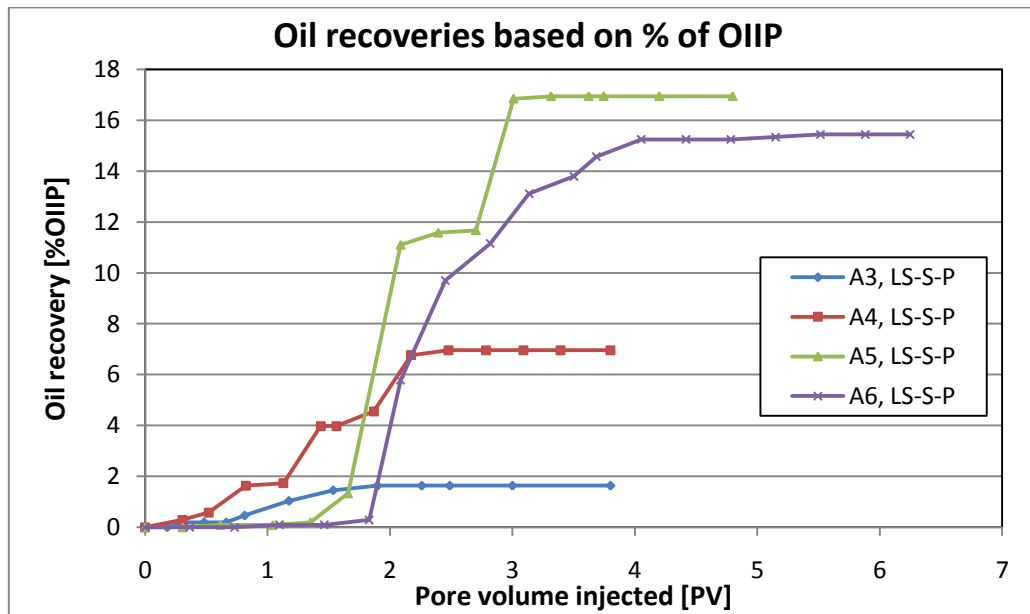


Fig. 9.11: Oil recovery of tertiary low salinity surfactant and polymer slugs injection done in the aged cores.

Core A3 which is flooded by 0.3 PV of surfactant followed by 0.5 PV of polymer showed low tertiary recovery of 1.6 % of OIIP. This would be explained by retention of surfactant due to adsorption, precipitation, and phase trapping therefore the efficiency of surfactant flooding will be reduced. In core A4 which is flooded by 0.5 PV of surfactant followed by 1 PV of polymer, the response was moderate and it gave a tertiary recovery of 7.0 % of OIIP. This increase in recovery is consistent with increase in the surfactant slug size which means that more oil has been mobilized by surfactant.

Cores A5 and A6 are flooded with 1 PV and 2 PV of surfactant respectively and then followed by 1 PV of polymer. The tertiary recovery is 16.9 and 15.4 % of OIIP from core A5 and A6 respectively. This high recovery compared to the other two cores is due to increase in the surfactant slug size injected. However core A5 showed higher recovery in terms of OIIP compared to core A6 even though the latter was flooded with larger slug size. This could be justified by that the residual oil saturation after secondary low salinity waterflooding is much higher in core A5 compared to core A6. The residual oil saturation before tertiary injection in core A5 is 25.3 %PV while in core A6 it is 18.5 %PV.

Figure 9.12 shows the oil recovery of tertiary low salinity surfactant and polymer slugs injection based on the residual oil after secondary low salinity waterflooding.

The lowest tertiary recovery is 6.2 % of residual oil which is obtained by injecting 0.3 PV of surfactant in core A3. The highest tertiary recovery is 65.0 % of residual oil obtained by injecting 2 PV of surfactant in core A6, which also resulted in lowest residual oil saturation, $S_{or @ LS-S-P}$, of 6.5 % PV at the end of floods as shown in table 9.9.

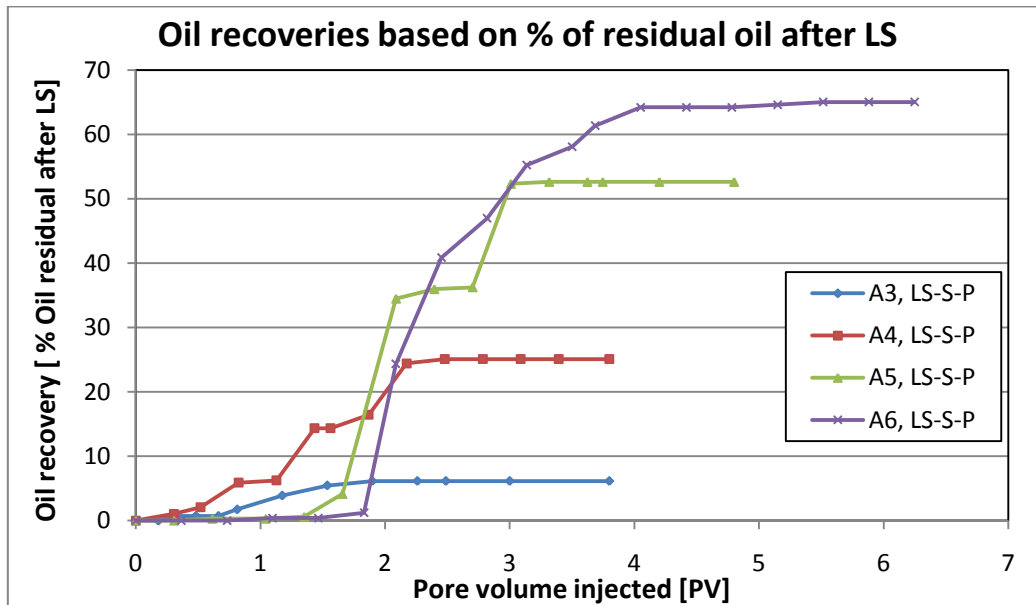


Fig. 9.12: Oil recovery of tertiary low salinity surfactant and polymer slugs injection based on the residual oil after secondary low salinity waterflooding.

The relation between the surfactant slug size injected and the final tertiary recovery factor based on the secondary residual oil is illustrated in figure 9.13. The figure clearly depicts that the tertiary recovery increases with increasing the size of the surfactant slug injected. However the injection of larger surfactant slug than 2 PV could lead to produce more oil and increase the recovery factor. Therefore the optimum surfactant slug size would be determined when there is no more increase in the recovery factor with further increase in the surfactant slug size at constant surfactant concentration.

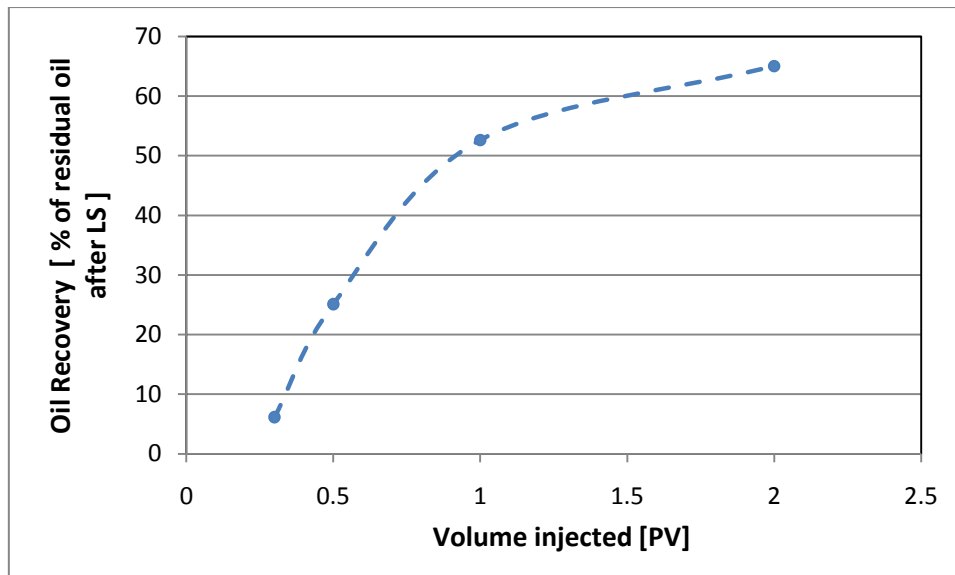


Fig. 9.13 : Relation between oil recovery and surfactant slug size injected at constant surfactant concentration.

After the low salinity waterflooding the residual oil saturation is most likely to be caused by capillary force which is responsible for trapping oil. Experimental studies showed that the surfactant flooding can improve the recovery after immiscible displacement by reducing the interfacial tension between oil and water which results in higher capillary number and mobilize the trapped oil [70]. In this study the interfacial tension of the surfactant used is about 10^{-2} mN/m which is low enough to mobilize the trapped oil and increase recovery.

The polymer slug injected after the surfactant slug could also contributed to the increase in the tertiary recovery by improving the volumetric sweep efficiency. However the main use of the polymer slug in this case was to maintain a stable displacement behind the surfactant and therefore having a better mobilization of oil.

9.5.2 Pressure Profiles:

The pressure profile of low salinity surfactant and polymer slugs injection is plotted with the oil production profile in figures 9.14 - 9.17. In all four aged cores, the pressure across the cores started increasing with injection of surfactant slug. Cores A3 and A4 showed during surfactant injection an early response by producing oil, however the produced volume was very small from both cores. Core A5 did not show any oil production during surfactant injection even it was flooded by 1 PV of surfactant. The pressure profile in core A6 which is flooded by 2 PV increased until it reached the peak value and then started dropping. However the significant oil production from the core started after 1.8 PV injection of surfactant.

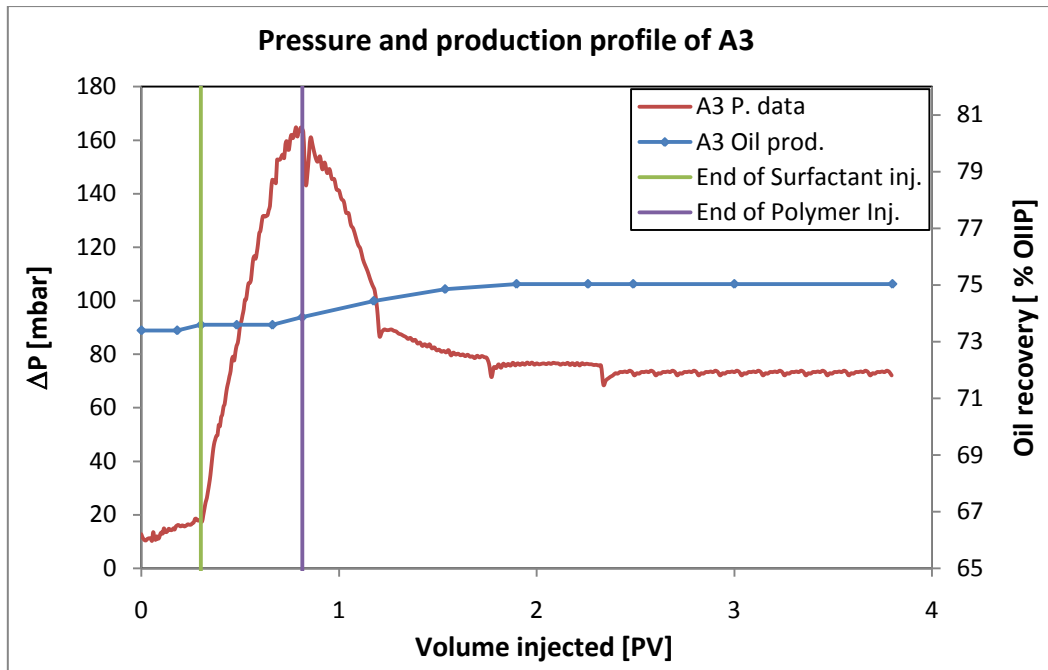


Fig. 9.14 : Pressure and production profile of LS-S-P flooding in core A3.

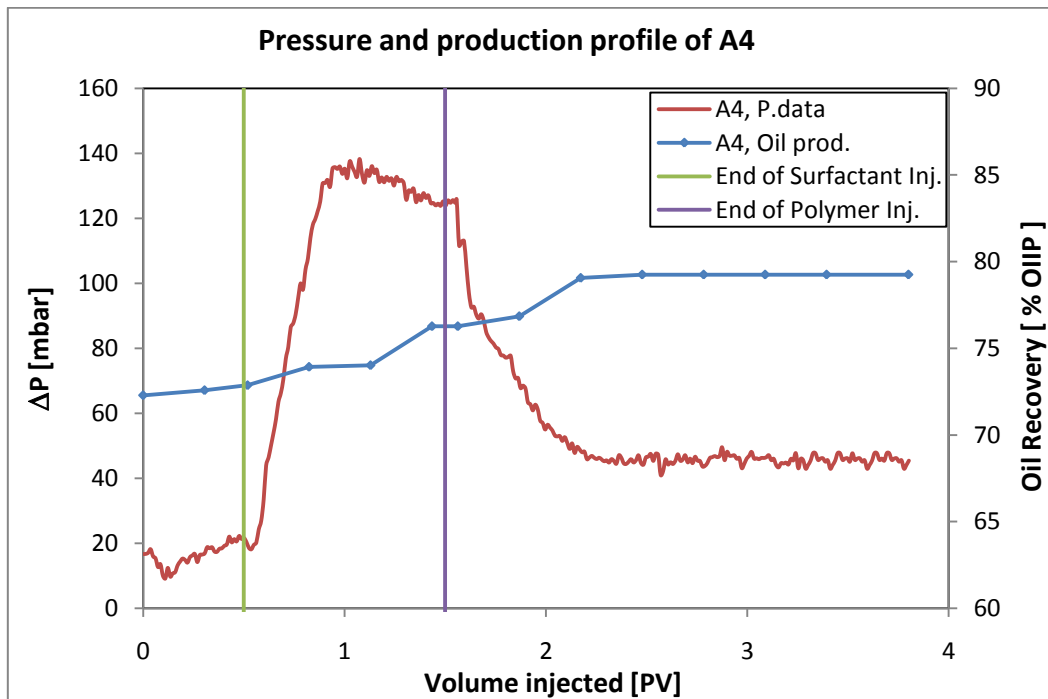


Fig. 9.15 : Pressure and production profile of LS-S-P flooding in core A4.

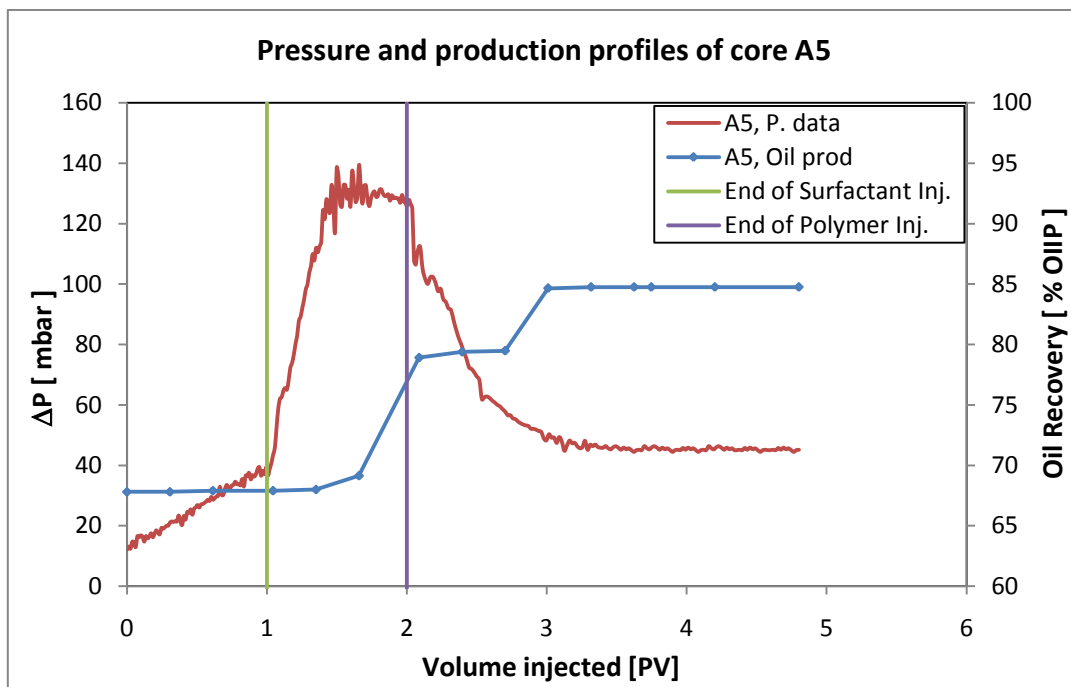


Fig. 9.16 : Pressure and production profile of LS-S-P flooding in core A5.

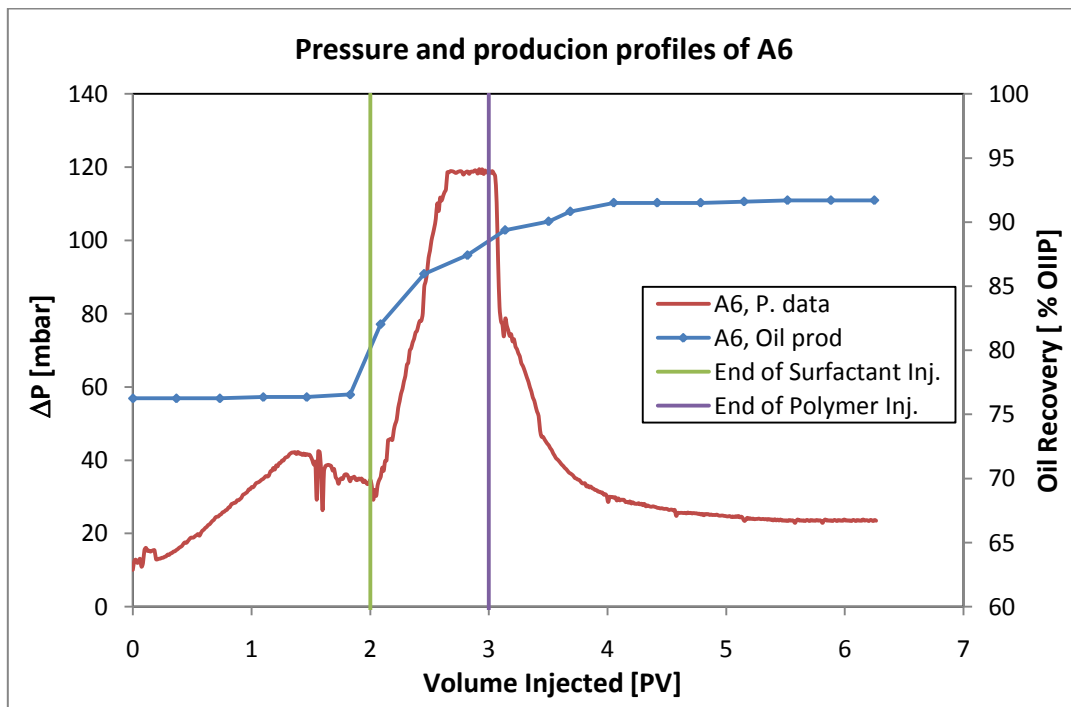


Fig. 9.17 : Pressure and production profile of LS-S-P flooding in core A6.

During the polymer slug injection the pressure across the cores increased significantly because of the increasing the viscosity of the injected brine. Core A3 was flooded by 0.5 PV of polymer and the pressure profile was increasing without any sign of polymer breakthrough. In the other cores, A4, A5, and A6, which flooded by 1 PV of polymer the pressure profile increased until the polymer breakthrough occurred and then stabilized or started to fall down. The breakthrough of the polymer occurred after 0.45, 0.51, and 0.65 PV of polymer injection in the cores A4, A5, and A6 respectively. All the cores showed an increase in the oil production during the polymer flooding. Generally the polymer flooding improves the volumetric sweep efficiency therefore increasing oil recovery.

After the polymer slug injection the cores were flooded by continuous low salinity brine (3000 ppm NaCl). The pressure profile in all cores declined once the low salinity waterflooding started and then leveled off. The cores continued producing oil during low salinity injection until the oil production is ceased.

9.5.3 Comparison of Tertiary Low Salinity Surfactant and Polymer Slugs Injection in Aged and Unaged Cores:

The tertiary low salinity surfactant and polymer slugs injection was also conducted in the unaged cores A1 and A2. The size of the slug injected in both unaged cores was 1 PV of surfactant followed by 1 PV of polymer then a continuous injection of low salinity brine. This slug size and injection procedure in the unaged cores is same as the slug size and injection procedure in the aged core A5. A comparison between the low salinity surfactant and polymer slug injection in these three cores is shown in figure 9.18 to determine the effect of wettability in the performance of tertiary recovery.

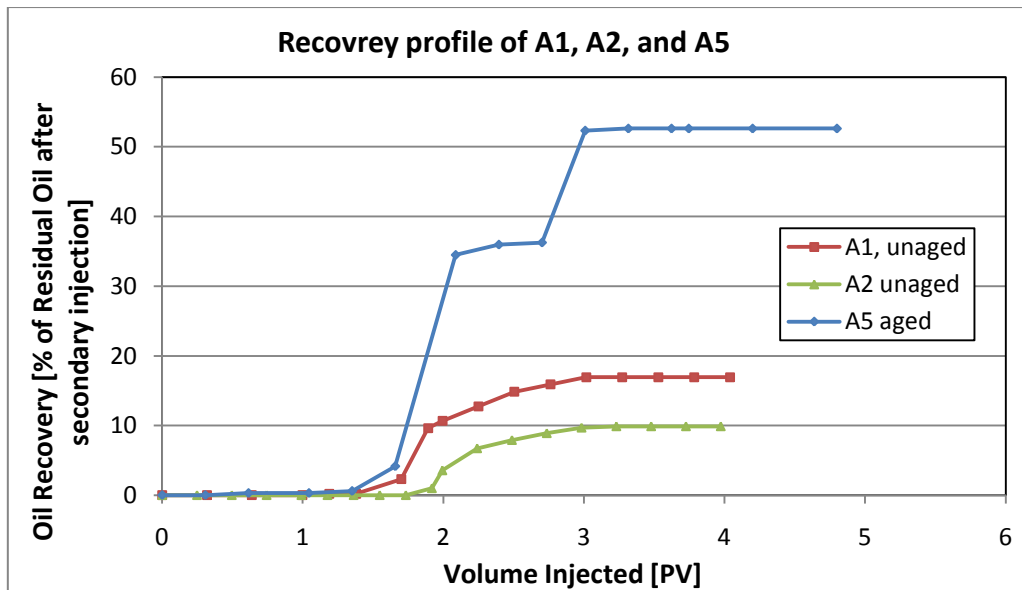


Fig. 9.18 : Recovery profiles of cores A1(unaged), A2 (unaged), and A5 (aged).

As it is clear from the above figure, the response of tertiary slug injection in all three cores started during the polymer injection. The aged core A5 gave tertiary recovery of 52.6 % of residual oil which is much higher than the unaged cores A1 and A2 that gave a tertiary recovery of 17.0 and 10.0 % of residual oil respectively.

It has been determined that the unaged cores has a strongly water-wet behavior, see section 9.3.2, while the wettability of core A5 was altered during the aging period to less water-wet state. This big difference in the tertiary recovery between aged and unaged cores indicates that the wettability of the core has a great influence in the performance of low salinity surfactant and polymer slugs injection. Although the strongly water-wet cores has a much higher residual oil after secondary low salinity waterflooding, see table 9.9, their response to the tertiary injection was much lower than the less water-wet core.

9.6 Low Salinity Polymer Slug Injection:

After the tertiary low salinity surfactant and polymer slugs injection, the cores were flooded by 1 PV of polymer followed by continuous low salinity brine injection to observe any further production. The concentration of the polymer solution used in this stage is 600 ppm which is double than the one used in the low salinity surfactant and polymer slugs injection stage. The recovery parameters of the cores are listed in table 9.10.

Table 9.10 : Recovery parameters of low salinity polymer injection.

| Core ID | A1 | A2 | A3 | A4 | A5 | A6 |
|-----------------------|------|------|------|------|------|-----|
| S_{or} after LS-S-P | 29.6 | 32.5 | 19.3 | 16.2 | 12.0 | 6.5 |
| PV inj | 3.5 | 3.7 | 5.2 | 3.7 | 3.6 | 4.7 |
| RF [S_{oi}] | 0.8 | 9.1 | 1.8 | 5.7 | 2.3 | 2.8 |
| S_{or} after LS-P | 28.9 | 25.2 | 17.8 | 11.8 | 10.2 | 4.3 |
| ΔS_{or} | 0.7 | 7.3 | 1.5 | 4.4 | 1.8 | 2.2 |

9.6.1 Oil Recovery :

The oil recovery from the six cores flooded by 1 PV of 600 ppm HPAM polymer solution is shown in figure 9.19. The results clearly indicate that the polymer slug injection has mobilized some oil from the cores. However the amount of the produced oil varies among the cores as illustrated in figure 9.19. Core A1, A3, A5 and A6 showed oil production of less than 3 % of OIIP while core A2 and A4 showed a significant amount of oil recovery of 9.1 and 5.7 % of OIIP. These two cores with highest recovery responded early to the polymer slug injection by starting oil production after injecting around 0.5 and 0.4 PV of polymer slug into core A2 and A4 respectively.

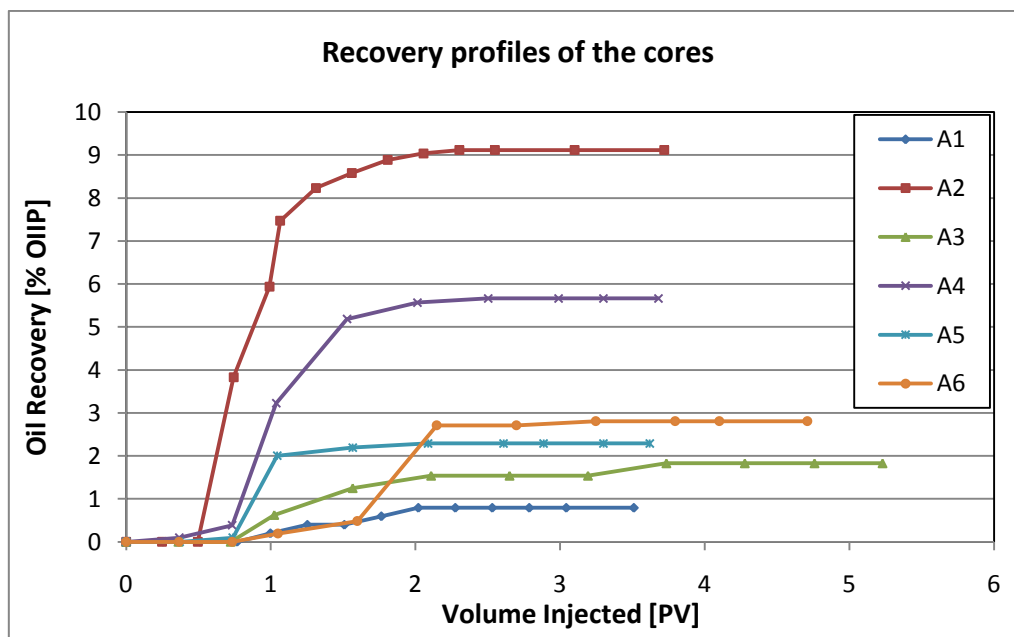


Fig. 9.19: Oil recovery of low salinity polymer slug injection.

The effect of polymer solution in improving oil recovery is mainly due to increasing the viscosity of the injected brine which lead to improve the volumetric sweep efficiency. In principle, increasing the viscosity of the injected water, μ_w , causes an

increase in capillary number, N_c , too and therefore gives lower residual oil, S_{or} , as described by equation 4.5. However, the reduction is small since it takes a major change of N_c (order of magnitudes) in order to affect the S_{or} significantly [1].

The recovery performance of the cores does not show the effect of wettability on the performance of the polymer slug injection. The highest recovery obtained from strongly water-wet core which is core A2 and in the other hand the lowest recovery obtained was from the other strongly water wet core A1. In addition the aged cores have a much lower residual oil before the low salinity polymer slug injection compared to the unaged cores, see table 9.10. Thus the responses to the polymer slug injection might differ from the cores.

9.6.2 Pressure Profiles:

The pressure profile of low salinity polymer slug injection done in the all cores is plotted with the oil production profile in figures 9.20 - 9.25. The pressure across the cores increased during the polymer slug injection as a response of increasing the viscosity of the injected brine. Then during the low salinity brine injection followed the polymer injection the pressure profile in all cores declined and leveled off. All the cores started producing oil during the polymer slug injection and continued producing during low salinity flooding until the oil production was ceased.

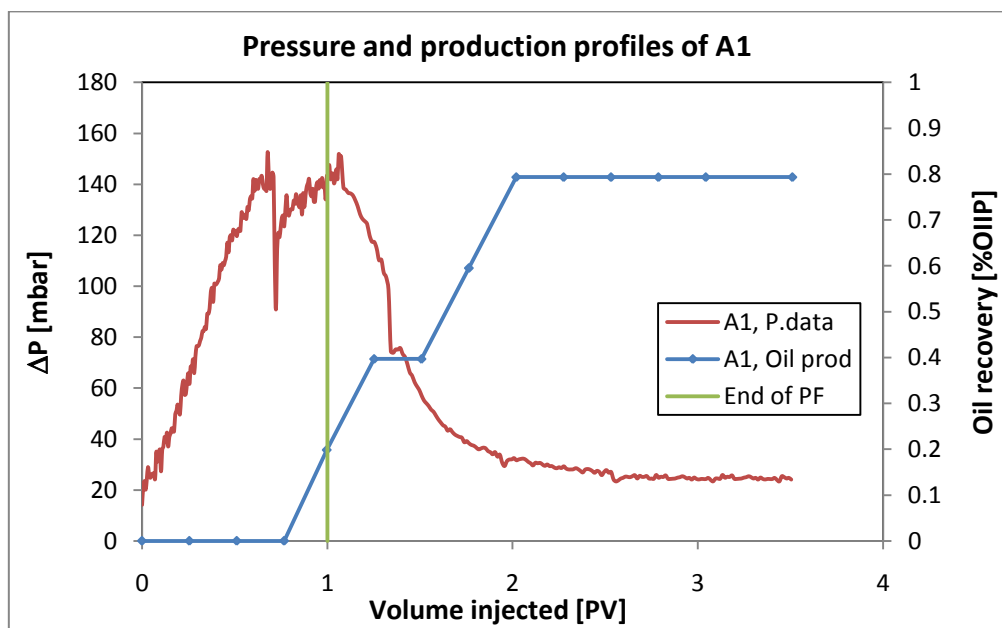


Fig. 9.20: Pressure and production profiles of LS-P flooding in core A1.

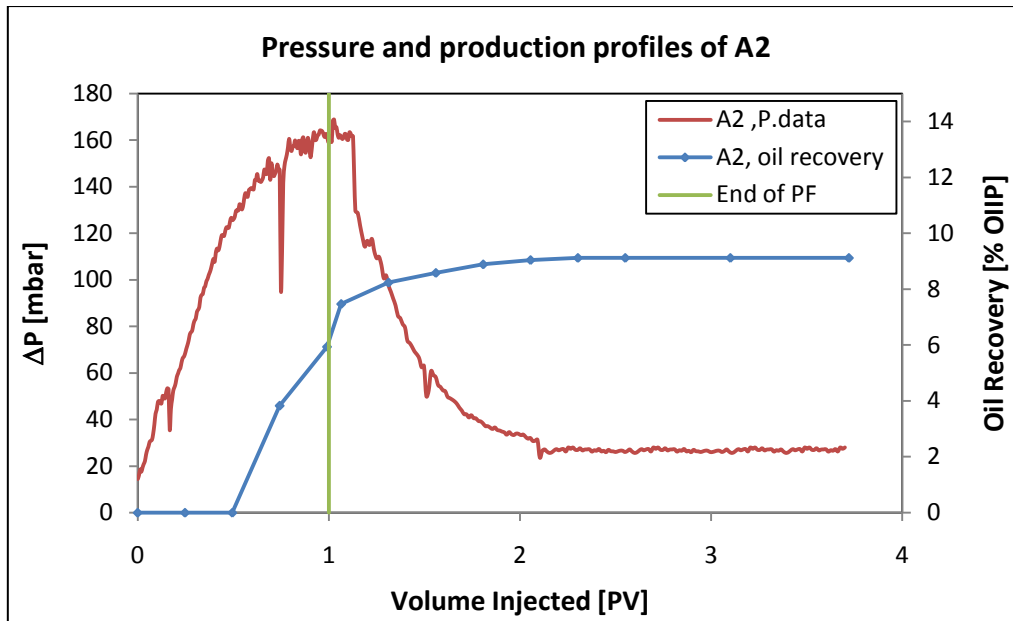


Fig. 9.21: Pressure and production profiles of LS-P flooding in core A2.

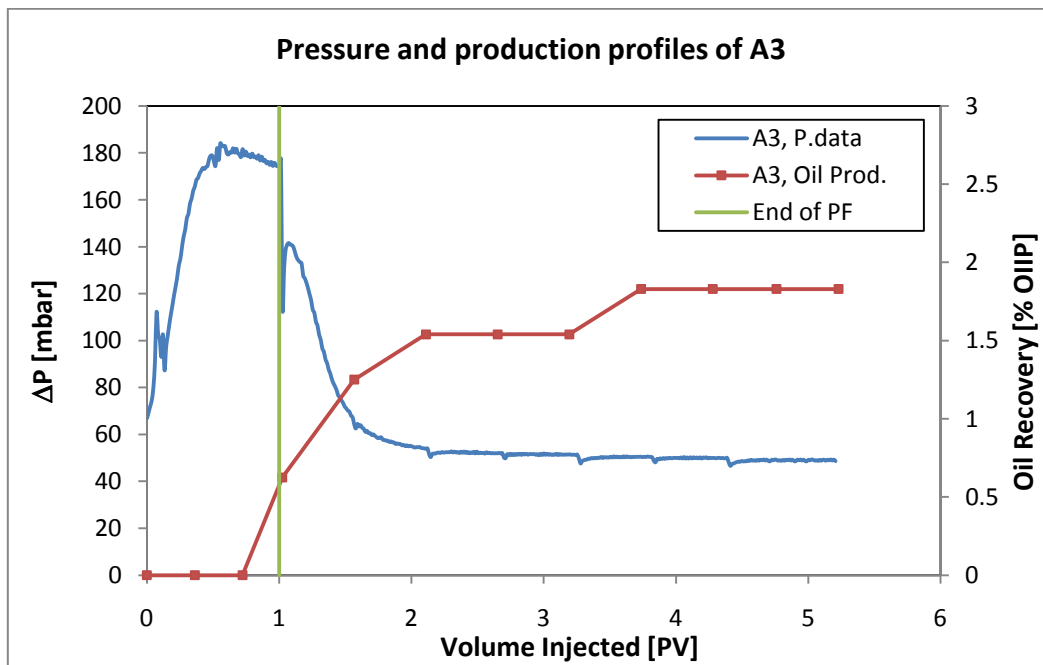


Fig. 9.22: Pressure and production profiles of LS-P flooding in core A3.

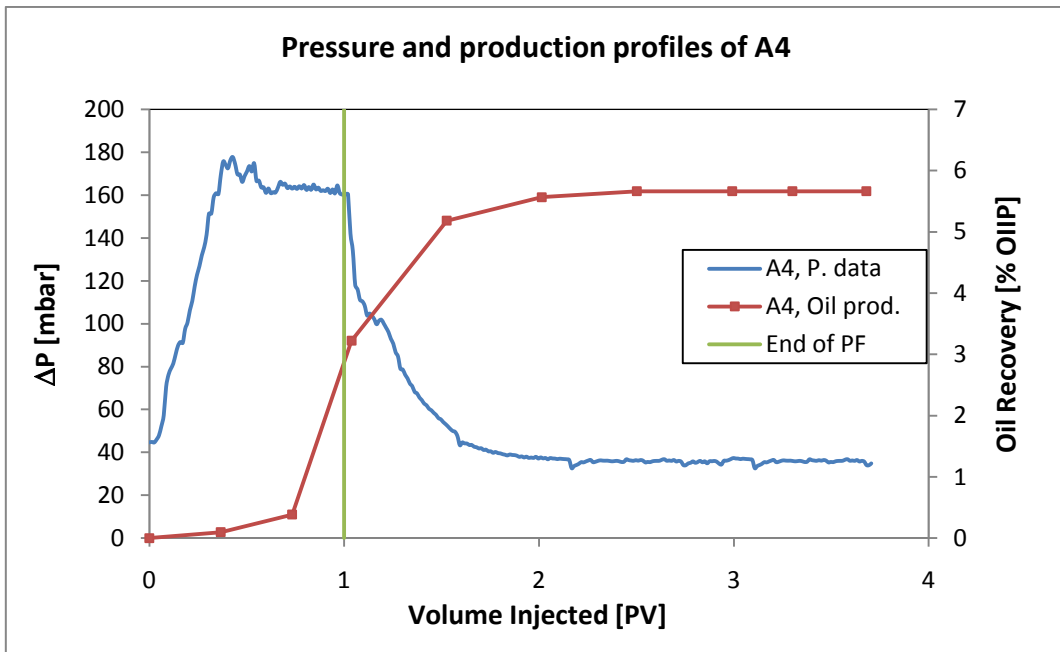


Fig. 9.23 : Pressure and production profiles of LS-P flooding in core A4.

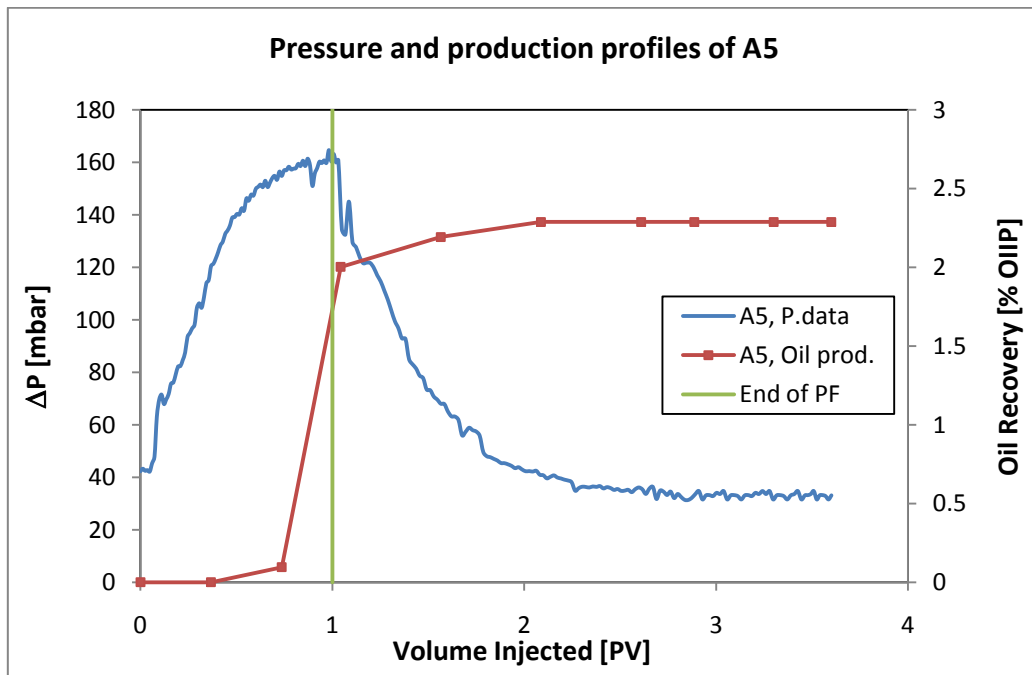


Fig. 9.24 : Pressure and production profiles of LS-P flooding in core A5.

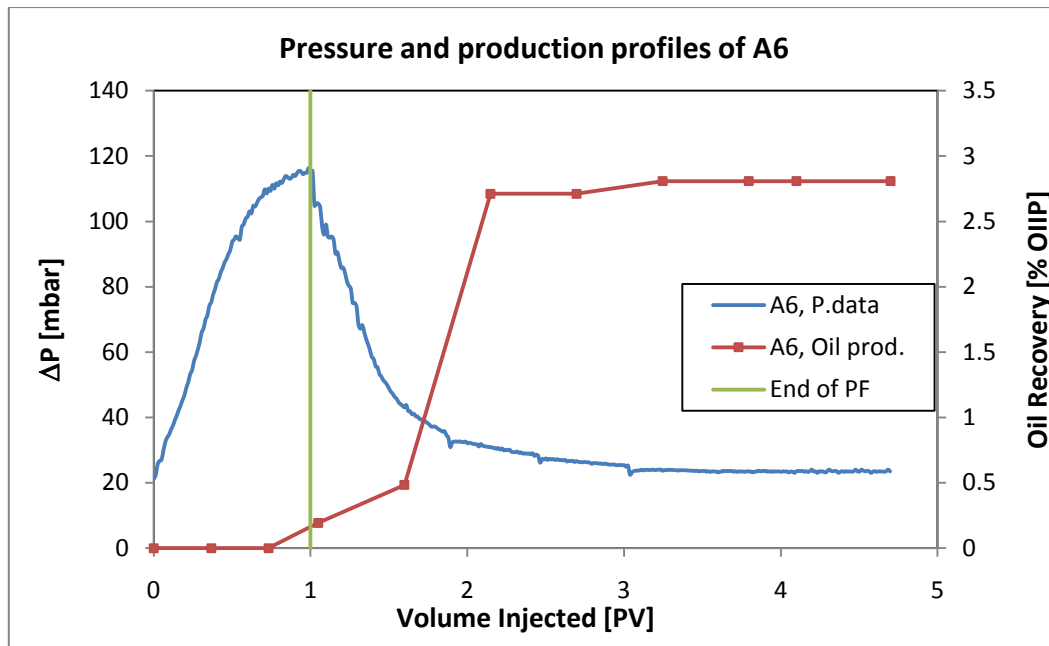


Fig. 9.25 : Pressure and production profiles of LS-P flooding in core A6.

9.7 Capillary Number, N_c :

The capillary number, N_c , which is the ratio between the viscous force and capillary force is calculated for both surfactant and polymer slugs injected in this study and is shown in table 9.11. As it is listed in the table, the surfactant gave a capillary number in order of 10^{-5} while the polymer solutions gave a capillary number in order of 10^{-4} .

Table 9.11 : Calculated capillary number (N_c) for surfactant and polymer injection.

| Core ID | A1 | A2 | A3 | A4 | A5 | A6 |
|--------------------------|----------------------|----------------------|----------------------|----------------------|----------------------|----------------------|
| N_c of Surfactant | 6.0×10^{-5} | 6.0×10^{-5} | 6.0×10^{-5} | 5.9×10^{-5} | 6.0×10^{-5} | 6.0×10^{-5} |
| N_c of 300 ppm Polymer | 2.7×10^{-4} | 2.6×10^{-4} | 2.6×10^{-4} | 2.6×10^{-4} | 2.6×10^{-4} | 2.6×10^{-4} |
| N_c of 600 ppm Polymer | 5.9×10^{-4} | 5.7×10^{-4} | 5.9×10^{-4} | 5.9×10^{-4} | 5.8×10^{-4} | 5.9×10^{-4} |

After secondary waterflooding, the capillary force is responsible for trapping oil in the porous media. Many studies have shown that the residual oil saturation is related to the capillary number and in order to achieve low, S_{or} , after water-flood, a high capillary number, N_c , is required [22,23,56].

The surfactant leads to reduce the interfacial tension between oil and water therefore increasing the capillary number, see equation 4.5. While the polymer increases the capillary number by increasing the viscosity of the injected brine. In this study as have been shown in the previous sections, the surfactant and polymer slugs injected have mobilized and produced oil from the cores which resulted in lower residual oil.

In the calculation of capillary number for polymer injection in this study, the interfacial tension between oil and injected brine is assumed to be constant after the surfactant slug injected. Therefore the capillary number of polymer injection is higher than the surfactant injection because of higher polymer viscosity.

9.8 Summary and Discussion:

In this study, it was expected that lowering the salinity of the injected brine could lead to increase oil recovery from Berea sandstone cores. This improved oil recovery by low salinity waterflooding requires necessary conditions which are significant clay fraction, initial formation water contains divalent cations, crude oil contains polar components, and exposure of the rock to crude oil to create mixed-wet conditions.

The experiments conducted on the two cores that were not subjected to aging period showed no dependence of oil recovery on the salinity of the injected brine either in secondary or tertiary mode. The recovery factor of secondary synthetic sea water flooding and low salinity water-flooding were 56.3% and 55.2% respectively. The tertiary low salinity waterflooding did not show any increase in the oil recovery in the unaged core.

While the secondary low salinity waterflooding in the aged cores gave a recovery factor in the range of $67.8 - 76.3 \pm 2\%$ which is higher than the unaged cores. This highlights the importance of initial wettability state of the core to observe the effect of low salinity waterflooding.

The injection of surfactant was believed to mobilize the trapped oil after waterflooding by significantly reducing the interfacial tension. However the amount of the mobilized oil will depend on the size of the surfactant slug injected at same surfactant concentration. The tertiary low salinity surfactant and polymer slugs injection done on the aged cores showed additional oil produced and the oil recovery increased with increasing the surfactant slug size injected. The sizes of surfactant slugs were 0.3, 0.5, 1, and 2 PV and the recovery increased from 6.2 % to 65.0 % of residual oil after secondary flooding. The determination of the optimum surfactant slug size requires injection of larger than 2 PV of surfactant with same concentration to observe the recovery performance. The comparison between aged and unaged cores flooded with same surfactant and polymer slugs size showed that the wettability of the

cores affects the performance of slugs injection in the recovery of trapped oil. The unaged cores A1 and A2 gave a tertiary recovery of 17.0 and 10.0 % of residual oil respectively while the aged core A5 which flooded with same slugs size gave 52.6 % of residual oil.

Garnes et al. [72] have plotted the capillary distribution curve (CDC) for the Berea sandstone core which has a wettability in the range of mixed-wet to weakly water-wet. They found that Berea sandstone has a critical capillary number in the range of 4×10^{-6} . In this study, the tertiary slugs injection has achieved a capillary number of 2.6×10^{-4} which lowered the residual oil saturation as listed in table 9.12. Figure 9.26 shows a comparison of the obtained results with the CDC measured by the work of Garnes et al.

Based on the CDC of Berea sandstone, the achieved capillary number in this study should reduce the residual oil saturation and give a value of $S_{or-LS-S-P} / S_{or-LS}$ in the range of 0.47. However in this study the decrease in the residual oil saturation is highly dependent on the size of the surfactant slug injected at constant surfactant concentration. The cores A3 and A4 which flooded by 0.3 and 0.5 PV of surfactant respectively show a significant deviation from the curve. This indicates that more surfactant is needed to be injected in order to satisfy surfactant retention and achieve lower residual oil saturation. Cores A5 and A6 which flooded by 1 and 2 PV of surfactant respectively gave a reasonable reduction in the residual oil saturation which are consistent with the CDC curve. However injection of 2 PV of surfactant resulted in higher tertiary recovery.

Although the unaged cores A1 and A2 have a high residual oil saturation after waterflooding, the tertiary slugs injection did not show a significant reduction in the residual oil saturation. The unaged cores have a strongly water-wet state and this indicates that the wettability affects the performance of tertiary recovery.

Table 9.12: Parameters of tertiary slugs injection in the cores

| Core ID | A1* | A2* | A3 | A4 | A5 | A6 |
|------------------------------------|----------------------|----------------------|----------------------|----------------------|----------------------|----------------------|
| S_{or-LS} [%PV] | 34.8 | 35.6 | 20.5 | 21.6 | 25.3 | 28.5 |
| Surfactant slug size injected [PV] | 1 | 1 | 0.3 | 0.5 | 1 | 2 |
| Polymer slug size injected [PV] | 1 | 1 | 0.5 | 1 | 1 | 1 |
| $S_{or-LS-S-P}$ [%PV] | 29.6 | 32.5 | 19.3 | 16.2 | 12.0 | 6.5 |
| $S_{or-LS-S-P} / S_{or-LS}$ | 0.85 | 0.91 | 0.94 | 0.75 | 0.47 | 0.35 |
| N_c of LS-S-P | 2.7×10^{-4} | 2.6×10^{-4} | 2.6×10^{-4} | 2.6×10^{-4} | 2.6×10^{-4} | 2.6×10^{-4} |

* Unaged core

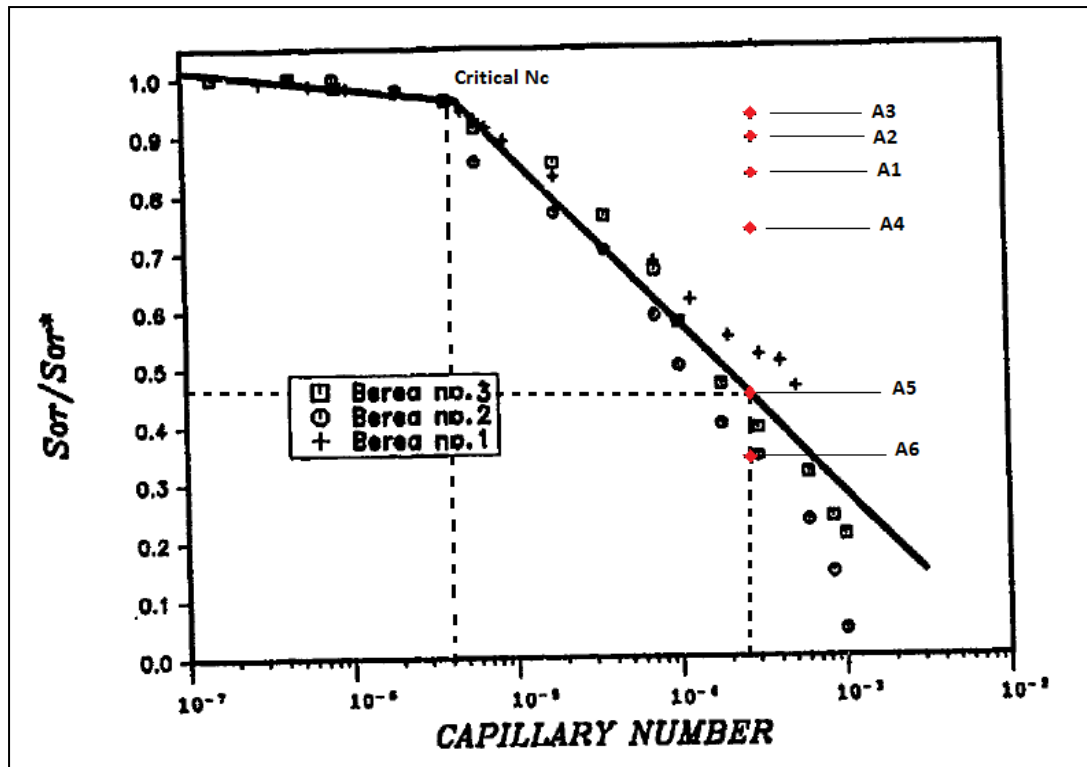


Fig. 9.26 : Capillary distribution curve of Berea sandstone [72].

10. Conclusions:

Core flooding experiments were carried out in six Berea sandstone cores to investigate the effect and different aspects of low salinity waterflooding followed by combined low salinity surfactant and polymer slugs injection.

Two cores out of the six were not been aged and were tested for effect of reducing salinity of injected brine in both secondary and tertiary mode. The two cores did not show any increase in oil recovery by low salinity waterflooding compared to high salinity water in both secondary and tertiary mode. The unaged cores showed a strongly water-wet behavior.

The other four cores were aged with crude oil and flooded by low salinity brine which is 3000 ppm NaCl brine as a secondary mode. The aging period altered wettability of the cores to less water-wet state which was confirmed by reduction in the oil permeability after aging. The oil recovery from these aged cores was higher than that of the unaged cores which indicates the effect of initial wettability state on performance of low salinity waterflooding. This confirms that the rock should be exposed to crude oil to create mixed-wet conditions in order to observe an effect of low salinity waterflooding. Fines particles were not been observed in the effluent during the coreflooding experiments and the pressure profiles were stable and increased only as a response of rising the flow rate.

In general, the results of tertiary low salinity surfactant and polymer slugs injection in all six cores showed that the slug injection has mobilized and produced different amount of oil from the cores. The aged cores were flooded with different surfactant slug size and the oil recovery increased with increasing the size of the surfactant slug injected at constant surfactant concentration.

The capillary number achieved by tertiary slugs injection was high enough to mobilize a significant amount of residual oil after waterflooding. However the reduction in the residual oil was highly dependent on the surfactant slug size injected. The injection of 0.3 and 0.5 PV of surfactant did not reduce the residual oil saturation as expected by the CDC of Berea sandstone which indicates that more surfactant should be injected to satisfy retention and achieve low residual saturation. The injection of 1 PV and 2 PV of surfactant gave increasing change in residual oil saturation with capillary number. The optimization of surfactant slug size requires injection of larger 2 PV of surfactant with same concentration to observe the recovery performance.

The comparison between aged and unaged cores flooded with same surfactant and polymer slugs size showed that the wettability of the cores affects the performance of slugs injection in the recovery of trapped oil. The unaged cores A1 and A2 gave a

tertiary recovery of 17.0 and 10.0 % of residual oil respectively while the aged core A5 which flooded with same slug size gave 52.6 % of residual oil.

The low salinity polymer slug injection performed at the end with higher concentration resulted in producing additional oil from the cores. However the performance of this injection varied because of different residual oil obtained after tertiary low salinity surfactant and polymer slugs injection.

11. Further work:

The understanding of aspects behind the effect of low salinity waterflooding in increasing the oil recovery requires an extensive researches to determine the different variables that contribute to the performance of the process.

The determination of initial wettability state and the changes in the wettability of the cores during the low salinity water flooding using quantitative methods such as Amott-Harvey and USBM will help to describe the improvements in the recovery. The effect of reducing salinity of the injected brine should be investigated in aged cores where the initial wettability of the cores reflects the reservoir wettability and the experiments should be performed in both secondary and tertiary mode.

Effluent analysis should be carried out to give a better understanding on how the low salinity waterflooding works and the mechanisms behind it that lead to improve oil recovery. These analysis are effluent pH and the concentration of the cations presents in the effluent compared to the injected brine.

The surfactant solution should be made with different concentrations and tested for interfacial tension measurements to obtain the optimum concentration that give low IFT with less amount of surfactant used.

The optimization of the surfactant slug size that gives high oil recovery requires more experiments with larger slug size at same surfactant concentration to determine the optimum slug in term of oil recovery. The analysis of the effluent from the tertiary low salinity slugs injection will help to identify the factors that affects the performance of the surfactant injection such as retention.

12. References:

- [1] M. Skarestad, and A. Skauge, (2007). " Reservoir Engineering II " , PTEK213 compendium, University of Bergen.
- [2] K. S. Sorbie and M. I. J. van Dijke, (2005). " Fundamentals of Three-Phase Flow in Porous Media of Heterogeneous Wettability ", Institute of Petroleum Engineering, Heriot-Watt University, Edinburgh, Scotland, UK.
- [3] L.P. Dake, (1985). " Fundamentals of Reservoir Engineering ", ELSEVIER Science B.V. Netherlands.
- [4] R. Meyer, (2002). " Anisotropy of sandstone permeability ", CREWES Research Report , Volume 14.
- [5] F.J. Lucia, (2007). " Carbonate Reservoir Characterization : An integrated Approach " , Second Edition.
- [6] H. Rueslatten, P.-E. Oren, M. Robin, E. Rosenberg, L.Cuiec. (1994) . " A Combined Use of CRYO-SEM and NMR-Spectroscopy for Studying the Distribution of Oil and Brine in Sandstones " , SPE/DOE 27804.
- [7] D. Myers, (1999). " Surfaces, Interfaces, and Colloids: Principles and applications " , Second Edition, Wiley & Sons Inc.
- [8] G. J. Hirasaki, C. A. Miller, and M. Puerto, (2008). " Recent Advances in Surfactant EOR " , SPE and Rice University, SPE 115386.
- [9] S. Lui, R. F. Li, C. A. Miller, and G. J. Hirasaki, (2008). " ASP Processes: Wide Range of Conditions for Good Recovery " , SPE, Occidental Oil and Gas Corporation, and Rice University, SPE 113936.
- [10] R. N. Healy, R. L. Reed, and D. G. Stenmark, (1976). " Multiphase Microemulsion Systems " , SPE 5565.
- [11] G. J. Hirasaki, (1991). " Wettability: Fundamentals and Surface Forces " , SPE Formation Evaluation, June.
- [12] W. G. Anderson, (1986). "Wettability Literature Survey – Part 1: Rock/Oil/Brine Interactions and the Effect of Core Handling on Wettability " , Journal of Petroleum Technology, October, SPE 13932.
- [13] W. G. Anderson, (1986). " Wettability Literature Survey – Part 2: Wettability Measurements " , Journal of Petroleum Technology, November, SPE 13933.
- [14] W. G. Anderson, (1987). " Wettability Literature Survey – Part 4: Effects of Wettability on Capillary Pressure " , Journal of Petroleum Technology, October, SPE 15271.

- [15] W. G. Anderson, (1987). " Wettability Literature Survey – Part 5: The of Wettability on Relative Permeability ", Journal of Petroleum Technology, November, SPE 16323.
- [16] W. G. Anderson, (1987). " Wettability Literature Survey – Part 6: The Effects of Wettability on Waterflooding ", Journal of Petroleum Technology, December, SPE 16471.
- [17] P. L. McGuire, J. R. Chatham, F. K. Paskvan, D. M. Sommer, F. H. Carini, (2005). "Low Salinity Oil Recovery: An Exciting New EOR Opportunity for Alaska's North Slope ", SPE 93903.
- [18] A. Lager, K. J. Webb, C. J. J. Black, M. Singleton, and K. S. Sorbie, (2008). " Low Salinity Oil Recovery – An Experimental Investigation ", Petrophysics Vol 49, No.1.
- [19] G.E. Leblanc, R.A. Secco, M. Kostic, (1999). " Viscosity measurement " CRC Press LLC.
- [20] A. Skauge, B. Ottesen, (2002). " A Summary of Experimentally Derived Relative Permeability and Residual Saturation on North Sea Reservoir Cores ", Norsk Hydro ASA, University of Bergen and Reservoir laboratories, Norway.
- [21] A. Skauge, K. Spildo, L. Hoiland, B. Vik, (2007). " Theoretical and experimental evidence of different wettability classes ", Journal of Petroleum Science and Engineering 57.
- [22] I. Chatzis, and N. R. Morrow, (1984). " Correlation of Capillary Number Relationships for Sandstone ", Society of Petroleum Engineering Journal, October.
- [23] G. L. Stegemeier, (1974). " Relationship of Trapped Oil Saturation to Petrophysical Properties of Porous Media ", Society of Petroleum Engineers of AIME, SPE 4754.
- [24] S. S. Ayatollahi, (2004). " Boundary Tension and Wettability ", Lecture note, Sultan Qaboos University, Fall 2004.
- [25] A. Skauge, (2013). " Wettability Two Phase Flow ", Lecture note, CIPR, University of Bergen, Norway.
- [26] A. Skauge, (2013). " Wettability and Oil Recovery ", Lecture note, CIPR, University of Bergen, Norway.
- [27] H. O. Yildiz, N. R. Morrow, (1995). " Effect of Brine Composition on Recovery of Moutray Crude Oil by Waterflooding", Journal of Petroleum Science and Engineering 14.

- [28] P. P. Jadhunandan, and N.R. Morrow, (1995). " Effect of Wettability on Waterflood Recovery for Crude-Oil/Brine/Rock Systems ", SPE Reservoir Engineering, February.
- [29] P. R. Filoco, and M. M. Sharma, (1998). " Effect of Brine Salinity and Crude Oil Properties on Relative Permeabilities and Residual Saturations ", SPE 49320.
- [30] M.M. Sharma and P.R. Filoco, (2000). " Effect of Brine Salinity and Crude-Oil Properties on Oil Recovery and Residual Saturations ", SPE Journal 5, September.
- [31] Y. Zhang, and N.R. Morrow, (2006). " Comparison of Secondary and Tertiary Recovery with Change in Injection Brine Composition for Crude Oil/Sandstone Combinations ", SPE 99757.
- [32] G.Q. Tang, and N.R. Morrow, (1997). " Salinity, Temperature, Oil Composition, and Oil Recovery by Waterflooding ", SPE Reservoir Engineering, November.
- [33] A. Lager, K.J. Webb, I. R. Collins, and D.M. Richmond, (2008). " LoSalTM Enhanced Oil Recovery: Evidence of Enhanced Oil Recovery at the Reservoir Scale ", SPE 113976.
- [34] H.O. Yildiz, M.Valat, and N.R. Morrow, (1999). " Effect of Brine Composition on Wettability and Oil Recovery of a Prudhoe Bay Crude Oil ", Journal of Canadian Petroleum Technology, Volume 38, No. 1.
- [35] A. K. Sarkar, and M. M. Sharma, (1990). " Fines Migration in Two- Phase Flow ", JPT, May.
- [36] P. Lemon, A. Zeinijahroma, P. Bedrikovetsky, and I. Shahin, (2011). " Effects of Injected-Water Salinity on Waterflood Sweep Efficiency Through Induced Fines Migration ", Journal of Canadian Petroleum Technology, September.
- [37] D.A. Musharova, I.M. Mohamed, and H.A. Naser-El-Din, (2012). " Detrimental Effect of Temperature on Fines Migration in Sandstone Formation ", SPE 150953.
- [38] Y.Zhang, X. Xie, and N.R. Morrow, (2007). " Waterflood Performance by Injection of Brine with Different Salinity for Reservoir Cores ", SPE 109849 .
- [39] J. C. Shaw, P. L. Churcher, and B. F. Hawkins, (1991). " The Effect of Firing on Berea Sandstone ", SPE Formation Evaluation.
- [40] E. D.Pittman, (1989). " Problems Related to Clay Minerals in Reservoir Sandstones ", Chapter 17, Amoco Production Company, Tulsa, Oklahoma.

- [41] A. RezaeiDoust, T. Puntervold, S. Strand, and T. Austad, (2009). " Smart Water as Wettability Modifier in Carbonate and Sandstone: A Discussion of Similarities/Differences in the Chemical Mechanisms ", University of Stavanger, Energy and Fuels article, 23, 4479–4485 : DOI:10.1021/ef900185q.
- [42] G. R. Jerauld, C.Y. Lin, K. J. Webb, and J. C. Seccombe, (2006). " Modeling Low-Salinity Waterflooding ", SPE 102239.
- [43] Yu-Shu Wu, and B. Bai (2009). " Efficient Simulation for Low-Salinity Waterflooding in Porous and Fractured Reservoirs ", SPE 118830.
- [44] D.J. Ligthelm, J. Gronsveld, J.P. Hofman, N.J. Brussee, F. Marcelis, and H.A. van der Linde. (2009). " Novel Waterflooding Strategy by Manipulation of Injection Brine Composition ", SPE 119835.
- [45] N. Morrow and J. Buckley, (2011). " Improved Oil Recovery by Low-Salinity Waterflooding ", JPT, SPE 129421, Distinguished Author Series.
- [46] S.Y. Lee, K.J. Webb, I.R. Collins, A. Lager, S.M. Clarke, M. O'Sullivan, A.F. Routh, and X. Wange, (2010). " Low Salinity Oil Recovery – Increasing Understanding of the Underlying Mechanisms ". SPE 129722.
- [47] T. Austad, A. R. Doust , and T. Puntervold, (2010). " Chemical Mechanism of Low Salinity Water Flooding in Sandstone Reservoir ", SPE 129767.
- [48] K.S. Sorbie and I.R. Collins, (2010). " A Proposed Pore-Scale Mechanism for Low Salinity Waterflooding Works ", SPE 129833.
- [49] W. Winoto, N. Loahardjo, X. Xie, P. Yin, and N. R. Morrow, (2012). "Secondary and Tertiary Recovery of Crude Oil from Outcrop and Reservoir Rock by Low Salinity Waterflooding ", SPE 154209.
- [50] A. Graue, (2006). " Experimental Reservoir Physics ", Lab Manual, Ptek 214, Department of Physics and Technology, University of Bergen.
- [51] J.J.M. Lewis, (1988). " Outcrop-Derived Quantitative Models of Permeability Heterogeneity for Genetically Different Sand Bodies ", SPE 18153.
- [52] NExT PERF, (1999). " Introduction to Capillary Pressure ", Short Course Note.
- [53] J.W. Amyx, D.M. Bass, and R.L. Whiting, (1960). " Petroleum Reservoir Engineering " New York.
- [54] A.B. Zolotuchin, and J.R. Ursin. (2000). "Introduction to Petroleum Reservoir Engineering". Hoyskoleforl, Kristiansand, 407.
- [55] J. L. Salager, (2002). " Surfactants Types and Uses ", FIRP Booklet #E300-A, Laboratory of Formulation, Interfaces Rheology and Processes, Universidad De Los Andes.

- [56] L. W. Lake, (1989). " Enhanced oil recovery ". Englewood Cliffs, N.J., Prentice Hall.
- [57] P.A. Winsor, (1954). " Solvent Properties of Amphiphilic compounds ", London, Butterworths.
- [58] K. Djurhuus, (2013). " Surfactant Flooding ", EOR Seminar, PTEK 313.
- [59] K. S. Sorbie, (1991). " Polymer – Improved Oil Recovery ", Blackie and Son Ltd. Heriot-Watt University, Edinburgh.
- [60] G. S. J. Kell, (1975). " Density measurements " Chern. Eng. Data, 20(1),97, Copyright by the American Chemical Society.
- [61] Malvern, (2009). " Kinexus rheometer and rSpace software " User Manual, MAN0380, Malvern Instruments Ltd.
- [62] G.Q. Tang, and N.R. Morrow, (1999). " Influence of brine composition and fines migration on crude oil/brine/rock interactions and oil recovery ", J. Petroleum Science Engineering, S09204105(99)00034-0.
- [63] A. Lager, K.J. Webb, and C.J.J. Black, (2007). " Impact of Brine Chemistry on Oil Recovery ", Paper A24 presented at the 14th European Symposium on Improved Oil Recovery, Cairo, Egypt, 22-24 April.
- [64] R. Ehrlich, and R. J. Wygal, (1977). " Interaction of Crude Oil and Rock Properties with the Recovery of Oil by Caustic Waterflooding ", SPE Journal, vol. 17, no. 4.
- [65] G. S. Kallevik, (2010). " Implementations of Methods for Modeling Low Salinity Waterflood and Low Salinity Surfactant Flooding ", Master Thesis in Petroleum Technology, CIPR, University of Bergen.
- [66] C. C. Agbalaka, A. Y. Dandekar, S. L. Patil, S. Khataniar, and J. R. Hemsath, (2008). "Coreflooding Studies to Evaluate the Impact of Salinity and Wettability on Oil Recovery Efficiency" Trans. Porous Media 76: 77-94.
- [67] G.J. Hirasaki, (1991). " Wettability : Fundamentals and Surface Forces ", SPEFE 6.
- [68] R. A. Nasralla, H. A. Nasr-El-Din, (2012). " Double-Layer Expansion: Is It A Primary Mechanism of Improved Oil Recovery by Low-Salinity Waterflooding? ", SPE 154334.
- [69] K. Skrettingland, T. Holt, M. T. Tweheyo, and I. Skjevraak, (2010). " Snorre Low Salinity Water Injection – Core Flooding Experiments and Single Well Field Pilot ", SPE 129877.

- [70] A. Skauge, Z. Ghorbani, and M. Delshad, (2011). " Simulation of Combined Low Salinity Brine and Surfactant Flooding ", 16th European Symposium on Improved Oil Recovery Cambridge, UK, 12-14 April.
- [71] E. Tzimas, A. Georgakaki, C. Garcia Cortes, and S.D. Peteves, (2005). " Enhanced Oil Recovery using Carbon Dioxide in the European Energy System", DG JRC, Institute for Energy, Petten, The Netherlands, Report EUR 21895 EN.
- [72] J.M. Games, A.M. Mathisen, A. Scheie, and A. Skauge, (1990). " Capillary Number Relations for Some North Sea Reservoir Sandstones ", SPE/DOE 20264.

Appendix A:

Table A.1 : Drainage data of cores A1 and A2

| Core ID | Volume of Marcol 152 Injected [PV] | Volume of produced water [ml] | S_{wi} [%] | S_{oi} [%] |
|---------|------------------------------------|-------------------------------|----------------|----------------|
| A1 | 15 | 12.60 ± 0.01 | 19.5 ± 0.1 | 80.8 ± 0.1 |
| A2 | 18 | 13.10 ± 0.01 | 18.9 ± 0.1 | 81.1 ± 0.1 |

Table A.2 : Drainage data of core A3

| Rate [ml/min] | Volume of Marcol 152 Injected [PV] | Volume of produced water [ml] | S_{wi} [%] | S_{oi} [%] |
|---------------|------------------------------------|-------------------------------|----------------|----------------|
| 0.1 | 2 | 10.30 ± 0.01 | 38.0 ± 0.1 | 62.0 ± 0.1 |
| 0.5 | 2 | 11.80 ± 0.01 | 28.9 ± 0.1 | 71.1 ± 0.1 |
| 1 | 4 | 12.40 ± 0.01 | 25.3 ± 0.1 | 74.7 ± 0.1 |
| 1.5 | 3 | 12.70 ± 0.01 | 23.5 ± 0.1 | 76.5 ± 0.1 |
| 2 | 3.5 | 12.80 ± 0.01 | 22.9 ± 0.1 | 77.1 ± 0.1 |

Table A.3 : Drainage data of core A4.

| Rate [ml/min] | Volume of Marcol 152 Injected [PV] | Volume of produced water [ml] | S_{wi} [%] | S_{oi} [%] |
|---------------|------------------------------------|-------------------------------|----------------|----------------|
| 0.1 | 2 | 10.36 ± 0.01 | 36.7 ± 0.1 | 63.3 ± 0.1 |
| 0.5 | 1.5 | 11.36 ± 0.01 | 30.6 ± 0.1 | 69.4 ± 0.1 |
| 1 | 4 | 12.36 ± 0.01 | 24.5 ± 0.1 | 75.5 ± 0.1 |
| 1.5 | 3 | 12.66 ± 0.01 | 22.7 ± 0.1 | 77.3 ± 0.1 |
| 2 | 4 | 12.76 ± 0.01 | 22.1 ± 0.1 | 77.9 ± 0.1 |

Table A.4 : Drainage data of core A5.

| Rate [ml/min] | Volume of Marcol 152 Injected [PV] | Volume of produced water [ml] | S_{wi} [%] | S_{oi} [%] |
|------------------|---------------------------------------|----------------------------------|----------------|----------------|
| 0.1 | 2 | 10.30 ± 0.01 | 36.8 ± 0.1 | 63.2 ± 0.1 |
| 0.5 | 2 | 11.30 ± 0.01 | 30.6 ± 0.1 | 69.4 ± 0.1 |
| 1 | 2 | 11.80 ± 0.01 | 27.5 ± 0.1 | 72.5 ± 0.1 |
| 1.5 | 4 | 12.50 ± 0.01 | 23.2 ± 0.1 | 76.8 ± 0.1 |
| 2 | 3 | 12.80 ± 0.01 | 21.4 ± 0.1 | 78.6 ± 0.1 |

Table A.5 : Drainage data of core A6

| Rate [ml/min] | Volume of Marcol 152 Injected [PV] | Volume of produced water [ml] | S_{wi} [%] | S_{oi} [%] |
|------------------|---------------------------------------|----------------------------------|----------------|----------------|
| 0.1 | 2 | 10.55 ± 0.01 | 35.6 ± 0.1 | 64.4 ± 0.1 |
| 0.5 | 2 | 11.55 ± 0.01 | 29.5 ± 0.1 | 70.5 ± 0.1 |
| 1 | 3.5 | 12.05 ± 0.01 | 26.5 ± 0.1 | 73.5 ± 0.1 |
| 1.5 | 2.5 | 12.35 ± 0.01 | 24.6 ± 0.1 | 75.4 ± 0.1 |
| 2 | 5 | 12.75 ± 0.01 | 22.2 ± 0.1 | 77.8 ± 0.1 |

Appendix B :

Table B.1: Density measurements of fluids with uncertainty of ± 0.0001 .

| Fluid | Density [g/ml] | | |
|---------------------------------|------------------|--------|--------|
| Temperature [C°] | 21 | 23 | 25 |
| Synthetic sea water | 1.0427 | 1.0247 | 1.0206 |
| Low salinity water | 0.9988 | 0.9987 | 0.9984 |
| North Sea Crude oil | 0.9137 | 0.8993 | 0.8982 |
| Diluted crude oil [40% octane] | 0.8227 | 0.8115 | 0.8084 |
| XOF 25s Surfactant solution | - | 0.9987 | - |
| XOF 26s Surfactant solution | - | 0.9961 | - |

Appendix C :

Table C.1: Viscosity measurements of brines and oils.

| Fluid | Viscosity [mPa.s] at different temperatures | | | |
|---------------------|---|--------------|--------------|--------------|
| | 20 C° | 22 C° | 24 C° | 26 C° |
| Marcol 152 Oil | 87.23 ± 4.36 | 78.72 ± 3.94 | 70.92 ± 3.55 | 64.31 ± 3.22 |
| North Sea crude oil | 38.72 ± 1.94 | 35.14 ± 1.76 | 32.05 ± 1.60 | 29.35 ± 1.47 |
| Diluted crude oil* | 2.86 ± 0.14 | 2.74 ± 0.14 | 2.62 ± 0.13 | 2.52 ± 0.13 |
| Synthetic sea water | 1.01 ± 0.05 | 0.96 ± 0.05 | 0.93 ± 0.05 | 0.90 ± 0.05 |
| 3000 ppm NaCl brine | 1.00 ± 0.05 | 0.95 ± 0.05 | 0.90 ± 0.05 | 0.86 ± 0.04 |

* Made of 40 wt% of Octane and 60 wt% of North Sea crude oil

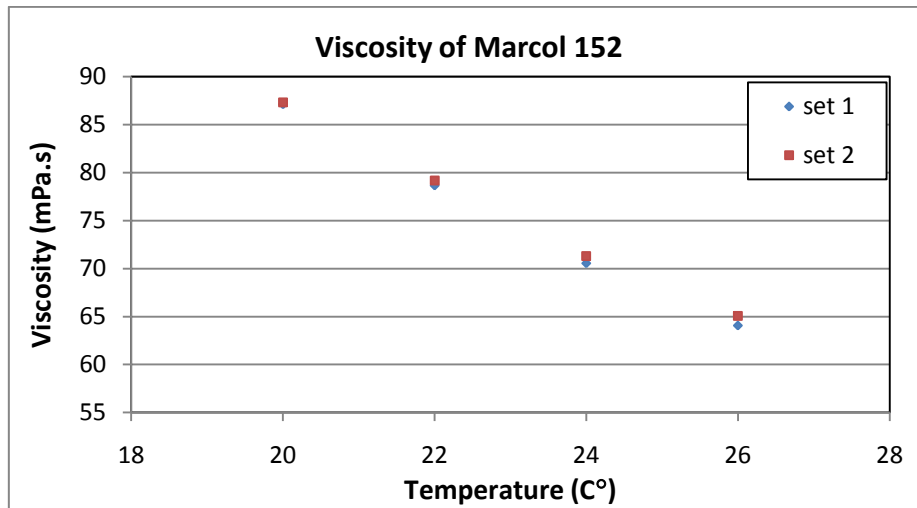


Fig.C.1: Viscosity of Marcol 152 measured at different temperature.

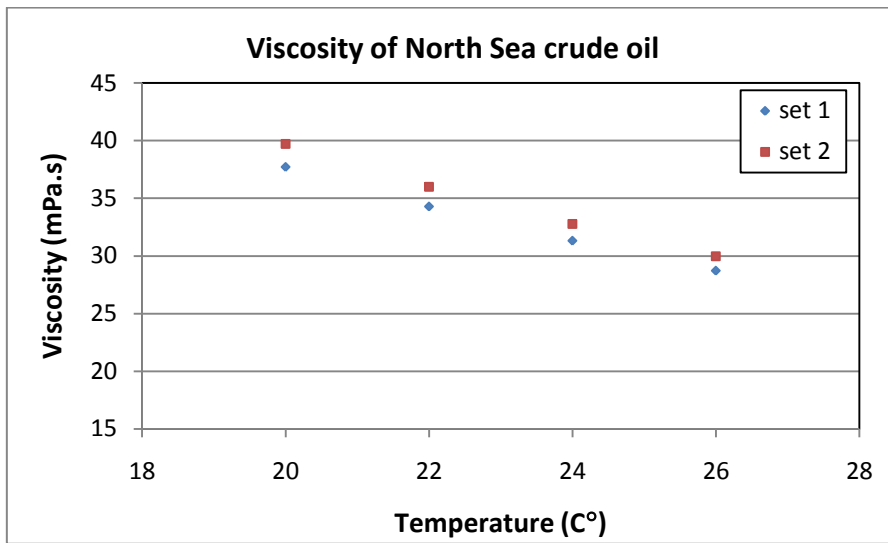


Fig.C.2 : Viscosity of North Sea crude oil measured at different temperature.

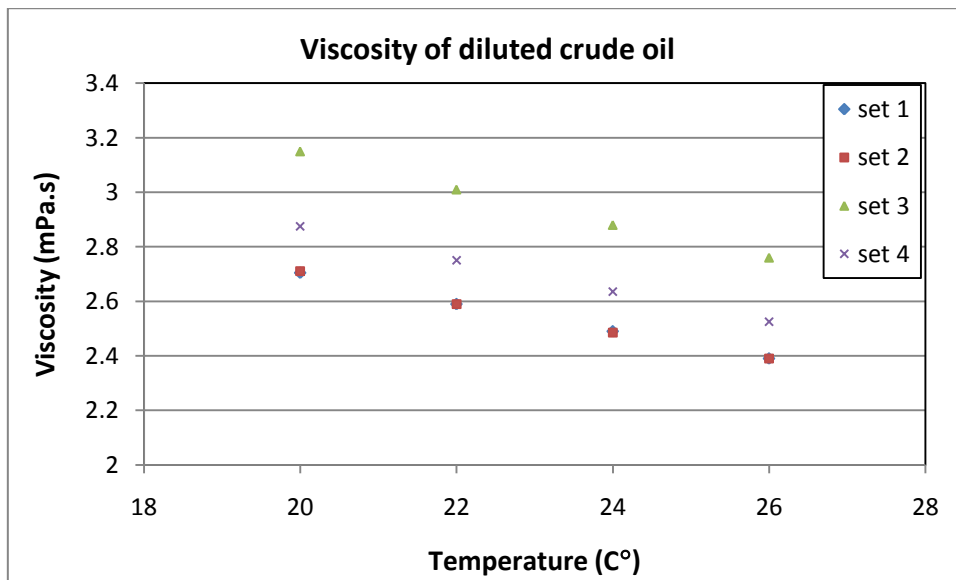


Fig.C.3 : Viscosity of diluted crude oil measured at different temperature.

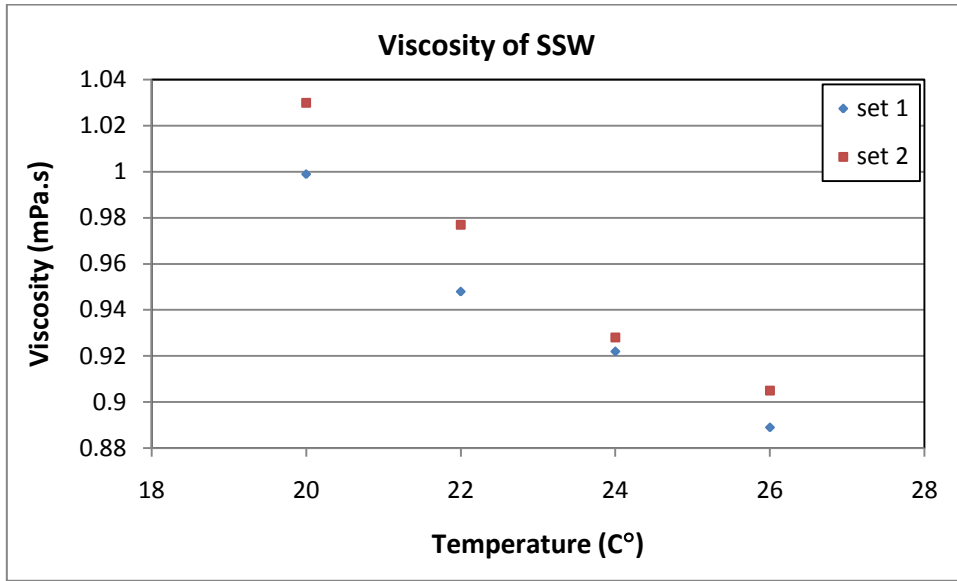


Fig.C.4 : Viscosity synthetic sea water measured at different temperature.

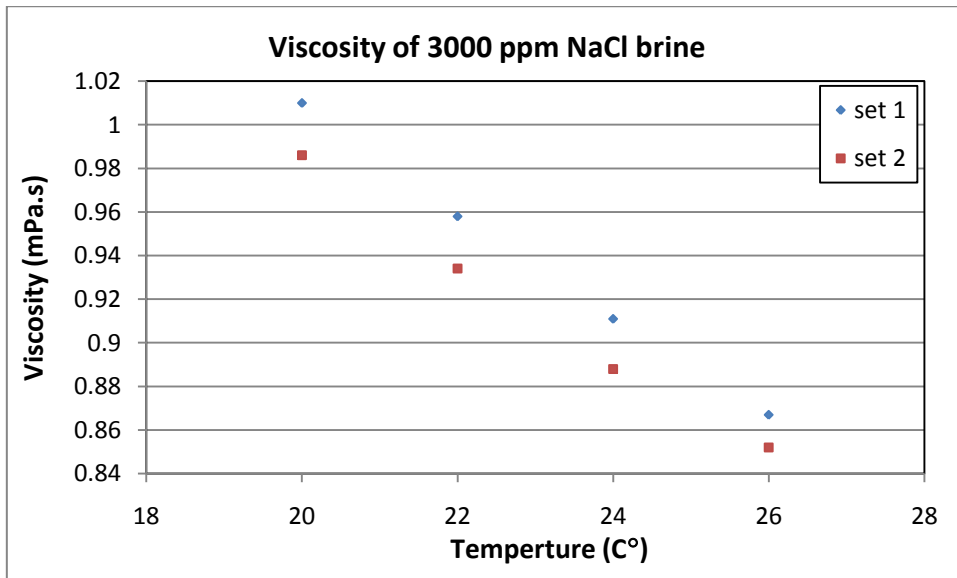


Fig.C.5 : Viscosity of 3000 ppm NaCl brine measured at different temperature.

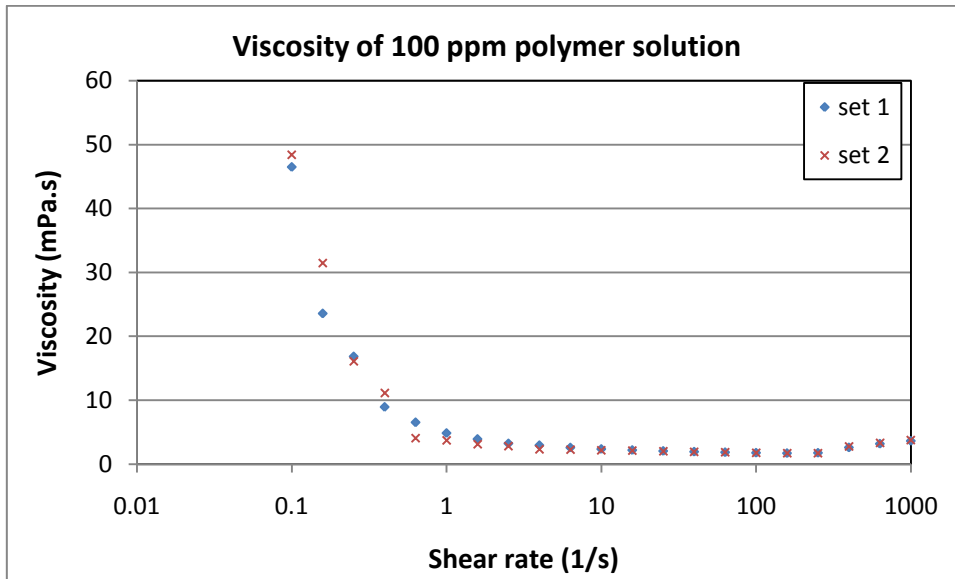


Fig.C.6 : Viscosity measurement of 100 ppm polymer solution.

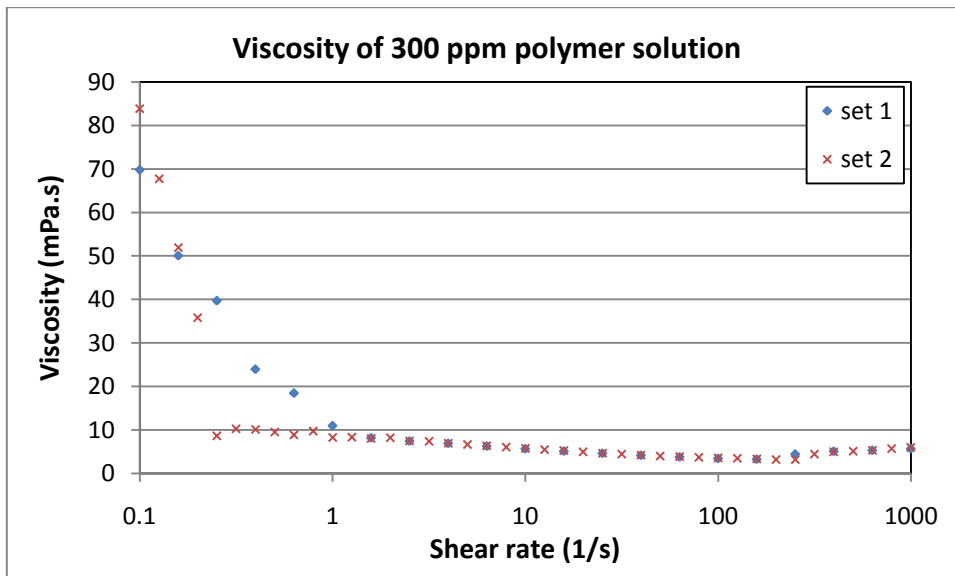


Fig.C.7 : Viscosity measurement of 300 ppm polymer solution.

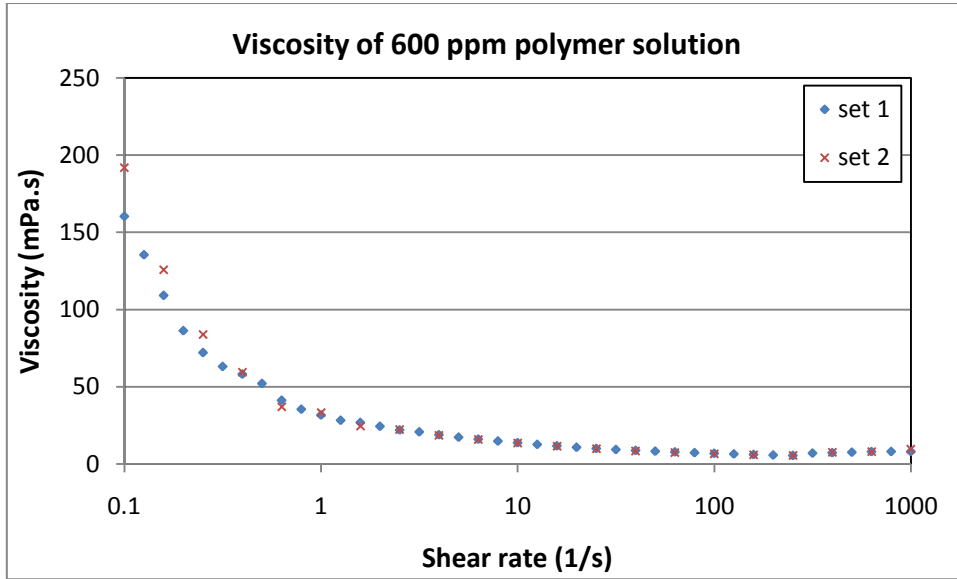


Fig. C.8 : Viscosity measurement of 600 ppm polymer solution.

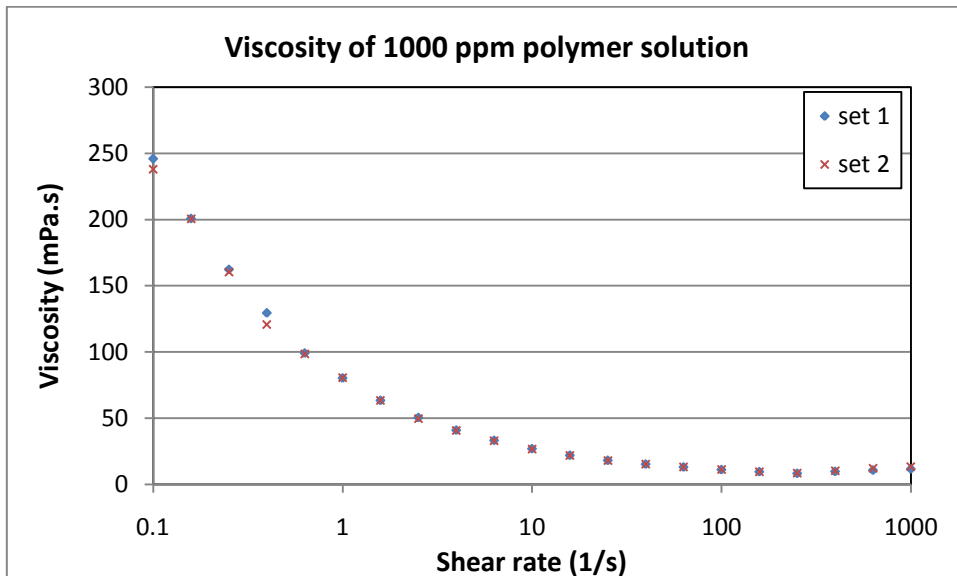


Fig.C.9 : Viscosity measurement of 1000 ppm polymer solution.

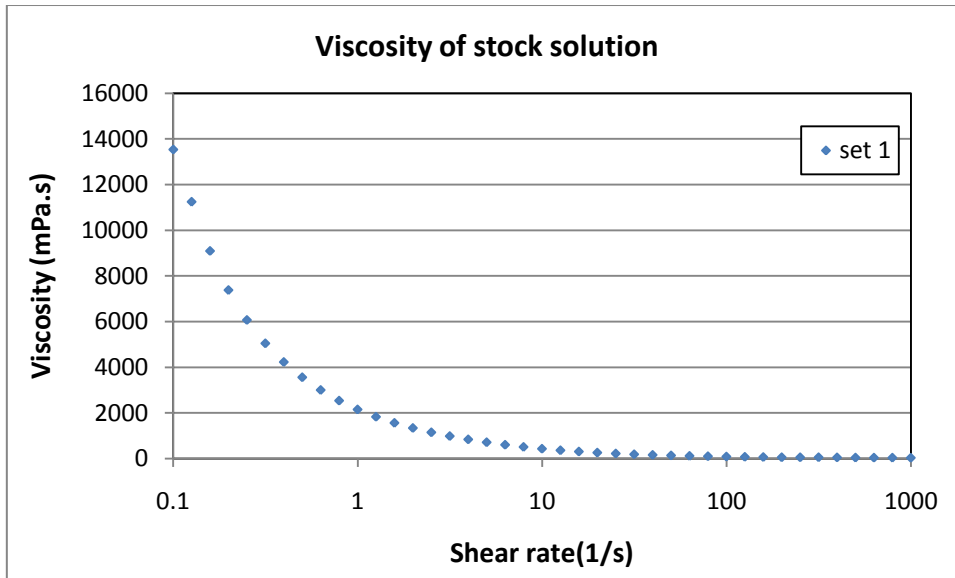


Fig.C.10 : Viscosity measurement of stock polymer solution.

Appendix D :

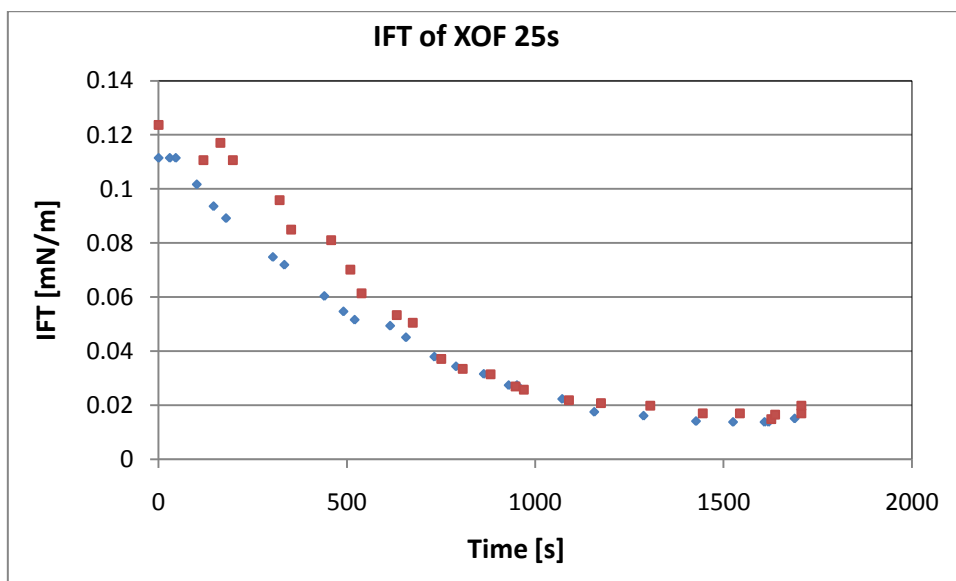


Fig.D.1: IFT measurements of fresh sample of XOF 25s surfactant with diluted crude oil.

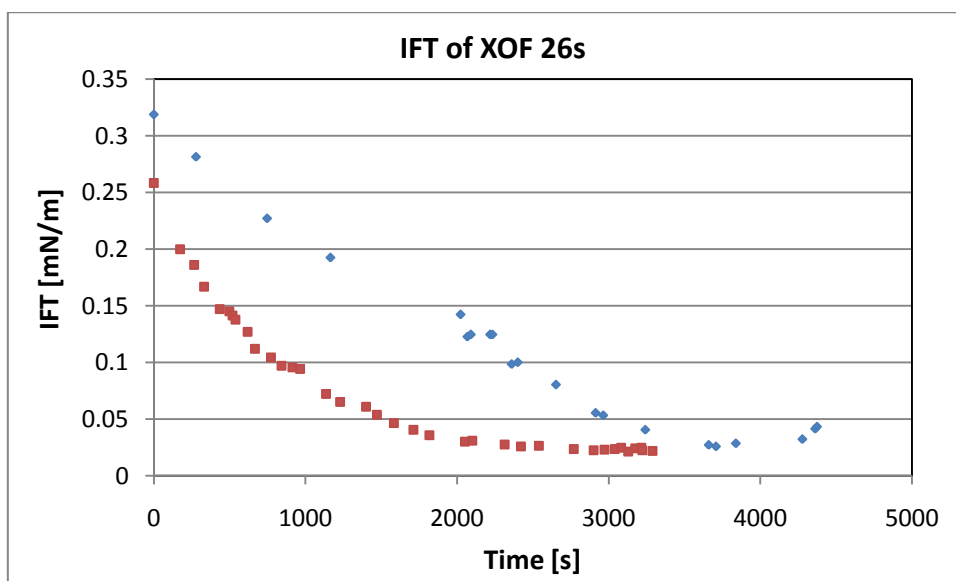


Fig.D.2 : IFT measurements of fresh sample of XOF 25s surfactant with diluted crude oil.

Appendix E :

Table E.1 : Measured diameters and lengths of the cores

| Core ID | Diameter [cm] | Average Diameter [cm] | Length [cm] | Average Length [cm] |
|---------|---------------|-----------------------|-------------|---------------------|
| A1 | 3.79 | 3.79 ± 0.01 | 6.29 | 6.29 ± 0.01 |
| | 3.79 | | 6.29 | |
| | 3.80 | | | |
| | 3.79 | | | |
| A2 | 3.79 | 3.80 ± 0.01 | 6.47 | 6.48 ± 0.01 |
| | 3.80 | | 6.48 | |
| | 3.80 | | | |
| | 3.80 | | | |
| A3 | 3.81 | 3.81 ± 0.01 | 6.40 | 6.40 ± 0.01 |
| | 3.82 | | 6.39 | |
| | 3.81 | | | |
| | 3.82 | | | |
| A4 | 3.81 | 3.82 ± 0.01 | 6.30 | 6.30 ± 0.01 |
| | 3.82 | | 6.29 | |
| | 3.82 | | | |
| | 3.83 | | | |
| A5 | 3.81 | 3.81 ± 0.01 | 6.34 | 6.33 ± 0.01 |
| | 3.81 | | 6.32 | |
| | 3.81 | | | |
| | 3.81 | | | |
| A6 | 3.81 | 3.81 ± 0.01 | 6.34 | 6.34 ± 0.01 |
| | 3.81 | | 6.34 | |
| | 3.81 | | | |
| | 3.81 | | | |